

**LOAD MANAGEMENT OF
ELECTRIC VEHICLES AND HEAT PUMPS
IN EMERGING ELECTRICITY SYSTEM**

THESIS SUBMITTED FOR THE DEGREE OF
DOCTOR OF PHILOSOPHY

RILWAN OLAOLU OLIYIDE

Institute of Energy
School of Engineering
Cardiff University, UK.



January 03, 2019

CONTENTS

CONTENTS	II
LIST OF TABLES	VII
LIST OF FIGURES	IX
DECLARATION	XII
ABSTRACT	XIII
DEDICATION	XV
ACKNOWLEDGEMENTS	XVI
LIST OF PUBLICATIONS	XVII
PROJECT PARTICIPATION	XVIII
LIST OF ABBREVIATIONS	XIX
CHAPTER 1	22
INTRODUCTION	22
1.1 Emerging Electricity System.....	22
1.2 Driving Factors for the Emerging Electricity System	22
1.3 Electric Vehicles	26
1.4 Heat Pumps	28
1.4.1 Principle of operation of HPs	28
1.4.1.1 Vapour compression cycle	28
1.4.1.2 Absorption cycle	31
1.4.2 Types of HPs	31
1.4.2.1 Types of HPs based on principle of operation	31
1.4.2.2 Types of HPs based on the source of heat.....	32
1.4.2.3 Types of HPs based on medium of heat distribution	33

1.4.2.4	Types of HPs based on the speed of compressor	33
1.4.2.5	Choice of HP for installation.....	34
1.5	Uptake Rate of EVs and HPs in the UK.....	34
1.6	Thesis Objectives	36
1.7	Thesis Structure.....	39
CHAPTER 2.....		41
LITERATURE REVIEW.....		41
2.1	EVs and GHG Emissions Reduction.....	41
2.2	Impacts of Charging Requirements and Charging Patterns of EVs on Power System Scheduling, GHG Emissions and Emissions Abatement Cost.....	44
2.2.1	EVs As Controllable Loads.....	44
2.2.2	EVs As Energy Storage System.....	45
2.2.3	EVs As Uncontrollable Loads.....	47
2.3	Impacts Of Load Demand OF EVs And HPs On LV Distribution Network .	49
2.4	Management Of Load Demand Of EVs and HPs In LV Distribution Network.....	51
2.4.1	Loading of Transformer	51
2.4.2	Immediate, Short-Term and Long-Term Effects of Transformer Overloading.....	53
2.5	Summary	58
CHAPTER 3.....		60
IMPACTS OF ELECTRIC VEHICLE CHARGING REQUIREMENTS AND CHARGING PATTERNS ON POWER SYSTEM SCHEDULING, GRID EMISSION INTENSITY AND EMISSION ABATEMENT COST.....		60
3.1	Introduction	60
3.2	Estimating the True GHG Emissions Reduction due to Electric Vehicles Integration	61

3.2.1	UK Mobility and Transport Statistics	61
3.2.2	The Algorithm for Estimating Real-Emissions-Reduction (RER).....	63
3.2.3	Application of the Algorithm	68
3.2.4	Results and Discussion.....	69
3.3	Dispatch Model for Analysing Impacts of EVs Charging Patterns on Power System Scheduling, Grid Emission Intensity and Emissions Abatement Cost.....	71
3.3.1	Generation mix and the system load	71
3.3.2	Model Description.....	73
3.3.3	Model Formulation.....	77
3.3.4	Model Testing	80
3.3.5	Results and Discussion.....	83
3.3.5.1	Results for Baseline scenario	83
3.3.5.2	Results for TOUC scenario	84
3.3.5.3	Results for WTOUC scenario	86
3.3.5.4	Comparison and analysis of results.....	87
3.4	Summary	89
CHAPTER 4.....		91
LOW CARBON TECHNOLOGIES INTEGRATION IN LOW VOLTAGE DISTRIBUTION NETWORK		91
4.1	Introduction	91
4.2	Description of Scenarios	92
4.3	Details of the Case Study LV Network.....	93
4.4	Calculation to Determine Future Baseline Electricity Demand Projection For the LV Network	94
4.5	Calculation to Determine EVs Uptake Projections For the LV Network	97
4.6	EVs Charging Load Requirement in the LV Network.....	102
4.7	Calculation to Determine HPs Uptake Projections For the LV Network	105

4.8	Modelling the HP Operation	107
4.9	Model Formulation of HP Operation in SH Mode.....	108
4.10	Model Formulation of HP Operation in DHW Mode	113
4.11	Implementation of the HP Operational Model.....	116
4.12	HP Model Validation	119
4.13	Data Sources.....	119
4.14	LV Network Modelling and Simulation Implementation	120
4.15	Simulation Results.....	121
4.16	Summary	126
CHAPTER 5.....		128
ADAPTIVE THERMAL MODEL FOR LOADING OF DISTRIBUTION TRANSFORMERS IN LOW CARBON LV DISTRIBUTION NETWORKS		128
5.1	Introduction	128
5.2	Assumption.....	129
5.3	Adaptive Thermal Loading Versus Static Loading of Transformer	129
5.4	Transformer Thermal Modelling.....	130
5.5	Mathematical Formulation of the Adaptive Thermal Modelling of Transformer.....	134
5.6	Case Study.....	137
5.6.1	Dumb Loading (DL).....	139
5.6.2	Capacity Enhancement (CE)	139
5.6.3	Adaptive Loading (AL).....	140
5.7	Results of the Case Study	140
5.7.1	Typical Winter Weekday Results.....	140
5.7.2	Typical Summer Weekday Results	144
5.8	Comparison of Results	148

5.9	Summary	149
CHAPTER 6		152
MANAGEMENT OF ELECTRIC VEHICLE CHARGING LOAD FOR OPTIMAL CAPACITY UTILISATION OF LOW VOLTAGE DISTRIBUTION TRANSFORMER		152
6.1	Introduction	152
6.2	Daily Commuting Patterns and EVs Use	153
6.3	The Architecture of the De-centralised Load Management Technique	154
6.4	The Design Formulation.....	156
6.5	Case Study.....	160
6.6	Results of Case study	162
6.7	Summary	164
CHAPTER 7		167
CONCLUSIONS AND SUGGESTIONS FOR FUTURE WORK		167
7.1	Fulfilling the Aim of the Study	167
7.2	Thesis Contributions	168
7.3	Conclusions	169
7.3.1	Estmiating the true GHG emissions reduction due to EVs integration.....	169
7.3.2	Dispatch model for analysing impacts of EVs charging patterns on power system scheduling, grid emission intensity and emission abatement cost.....	170
7.3.3	EVs and HPs integration in LV distribution networks.....	170
7.3.4	Adaptive thermal loading of distribution transformers	171
7.3.5	Management of EVs charging.....	172
7.4	Suggestions for Further Work.....	173
REFERENCES.....		175
APPENDIX A.....		194
APPENDIX B.....		205

LIST OF TABLES

Table 2.1 EV and domestic load suitability to support the grid	47
Table 3.1 Motor traffic by vehicle type in GB	61
Table 3.2 Vehicles licensed by body type in GB.....	62
Table 3.3 Vehicles licensed by body type in NI	62
Table 3.4 Cars licensed by propulsion/fuel type in NI.....	63
Table 3.5 Car licensed by propulsion/fuel type in GB.....	63
Table 3.6 Electricity generated, and fuel used in generation	68
Table 3.7 Emissions by ICE cars in the UK	68
Table 3.8 Emission intensity of ICE cars in the UK, 2009-2013	69
Table 3.9 UK's Transmission-Entry-Capacity generating technologies as at December 2015	72
Table 3.10 UK's most popular electric cars in 2015	81
Table 3.11 Parameters of the generating technologies	83
Table 3.12 Emissions, average grid intensity and generating costs for Baseline, TOUC and WTOUC scenarios	87
Table 3.13 Comparison of TOUC and WTOUC scenarios	89
Table 4.1 Feeder analysis.....	94
Table 4.2 GB residential annual baseline demand and relative baseline demand	95
Table 4.3 Calculated projected annual baseline demand of the LV network.....	96
Table 4.4 Average household size, cars/household, cars/head and number of cars, GB, 2020-2050	100
Table 4.5 Percentage uptake of EVs, GB, 2020-2050	101
Table 4.6 Number of households and number of EVs per scenario in the LV network, 2020-2050	102
Table 4.7 Percentage uptake of HPs, GB, 2020-2050.....	106
Table 4.8 Number of households and number of HPs per scenario in the LV network, 2020-2050	107
Table 4.9 Distribution of EVs and HPs amongst the feeders	121
Table 5.1 Thermal parameters of distribution transformer	138
Table 5.2 Comparison of transformer performances under different situations	148

Table 6.1 Analysis of the charge requirements of EVs	162
Table A.1 Parameters of building	194
Table A.2 Parameters of domestic hot water tank	196
Table A.3 Parameters of radiator	196
Table A.4 Temperature, Solar radiation and water draw events	197
Table B.2 Technical parameters of the LV network	206

LIST OF FIGURES

Fig. 1.1 Emerging electricity system	23
Fig. 1.2 Global GHG emissions by sectors	23
Fig. 1.3 Historical and projected GHG emissions and warming temperatures	24
Fig. 1.4 GHG emissions by sector, UK, 2016.....	25
Fig. 1.5 Vapour compression cycle of HP	29
Fig. 1.6 Reversed Carnot cycle	30
Fig. 1.7 Plug-in eligible cars registered for the first time in the UK, 2010-2017.....	35
Fig. 1.8 Total number of Domestic RHI approved per heating system	35
Fig. 2.1 Model for comparing LCAs of EVs and ICE vehicles	42
Fig. 2.2 Comparison of countries: Share of EV sales and EV emissions in EU	43
Fig. 2.3 Concept of peak load shaving and load levelling by EVs	45
Fig. 3.1 UK Mobility pattern	61
Fig. 3.2 Flowchart of algorithm for estimating RER	67
Fig. 3.3 Electricity generation from different sources	68
Fig. 3.4 Emissions at the grid due to EVs, RER and AER in the UK, 2009-2013	69
Fig. 3.5 Simplified diagram of UK power system showing Transmission-Entry-Capacity generating technologies as at December 2015.....	72
Fig. 3.6 Average half-hourly system load demand and generation dispatch mix, December 2015 (Historical).....	73
Fig. 3.7 Average contribution of different generating technologies into the generation mix, December 2015 (Historical).....	74
Fig. 3.8 Average half-hourly capacity factor vs average half-hourly system load	74
Fig. 3.9 Average half-hourly EV charging profiles: WTOUC and TOUC	82
Fig. 3.10 Half-hourly system average load demand	82
Fig. 3.11 Baseline: Half-hourly generation from different generating technologies (modelled)	83
Fig. 3.12 Baseline: Average daily contributions from different generating technologies (modelled)	84
Fig. 3.13 TOUC: Half-hourly generation from different generating technologies (modelled).	85

Fig. 3.14 TOUC: Average daily contributions from different generating technologies (modelled)	85
Fig. 3.15 WTOUC: Half-hourly generation from different generating technologies (modelled)	86
Fig. 3.16 WTOUC: Average daily contributions from different generating technologies (modelled)	87
Fig. 3.17 Grid emission intensities for Baseline, TOUC and WTOUC scenarios	88
Fig. 4.1 Simplified diagram of the case study LV network	93
Fig. 4.2 Average household size and cars per household, GB, 1994-2017.....	98
Fig. 4.3 Average household size and cars per head of population, GB, 1994-2017...98	
Fig. 4.4 EVs daily charge requirements distribution.....	104
Fig. 4.5 Average half-hourly EV charging profile.....	105
Fig. 4.6 Block daigram of HP system configuration.....	108
Fig. 4.7 The COP-curve from test data at Test Centre WPZ	112
Fig. 4.8 DHW tank in single-node state.....	113
Fig. 4.9 Block diagram of implementation process of HP operation.....	117
Fig. 4.10 HP average daily demand	118
Fig. 4.11 Screenshot of HP average demand from Carbon, Control and Comfort project	119
Fig. 4.12 Normalised DHW tapping profile	120
Fig. 4.13 (a-d) Half-hourly percentage transformer loading of the LV network, 2020-2050	122-123
Fig. 4.14 Voltage profiles at the farthest end of feeders in TDWtrWd, 2050	125
Fig. 4.15 Percentage ampacity loading of feeders in TDWtrWd, 2050	125
Fig. 5.1 Transformer thermal diagram	131
Fig. 5.2 Algorithm for adaptive thermal loading of transformer and optimal DRU	136
Fig. 5.3 Transformer loading and load losses	139
Fig. 5.4 (a) Transformer loading profiles on a Winter weekday.....	141
Fig. 5.4 (b) Transformer utilisation factor on a Winter weekday	141
Fig. 5.5 (a) HST curves of transformers on a Winter weekday	142
Fig. 5.5 (b) Daily cumulative LoL plots of transformers on a Winter weekday	143
Fig. 5.6 Daily return on utilisation of transformer on a Winter weekday	144
Fig. 5.7 (a) Transformer loading profiles on a Summer weekday	145

Fig. 5.7 (b) Transformer utilisation factor on a Summer weekday	146
Fig. 5.8 (a) HST curves of transformers on a Summer weekday	146
Fig. 5.8 (b) Daily cumulative LoL plots of transformers on a Summer weekday ...	147
Fig. 5.9 Daily return on utilisation of transformers on a Summer weekday	148
Fig. 6.1 Daily trip patterns of commuters (National Travel Survey)	154
Fig. 6.2 The architecture of the load management	155
Fig. 6.3 The algorithm of the load management	159
Fig. 6.4 Half-hourly Non-EV and EV load demand on a Winter weekday, 2050 ...	160
Fig. 6.5 Half-hourly Non-EV and EV load demand on a Summer weekday, 2050...	161
Fig. 6.6 Half-hourly contribution of Non-EV and EV load components to transformer load after applying load management technique.....	163
Fig. B.1 One-line diagram of the LV network	205


DECLARATION

This work has not been submitted in substance for any other degree or award at this or any other university or place of learning, nor is being submitted concurrently in candidature for any degree or other award.

Signed.....  Date..... 03-01-2019


STATEMENT 1

This thesis is being submitted in partial fulfilment of the requirements for the degree of PhD

Signed.....  Date..... 03-01-2019

STATEMENT 2

This thesis is the result of my own independent work/investigation, except where otherwise stated. Other sources are acknowledged by explicit references. The views expressed are my own.

Signed.....  Date..... 03-01-2019


STATEMENT 3

I hereby give consent for my thesis, if accepted, to be available for photocopying and for inter-library loan, and for the title and summary to be made available to outside organisations.

Signed.....  Date..... 03-01-2019

STATEMENT 4: PREVIOUSLY APPROVED BAR ON ACCESS

I hereby give consent for my thesis, if accepted, to be available for photocopying and for inter-library loans **after expiry of a bar on access previously approved by the Academic Standards & Quality Committee.**

Signed.....  Date..... 03-01-2019

ABSTRACT

The uptake of electric vehicles (EVs) and heat pumps (HPs) have been identified as means of cutting down on emissions in the transport and domestic sectors. Increasing uptake of EVs and HPs must be managed to avoid unintended consequences on the power system and the environment. This thesis describes an investigation of the management of the load demand of EVs and HPs such that they would help achieve the CO₂ emission reduction targets in the most economic manner.

Policies encouraging uptake of EVs and HPs must be guided by facts. Therefore, an algorithm for estimating reduction of emissions due to EVs replacing internal combustion engine (ICE) cars was developed and tested on data from the United Kingdom (UK). Results showed that a point could be reached when further uptake of EVs might be counterproductive if the declining average gram of CO₂ emitted per kilometre driven of ICE cars was not matched by the increasing use of low-carbon sources for the generation of electricity.

As the uptake of EVs increases, the impacts of their charging requirements and charging patterns on the generating infrastructure in terms of capacity, scheduling of resources, grid emission intensity and emission abatement cost must be understood. To this effect, a dispatch model based on correlation between system load demand and capacity factors of generating units was developed and tested on data from the UK power system with 50% uptake of EVs under two charging patterns.

The low voltage (LV) distribution networks are the hosts of EVs and HPs, therefore, their impacts on the LV distribution networks was investigated through a powerflow simulation study of a typical urban LV distribution network in the UK hosting future uptake number of EVs and HPs up to 2050 using GridLAB-D. The operating model of domestic variable speed Air-Source HP for the provision of both hot water and space heating was developed and used in the powerflow study. Results showed that overloading of transformers was likely to be the first restricting factor to further uptake of EVs and HPs.

Hence, distribution transformers, being the most expensive components of the LV distribution network need to be optimally utilised to cost-effectively support high

uptake of EVs and HPs. In this regard, an adaptive thermal loading method of distribution transformers was developed. The adaptive thermal loading method was combined with a proposed load management technique in an optimisation objective function. This was tested on a typical urban LV distribution network in the UK characterised by significant uptake of EVs and HPs when carrying the future load demand of the area up to 2050. Results proved that the transformer of a typical LV distribution network area could support high uptake of EVs and HPs beyond 2050.

DEDICATION

To GOD alone be all the glory

“Be merciful unto me, O God, be merciful unto me: for my soul trusteth in thee: yea, in the shadow of thy wings will I make my refuge, until these calamities be overpast.

I will cry unto God most high; unto God that performeth all things for me.

He shall send from heaven, and save me from the reproach of him that would swallow up. God shall send forth His mercy and His truth”

ACKNOWLEDGEMENTS

I gratefully acknowledge the Almighty God for His mercies, blessings and grace upon me to complete the Ph.D. ‘journey’ successfully.

My immense gratitude to my supervisor Dr. Liana M. Cipcigan for her constant motivation, support and advice that all combined to spurring me to accomplish this feat. Ma, supervisors like you are very rare – you are one in a million. My appreciation goes to my second supervisor Prof. N. Jenkins for his patience and always wise suggestions and pieces of advice.

To Babis and Kriton, the two wise Greeks, I am always thankful for your contributions and collaborations. Also, I want to appreciate the comraderies of the following people: Emmanuel Fasina, Hector Jose, Sambu Sakiliba, Sonia Cobo, Kess, Nur, Noraidah, Daniel Adewuyi, Bamise Ogunbunmi and other members of the Smart Grids and Electric Vehicles group.

To Naphiri V. Chona, words alone cannot express my gratitude for all the roles you played and how you blessed my life. My prayer for you, your children and your entire lineage is that God Himself will always take care of you and satisfy you with all good things here and thereafter.

I appreciate and acknowledge TETFund Nigeria for the sponsorship and MAPOLY for the support given.

To my spiritual father, Pst. S.O. Opalanwo, God bless you and your household more abundantly. I appreciate Pst. S.O. Sobowale as well. God bless you and your family.

Most importantly, I appreciate in no small measure the great sacrifice, love, prayers and patience of my family, especially of my wife and children and the extended family in general. Tunrayo, Timilehin, Ayanfe, Ire and Anu my prayer for you all is that God will always be merciful and gracious unto you.

Thank you all.

LIST OF PUBLICATIONS

The following papers were published based on work done for this thesis, or work done within the framework of the doctorate degree, or collaboration with other researchers:

CONFERENCE PAPERS

1. R. O. Oliyide, C. Marmaras, E. T. Fasina, and L. M. Cipcigan, “Low carbon technologies integration in smart low voltage network,” In *Proceedings - 2017 IEEE 15th International Conference on Industrial Informatics, INDIN 2017* (pp. 462–467). Institute of Electrical and Electronics Engineers Inc. <https://doi.org/10.1109/INDIN.2017.8104816>
2. E. T. Fasina, R. O. Oliyide, and L. M. Cipcigan, “Localised energy systems in Nigerian power network,” In *Proceedings - 2017 IEEE 15th International Conference on Industrial Informatics, INDIN 2017* (pp. 456–461). Institute of Electrical and Electronics Engineers Inc. <https://doi.org/10.1109/INDIN.2017.8104815>
3. R. O. Oliyide, C. Marmaras, E. Xydias, and L. M. Cipcigan, “Estimating the true GHG emissions reduction due to electric vehicles integration,” In *Proceedings of the Universities Power Engineering Conference* (Vol. 2015-November). IEEE Computer Society. <https://doi.org/10.1109/UPEC.2015.7339804>

SUBMITTED JOURNAL PAPERS

4. R. O. Oliyide and L. M. Cipcigan, “Adaptive thermal modelling for transformer in a low carbon electricity distribution network,” Elsevier, *Electric Power Systems Research*. (Submitted on 10-02-2019)
5. R. O. Oliyide and L. M. Cipcigan, “Management of charging load of electric vehicles for optimal capacity utilisation of distribution transformers,” Elsevier, *International Journal of Electrical Power & Energy Systems*. (Submitted on 16-02-2019)

PROJECT PARTICIPATION

EU FP7 - 619682 Project: **Multi-Agent Systems and Secured coupling of Telecom and Energy gRIDs for Next Generation smart grid services (MAS²TERING)**

- Deliverable 6.1: Detailed Use Cases Scenarios

LIST OF ABBREVIATIONS

AC	Alternating Current
AER	Apparent Emissions Reduction
AL	Adaptive Loading
ASHP	Air Source Heat Pump
ATL	Adaptive Thermal Loading
BEV	Battery Electric Vehicle
BMW	Bavarian Motor Works
CAGR	Compound Annual Growth Rate
CCGT	Combined Cycle Gas Turbine
CCR	Controlled Charging Regime
CE	Combined Heat and Power
CHP	Capacity Enhancement
COP	Coefficient Of Performance
CO ₂	Carbon IV Oxide
DG	Distributed Generation
DHW	Domestic Hot Water
DL	Dumb Loading
DNO	Distribution Network Operator
DRU	Daily Return on Utilisation
DSR	Demand Side Response
DTM	Distribution Transformer Monitor
ESS	Energy Storage System
EV	Electric Vehicle
EVSCC	Electric Vehicle Smart Charge Controller
EVLC	Electric Vehicle Load Controller
EU	European Union
GB	Great Britain
GHGs	Greenhouse Gases
GSHP	Ground Source Heat Pump
G2V	Grid to Vehicle

HEV	Hybrid Electric Vehicle
HGV	Heavy Goods Vehicle
HP	Heat Pump
HST	Hot Spot Temperature
IBM	International Business Machines
ICE	Internal Combustion Engine
IEC	International Electrotechnical Commission
IEEE	Institute of Electrical and Electronic Engineers
IPCC	Inter-governmental Panel on Climate Change
ISO	Independent System Operator
LCA	Life Cycle Assessment
LCTs	Low Carbon Technologies
LGV	Light Goods Vehicle
LoL	Loss of Life
LV	Low Voltage
NI	Northern Ireland
OCGT	Open Cycle Gas Turbine
Ofgem	Office of Gas and Electricity Markets
ONAN	Oil Natural Air Natural
PHEV	Plug-in Hybrid Electric Vehicle
PSO	Power System Operator
PV	Photovoltaic
RER	Real Emissions Reduction
RES	Renewable Energy Source
RHI	Renewable Heat Incentive
SH	Space Heating
SHGC	Solar Heat Gain Coefficient
SoC	State of Charge
SmrWd	Summer Weekday
SS	Steady State
TD	Two Degrees
TOUC	Time Of Use Charging
UCR	Uncontrolled Charging Regime

UK	United Kingdom
US	United States
U-value	Thermal transmittance value
V2G	Vehicle to Grid
WTOUC	Without Time Of Use Charging
WtrWd	Winter Weekday

CHAPTER 1

INTRODUCTION

1.1 EMERGING ELECTRICITY SYSTEM

The electricity system is changing from large, centralised, fossil-fuel based electricity generation and power that is transported unidirectionally over the transmission and distribution networks to end consumers with non-smart meters, who are heavily dependent on fossil fuel for heating and transportation.

The emerging electricity system consists increasingly of de-centralised, low-carbon and renewable based electricity generation, and power that is transported over bi-directional transmission and distribution networks to end consumers with smart meters, whose heating and transportation are now mostly electrified.

Fig. 1.1 is the diagram of emerging electricity system. Distribution networks now include distributed generation and energy storage systems with control capabilities, thereby becoming active distribution networks. The distribution networks have to cope with the increasing demand from the electrification of heating and transportation. To enable high integration of HPs and EVs in the distribution networks, active management methods and techniques are required.

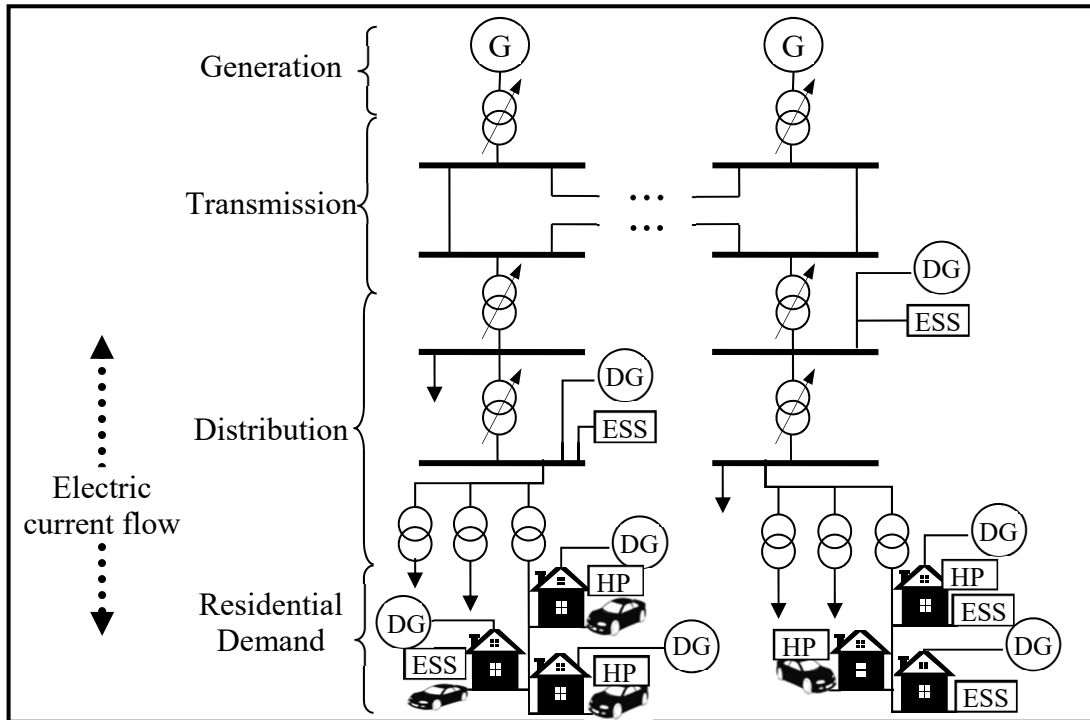


Fig. 1.1 Emerging electricity system

1.2 DRIVING FACTORS FOR THE EMERGING ELECTRICITY SYSTEM

How electricity is generated and used must change for the sake of environmental sustainability. Electricity generation and heat production, constitute a quarter of global GHG emissions [1]. Fig. 1.2 shows the statistics of the contribution to global GHG emissions by different sectors.

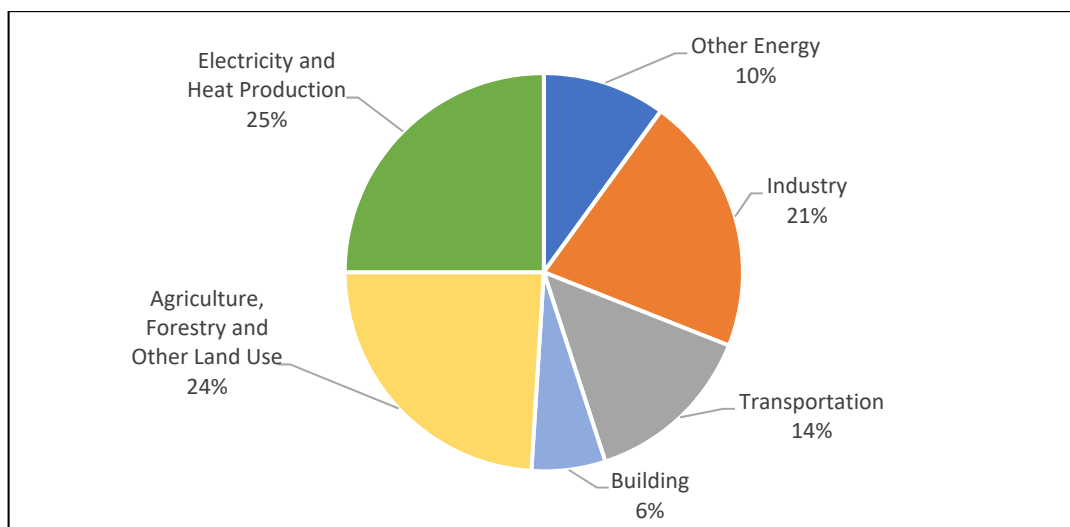


Fig.1.2 Global GHG emissions by sectors [1]

Global warming and its destructive climate change impacts are direct consequence of GHG emissions. Not doing enough to reduce GHG emissions in all the economic sectors holds potential danger for modern civilisation [2]. A report by the Intergovernmental Panel on Climate Change (IPCC) of the United Nations concluded that global warming must be limited to 1.5°C above the pre-industrial levels by 2100 to reduce catastrophic climate change impacts [3].

Fig. 1.3 shows the historic and projected global GHG emissions in GtCO₂e on the primary y-axis and corresponding global warming temperatures in °C on the secondary y-axis under five scenarios from 2000 to 2100.

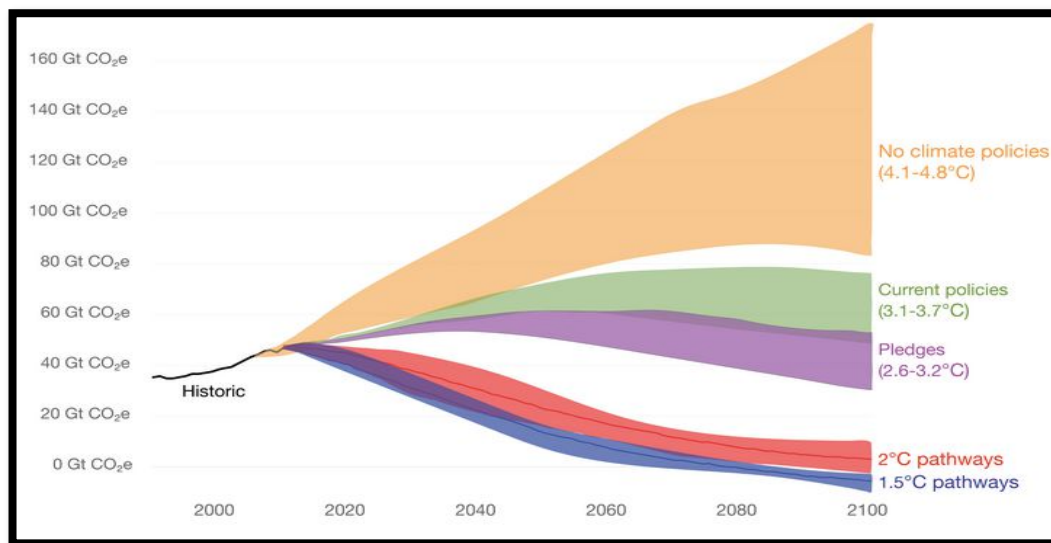


Fig. 1.3 Historic and projected GHG emissions and warming temperatures [4]

It is seen that with current policies and pledges of different governments, average global warming temperature would respectively be 3.4°C and 2.9°C by the year 2100. To meet the target of limiting warming temperature to 1.5°C above the pre-industrial levels by 2100, radical paradigm shifts towards low-carbon must take place in all the sectors. The quota of low-carbon and renewable sources must significantly increase in the electricity generation mix. Means of meeting heating demand must be efficiently and economically decarbonised. Also, the transportation sector, especially road transport, must be decarbonised.

To bring the UK into perspective, Fig. 1.4 shows the UK's GHG emissions by sector in 2016.

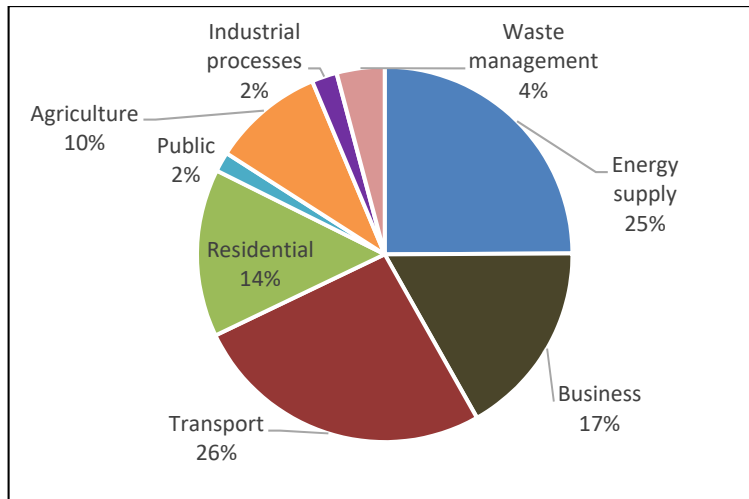


Fig. 1.4 GHG emissions by sector, UK, 2016 [5]

As seen in Fig. 1.4, the transport and power sectors were the two largest producers of GHG emissions in the UK in 2016, constituting more than 50%. The residential sector contributed 14% of the total GHG emissions. In the residential sector, GHG emissions are dominated by natural gas combustion for space heating [5].

In an effort to reduce GHG emissions, the UK Government enacted a legally binding parliamentary act called the ‘Climate Change Act 2008’ to reduce UK’s GHG emissions by 80% relative to the 1990 level by 2050 [6]. In order to meet this target, Government introduced different schemes to promote low-carbon and renewable electricity generation and usage. The UK Government also initiated an incentive scheme to encourage the uptake of EVs to replace ICE cars for road transport. Amongst the schemes introduced are:

- **Climate Change Levy (CCL):** CCL was introduced in 2001 under the Finance Act 2000 [7]. It is a tax on energy supplied from non-renewable sources to non-domestic users. It aims to promote electricity generation from renewable sources.
- **Renewable Obligation:** In this scheme, a mandatory obligation is placed on the UK’s electricity suppliers to source a particular proportion of their electricity from renewable sources [8].
- **Feed-in Tariffs (FITs):** FITs aim to promote rapid and widespread deployment of a range of small-scale renewable and low-carbon distributed

generation (DG) of electricity. In the scheme, licensed electricity suppliers are required to pay a generation tariff to these small-scale generators for the electricity generated, whether or not it is exported to the electricity grid [9]. Eligible technologies for this scheme include solar photovoltaic (PV), wind, hydro, and anaerobic digestion up to a maximum installed capacity of 5 MW, and micro combined heat and power (CHP) up to 2 kW [9].

- **Renewable Heat Incentive (RHI):** This scheme is applicable to both residential and non-residential buildings under domestic RHI and non-domestic RHI. It is a Government financial incentive to encourage landlords and building owners to switch from conventional fossil fuel heating to renewable heating [10]. Eligible technologies include biomass, air-source heat pump, ground-source heat pump and solar thermal for both domestic and non-domestic RHI, and geothermal, biogas and CHP (generating from solid biomass, solid biomass contained in waste, biogas and geothermal) for non-domestic RHI [10].
- **Plug-in Car Grant (PICG):** PICG is a UK Government financial incentive in the form of purchase subsidy for ultra-low emission vehicles. This aims to encourage the uptake of EVs. Vehicles eligible for PICG, must amongst other things, have a zero emission range of at least 70 miles and must emit less than 50g of CO₂ per kilometre driven [11].

1.3 ELECTRIC VEHICLES

Electric vehicles according to [12] are automobiles that use electric motors for their traction, and chemical batteries, fuel cells, ultracapacitors, and/or flywheels for their energy sources. This broad definition embraces different types of EVs. However, the three main types of EVs are:

- i) **Battery Electric Vehicles (BEVs):** Also known as Pure Electric Vehicles (PEVs). These vehicles use only battery to power the electric motor for their traction. They have no internal combustion engine. Their battery is charged entirely by electricity from the grid. They produce no tail-pipe emissions.

With improvement in the lithium ion batteries, BEVs are now capable of making longer range per charge than in the past. Some common examples of BEVs are: Nissan Leaf 2015 and Tesla Model S [13].

- ii) **Plug-in Hybrid Electric Vehicles (PHEVs):** PHEVs have both internal combustion engine and electric motor powered by rechargeable battery for traction generation. The battery can either be charged on-board by the internal combustion engine or directly from the grid. The internal combustion engine and the electric motor complementarily run the vehicle together in a fuel-saving manner. When the all-electric range reaches its limit, the internal combustion engine takes over and provides the necessary power. Examples of PHEVs include Toyota Prius 1.8 2015 and Chevrolet 2015 [13].

- iii) **Hybrid Electric Vehicles (HEVs):** HEVs incorporate both an internal combustion engine and electric motor for their traction. But for these types of EVs the battery for powering the electric motor is solely charged on-board by the internal combustion engine. They are not connected to the grid for charging of battery. Sub-categories of HEVs are series full-HEV, parallel full-HEV, series-parallel full-HEV and complex full-HEV [14]. Examples of HEVs include BMW Active Hybrid3 2015, Ford Fusion Hybrid FWD 2016 and Honda Civic Hybrid 2015 [13].

Other types of EVs are **Fuel Cell Electric Vehicles (FCEVs)** and **Fuel Cell Hybrid Electric Vehicle (FCHEVs)** [14]. FCEVs use only electric motor for traction like the BEVs. However, the energy source of the electric motor used in FCEVs for traction is either direct hydrogen which is stored in a tank mounted in the vehicle, or hydrogen extracted from fuel using a fuel processor [14]. FCEVs emit only water and heat from their exhaust pipes. **FCHEVs** incorporate battery or ultra-capacitor as auxiliary energy source for supporting the hydrogen of the fuel cell to power their electric motor for traction [14].

In this thesis only EVs whose batteries are connected to the grid for charging are considered, i.e. BEVs and PHEVs. If not otherwise mentioned, the term EV in this thesis will refer to these two types of electric vehicles.

1.4 HEAT PUMPS

In simple terms, a heat pump (HP) is a device that transfers heat from one location to another. Usually, the heat is taken from a low temperature source and worked upon before transferring it to another location at a higher temperature. In order to transport heat from a heat source to a heat sink, external energy (usually electricity or fuel) is needed to drive the heat pump. Theoretically, the total heat delivered by the heat pump is equal to the heat extracted from the heat source, plus the amount of drive energy supplied. Carnot and Kelvin were instrumental to developing the concept of HP, but the first patent of the device was issued to TGN Haldane in 1927 [15].

1.4.1 Principle of Operation of HPs

The two main principles upon which the operation of HPs is based according to [16] are:

- i) Vapour compression cycle and
- ii) Absorption cycle

Detailed attention would be given to vapour compression cycle because it is the principle upon which commercially available domestic HPs are operating [17]–[19].

1.4.1.1 Vapour Compression Cycle

The main components of HPs based on this principle are compressor, expansion valve, evaporator and condenser. Fig. 1.5 shows the arrangement of the components.

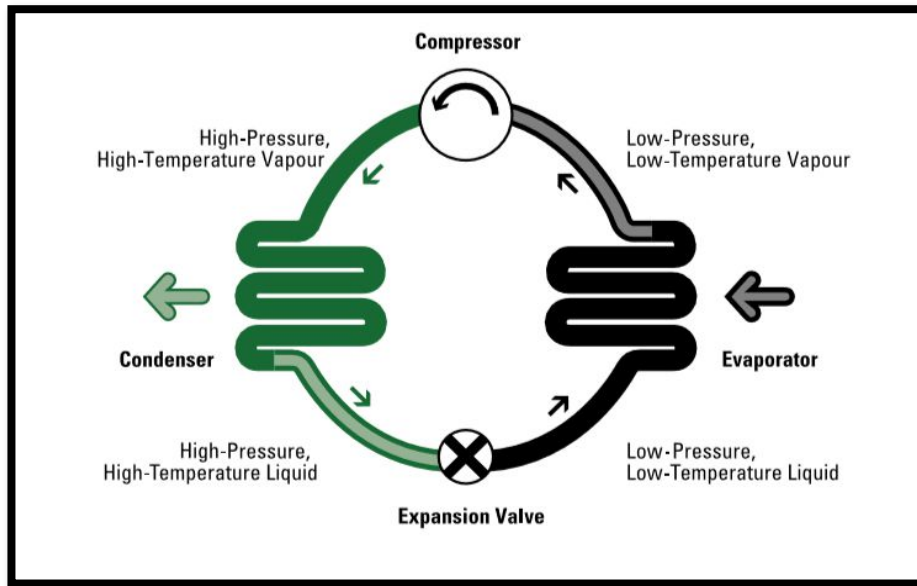


Fig. 1.5 Vapour Compression Cycle of HP [20]

The working fluid, also called the refrigerant, circulates through four components. The working fluid, which is a volatile liquid, is usually of lower temperature than the heat source while inside the evaporator. It thus turns into vapour inside the **evaporator** at low pressure and temperature due to the heat received from the heat source. Vapour from the evaporator is then compressed to a higher pressure and temperature inside the **compressor**. The hot vapour then enters the **condenser**, where it condenses and ejects the useful heat. Finally, the high-pressure working fluid is expanded to the evaporator pressure and temperature in the **expansion valve**. The working fluid is returned to its original state and once again enters the evaporator. The compressor is usually driven by an electric motor or sometimes by a combustion engine. HPs with electric motor driven compressors are considered in this thesis.

The efficiency of an electric compression HP, which is also called coefficient of performance (COP), is defined as the ratio of the heat delivered by the HP and the electricity supplied to the compression [16]. The COP of an ideal HP is inversely related to the difference between the temperature of the heat sink and the heat source. That is the difference between the condensation temperature and the evaporation temperature. The theoretical maximum COP achievable by an ideal HP can be derived from the reversed Carnot cycle's temperature-entropy diagram of Fig. 1.6, in which the thermodynamic state at a point on the diagram is specified by entropy 'S' on the horizontal axis and temperature 'T' on the vertical axis.

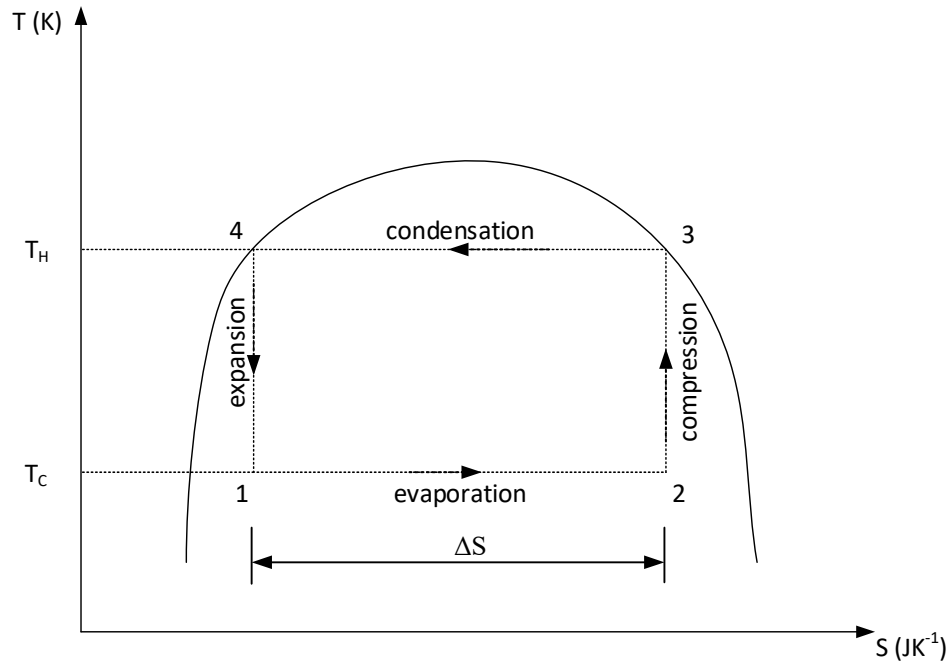


Fig. 1.6 Reversed Carnot cycle [18]

The theoretical maximum COP can be expressed as in equation (1.1) below.

$$COP_{th} = \frac{\text{useful heat ejected on condensation}}{\text{compression energy} - \text{expansion energy}} \quad (1.1)$$

The terms in equation (1.1) can be expressed in terms of temperature and entropy as in equation (1.2).

$$COP_{th} = \frac{T_H \times \Delta S}{(T_H - T_C) \times \Delta S} = \frac{T_H}{(T_H - T_C)} \quad (1.2)$$

Where:

COP_{th} is the theoretical maximum COP,

T_H is the heat sink temperature /condensation temperature (K),

T_C is the heat source temperature (K),

ΔS is the change in entropy (J/K).

While an ideal HP might not exist in reality because of some heat loss to the surroundings, but the COP of a practical HP is always greater than unity and maintains a strong dependence on the difference between the heat sink temperature and heat source temperature.

This underscores the importance of deploying an adequate heat source with reasonable temperature level and moderating the heat sink temperature if possible. Presently, modern heat pumps operate at a COP in the range of 4-5 at a heat source temperature of 0°C and 35°C heat sink temperature [21]. This means that 1-kWh of electricity could be transformed to 4-5 kWh of heating. In comparison modern condensing boilers exhibit efficiencies of more than 90% and under some favourable conditions (low temperature, wet system systems) their efficiencies increase close to 100% [22]. Thus, the HP has better efficiency (always greater 100%) than the condensing boiler and coupled with the fact that a HP produces no direct emissions in its operation makes it the technology of choice in space heating and domestic hot water provision in the quest of cutting down on GHG emissions.

1.4.1.2 Absorption Cycle

Absorption heat pumps are thermally driven, which means that heat rather than mechanical energy is supplied to drive the cycle. Absorption systems utilise the ability of liquids or salts to absorb the vapour of the working fluid [16]. The COP of an absorption heat pump is much less than what can be achieved by an electric compression heat pump, typical COPs range in between 1.4-1.7 [19].

1.4.2 Types of HPs

The naming and therefore, the classification of HPs is based on the following criteria:

- i) principle of operation
- ii) source of heat energy
- iii) medium of heat transfer
- iv) type of compressor

1.4.2.1 Types of HPs based on principle of operation

Many thermodynamic principles exist that could be used for a HP operation. Almost all HPs currently in operation are either based on a **vapour compression cycle**, or on an **absorption cycle** (see Section 1.3.1). Other principles of operation include **Stirling**

and Vuilleumier cycles, solid-vapour sorption systems, hybrid systems (notably combining the vapour compression and absorption cycle) and thermoelectric and acoustic processes [16].

1.4.2.2 Types of HPs based on the source of heat

Based on the source of heat, the following types of HPs are available:

- i) **Air-Source HPs:** These types of HPs use either ambient air or exhaust air from mechanical ventilation systems of buildings. Thus, we have ambient air HPs and exhaust air HPs.
 - HPs using ambient air as heat source are the most common HPs [19] because ambient air is free and unlimitedly available. The major drawback of ambient air HPs is that their performances attenuate with decreasing outdoor temperature. At ambient temperature range between -15°C and -20°C , ambient air HP might stop operating due to large temperature difference between the heat source and the heat sink [19]. In mild and humid climates, frost might accumulate on the evaporator surface especially at temperatures around $+7^{\circ}\text{C}$ and below [16]. Thereby increasing the thermal resistance of the evaporator and requiring it to be defrosted. Defrosting is achieved by reversing the heat pump cycle or by other, less energy-efficient means. Energy consumption increases and the overall COP of ambient air HPs are thus affected during defrosting.
 - Exhaust air HPs suffer no drawback of large temperature difference between the heat source and the heat sink, as the temperature of the exhaust air is in the range of $+20^{\circ}\text{C}$. The drawback of exhaust air HPs is the limited availability of the airflow through the ventilation system of the building.
- ii) **Ground-Source HPs:** These are the types of HPs which make use of heat from the ground (soil). The ground serves as seasonal storage of solar energy. During winter the ground serves as heat source for heating and

during summer could serve as heat sink for cooling if the HP cycle is reversed [23].

- iii) **Water- Source HPs:** These are the types of HPs that use heat energy from sources like aquifers, rivers, lakes or the sea, wastewater, cooling water from industrial systems, or a district heating system [17].
- iv) **Hybrid-Source HPs:** These are the types of HPs which make use of more than one sources of heat [17]. Usually two sources of heat are combined to compliment each other. Examples include ambient air and exhaust air HPs, heat pump and biomass boiler, heat pump and thermal collector, heat pump and electric heater, etc.

1.4.2.3 Types of HPs based on medium of heat distribution

Based on the medium of heat distribution, there are two main types of HPs.

- i) **Hydronic HPs:** These are HPs in which the medium of heat distribution is water. The heat generated by the HPs is transferred to radiators or underfloor panel heating that then heat up the room via radiation and convection [17].
- ii) **Air-based HPs:** These are the types of HPs in which the heat is distributed via ducts, distributing air through a series of grilles or diffusers to the room [16].

1.4.2.4 Types of HPs based on the speed of compressor

Based on the speed of compressor, there are three types of HPs.

- i) **Single-speed HPs:** These are HPs whose compressors have constant speed of operation. In heating mode, they turn ON at 100% output capacity when the indoor temperature drops below the minimum set point, operating until they reach the maximum set point, and turn OFF completely [24].

- ii) **Two-speed HPs:** These are HPs whose compressors are capable of two levels of operational speed. A low-capacity speed to meet smaller demand and a high-capacity speed to meet heavy demand. In comparison to single-speed HPs, the power needed to meet the smaller demand would be reduced [25].

- iii) **Variable-speed HPs:** These are HPs whose compressors are capable of modulating their operational speeds to adjust capacity in effort to run at the best speed to meet the demand [24], [26].

1.4.2.5 Choice of HP for installation

The three main factors for consideration in the installation of HPs are technical, economic and logistic factors. Technically, a good choice of HP for installation is that whose heat source is abundantly available with moderate level of temperature, especially during the heating season. In terms of economics, a good choice of HP is that with moderate investment, installation and operational costs. Logistic factors include nearness of the heat source to the point of installation, obtaining installation permit from the authorities and ease of retrofitting into existing building.

In thesis, the full description of the type of HP considered based on technical, economic and logistic factors is the **Air-to-Water, Variable-speed, electric-compression HP**.

1.5 UPTAKE RATE OF EVS AND HPs IN THE UK

Fig. 1.7 is the statistical bar chart of the number of plug-in eligible cars registered for the first time in the UK between 2010 and 2017.

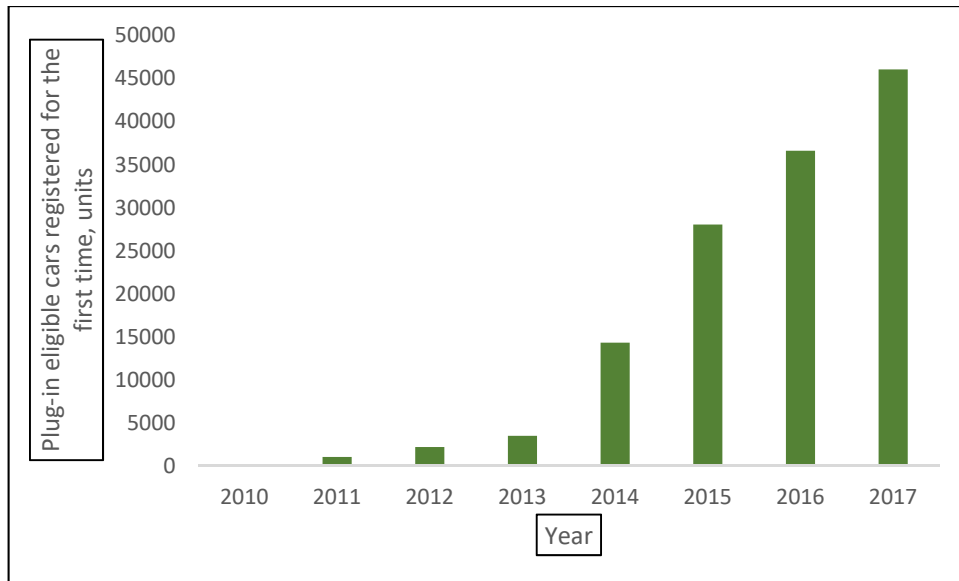


Fig. 1.7 Plug-in eligible cars registered for the first time in the UK, 2010-2017 [27]

There was an almost 100% increase in the plug-in eligible cars registered for the first time between 2014 and 2015. Between 2015 and 2017 the annual uptake rate had been more than 25% reaching 46,058 plug-in eligible cars in 2017 that registered for the first time.

Fig. 1.8 shows the statistics of the total number of different types of renewable heating systems approved under the Domestic RHI scheme between May 2015 and June 2018.

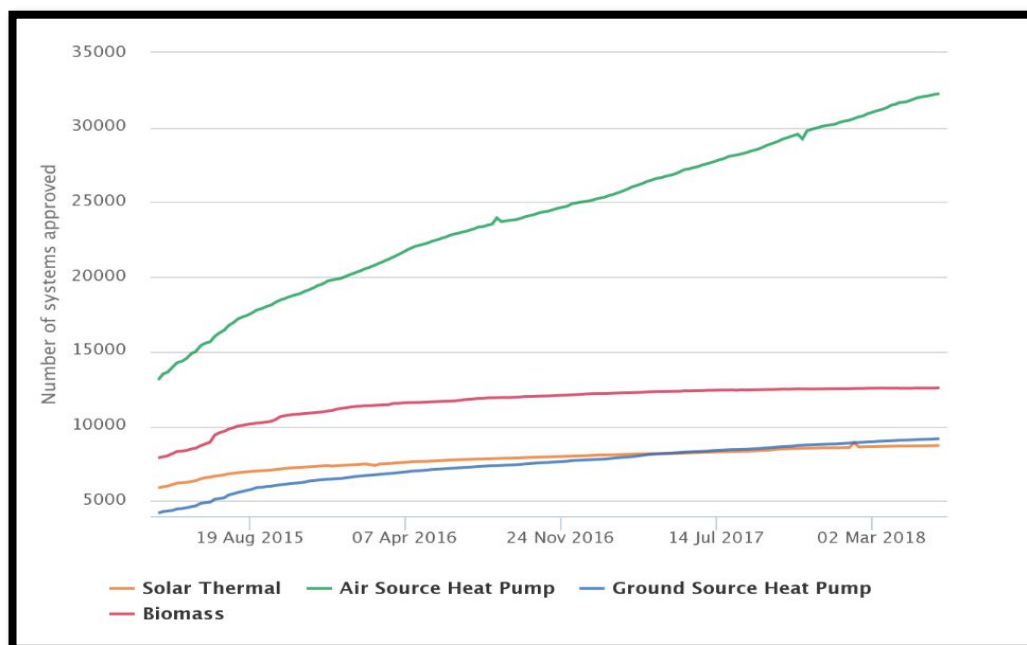


Fig. 1.8 Total number of Domestic RHI approved per heating system [28]

The uptake of ASHP under the Domestic RHI scheme increased by about 150% between 2015 and 2018, reaching a total of 32,268 by June 2018.

1.6 THESIS OBJECTIVES

The key question that this thesis aims at addressing is - how can the new and additional electric load demand of EVs and HPs on the Electricity System be managed to help achieve the CO₂ emissions reduction targets in the most economic manner?

To this end, the following objectives were set:

Objective 1

Review of the environmental and technical impacts of EVs and HPs on the traditional grid and the state-of-the-art smart grid approaches to minimise the impacts.

Methodology:

1. To provide a detailed review of the topics on environmental and technical impacts on the grid of EVs and HPs.
2. To review the current findings in the field of smart grids and ongoing research activities in the load management of EVs and HPs at the LV distribution network.

Objective 2

Estimate the ‘real’ emission reduction on the road due to EVs replacing ICE cars.

Methodology:

1. To develop an algorithm for estimating the ‘actual’ emission reduction on the road due to uptake of EVs. The algorithm will compare the ‘apparent’ emission reduction on the road with the marginal increase of emissions at the grid to arrive at ‘real’ emission reduction.
2. To source for relevant data and apply the algorithm.

Objective 3

Investigate the impacts of charging requirements of EVs and charging patterns of EVs on the existing generating infrastructure of the power system in terms of capacity, scheduling of generating resources, grid emission intensity and emission abatement cost.

Methodology:

1. To develop a dispatch model for generating resources.
2. To obtain data from the UK power system and test the developed dispatch model.

Objective 4

Investigate the impacts of EVs and HPs on the LV distribution network.

Methodology:

1. Scale down the national projection figures of future uptake of EVs and HPs to the level of a typical and real LV distribution network to be used as case study.
2. To develop an algorithm for the operational model of variable speed ASHP in order to obtain its operating profile in providing space heating and hot water in residential buildings.
3. To perform powerflow simulation of the case study LV network with future uptake of EVs and HPs up to the year 2050 integrated in the LV network. This is to find out the impacts of EVs and HPs on the LV network in terms of transformer loading, cable loading and violation of voltage drop limit.

Objective 5

Investigate how the loadability and utilisation of distribution transformers, serving LV distribution networks characterised by significant uptake of EVs and HPs, be optimised based on their thermal properties.

Methodology:

1. To develop a detailed thermal model of distribution transformer.
2. To develop an adaptive thermal model for loading of distribution transformers. This is to ensure high capacity utilisation of distribution transformers without compromising their normal life expectancy.
3. To test the model on the case study LV distribution network when hosting future uptake level of EVs and HPs up to the year 2050.

Objective 6

Examine the potentials of combining load management technique with adaptive thermal loading of transformers to increase the hosting capability of LV distribution networks for EVs and HPs.

Methodology:

1. To develop a de-centralised load management technique incorporating an assumed two-way wireless communication link between EV chargers and distribution transformer.
2. To develop a model that integrate both the proposed load management technique and adaptive thermal loading of distribution transformers.
3. To test the integrated model on the case study LV distribution network when hosting future uptake level of EVs and HPs up to the year 2050.

1.7 THESIS STRUCTURE

This thesis is structured in the following way:

Chapter 2: Relevant literature used in the thesis is presented. An overview is given with regard to: i) EVs and GHG emissions reduction, ii) charging patterns of EVs and power system scheduling iii) impacts of EVs and HPs load demand on LV distribution networks and iv) management of load demand of EVs and HPs in LV distribution networks.

Chapter 3: An algorithm for estimating the emissions reduction due to the uptake of EVs is presented. In addition, a dispatch model for Power System, suitable for analysing the impacts of charging patterns of EVs on power system scheduling, GHG emissions, grid emissions intensity and emissions abatement cost, is also presented. The results of the dispatch model were compared to the results from observed historical data of the UK grid.

Chapter 4: A methodology for scaling down national projected figures for the future uptake of EVs and HPs to a LV distribution network level is described. Also, an algorithm for the operational model of variable speed Air-Source HP for the provision of both domestic hot water and space heating in residential buildings is developed. The operational profile of HP from the model is comparable to that of a trial field project. Finally, GridLAB-D power system simulation software is used in a powerflow study to investigate the impacts of uptake of EVs and HPs on a typical real urban LV distribution network.

Chapter 5: An adaptive thermal model for loading of distribution transformer is developed. The model is tested on the transformer of a typical real urban LV distribution network area characterised by significant uptake of EVs and HPs when carrying the future load demand of the area up to 2050.

Chapter 6: A de-centralised load management technique for optimal capacity utilisation of LV distribution transformer is presented. As the main core of the load management technique, a wireless two-way communication between EVs and a distribution transformer of residential LV network area to manage the charging of EVs and avoid transformer overloading is described. The technique is tested on the transformer of a real and typical urban LV distribution network area.

Chapter 7: The main conclusions of the work described in the thesis are summarised. Suggestions for future work are given.

CHAPTER 2

LITERATURE REVIEW

2.1 EVS AND GHG EMISSIONS REDUCTION

Transportation accounts for about 14% of the global GHG emissions [1]. Light-duty vehicles accounts for about two-thirds of the global GHG emissions from the transportation sector [29]. It is projected that the number of light-duty vehicles is expected to double in the next three decades [30]. Already, about a quarter of the global demand for fossil fuel is for the consumption of the light-duty vehicles [31]. Thus, the projected increase in the number of the light-duty vehicles means increasing demand and consumption of the fossil fuel. This implies more GHG emissions from the transportation sector.

One solution to the heavy dependence of light-duty vehicles on fossil fuel is to change their traction engines from internal combustion types to electric types. Vehicles with electric traction engines are broadly called electric vehicles (EVs) [12]. Unlike the conventional vehicles that use fossil fuel for traction, EVs use electricity stored in rechargeable batteries for traction. Therefore, EVs produce no direct emission. For this reason, EVs are good alternatives to conventional vehicles in the quest to keeping down emissions from the transportation sector.

Governments around the world are providing purchase subsidies and tax incentives to encourage the uptake of EVs [11], [32], [33]. However, considering the life-cycle assessment (LCA) impacts of EVs and the source of electricity for charging their batteries, some researchers claimed that EVs are no better than conventional vehicles [29], [34], [35].

However, according to [36], LCA calculations require large sets of data, and therefore tend to be more complex and less transparent. In [33] further clarification is made about comparing LCA impacts of EVs and ICE vehicles. Fig. 2.1 illustrates the model for comparing the LCA impacts of EVs and ICE vehicles. In the model, LCA is further categorised into LCA for vehicle fuel and LCA for vehicle. For the ICE cars,

LCA for vehicle fuel consists of **well-to-pump**, which is the energy consumption and GHG emissions in the fuel exploration and production and **pump-to-wheel**, which is the energy consumption and GHG emissions during vehicle operation. For EVs, LCA for vehicle fuel is made up of **mine-to-meter**, which is the energy consumption and GHG emissions in production, transmission, distribution and charging and **meter-to-wheel**, which is the energy consumption and GHG emissions in vehicle operation. LCA for vehicle in both ICE cars and EVs include energy consumption and GHG emissions in the material production and transportation, the production of and assembly of vehicle parts and components, vehicle operation and vehicle scrapping.

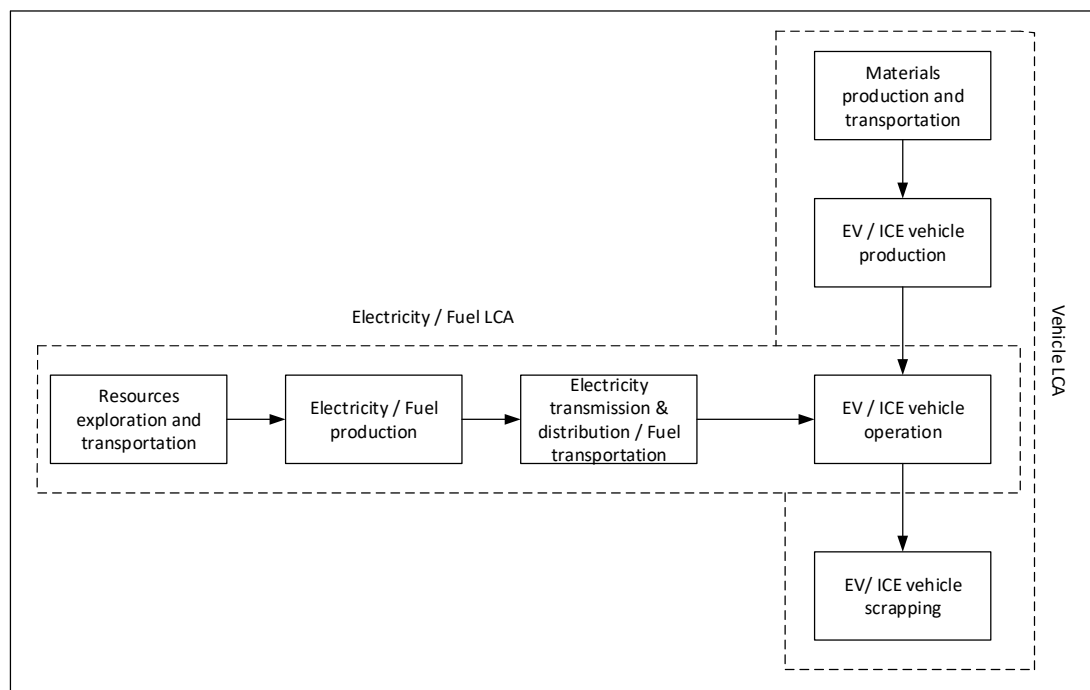


Fig. 2.1 Model for comparing LCAs of EVs and ICE vehicles [33]

In [30], a comparison of the full LCA environmental performance of a PHEV and a class-equivalent ICE car was made using electricity supply mix and observed charging behaviour. Conclusion was that PHEVs have lower full life cycle GHG emission than ICE cars but have higher acidification and human toxicity impacts. However, empty-to-full charging cycles were assumed rather than top-up charging. Also, Monte Carlo simulation was used for modelling the environmental impacts which make them probabilistic in nature.

Comparative analysis of LCA of EVs and ICE cars in the UK and California was performed in [37]. The work concluded as follows:

- i) EVs perform better than ICE cars in terms of GHG emissions in low speed urban driving and when lightly loaded with weight and auxiliaries
- ii) based on marginal grid intensity, EVs have higher life cycle GHG emissions than ICE cars and
- iii) vehicle life cycle emissions are higher for EVs due to the emissions associated with battery manufacture.

However, the authors acknowledged limited data availability in their LCA emissions analysis.

A study on how the EVs life-cycle emissions vary when compared to the ICE vehicles based on electricity generation and efficiency during use-phase under various standard driving conditions in five EV most selling European countries was described in [38]. Fig. 2.2 shows the results of comparison to determine in which countries there are immediate emissions reduction by switching to EVs from ICE vehicles.

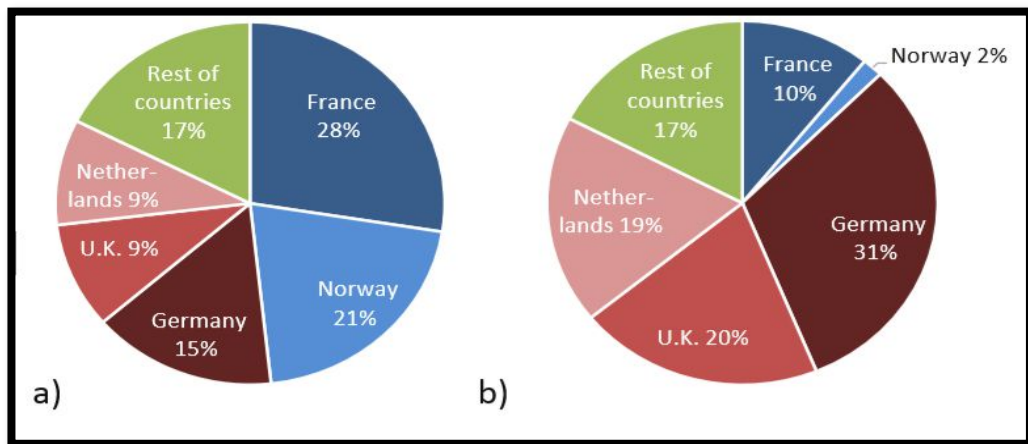


Fig. 2.2 Comparison of countries: a) Share of EV sales in EU and b) Share of EV emissions in EU [38]

Norway and France performed well, together accounting for 49% of EV market share and contributing only 12% of emissions from EVs. UK controls 9% of EV market share and is responsible for 20% of emissions from EVs.

2.2 IMPACTS OF CHARGING REQUIREMENTS AND CHARGING PATTERNS OF EVs ON POWER SYSTEM SCHEDULING, GHG EMISSIONS AND EMISSIONS ABATEMENT COST

EVs represent a new kind of load with new opportunities and challenges in the electricity system [39]–[41]. EVs, from the power system viewpoint, can be seen as controllable loads, energy storage system and uncontrollable loads [42].

2.2.1 EVs As Controllable Loads

EV is considered to be a controllable load if its charging process can be interrupted and/or its charging rate can be varied. As a controllable load, the flow of power between the grid and the EV battery is unidirectional [43]. The EV only receives power from the grid. The unidirectional flow of power from grid to EV is denoted here as G2V. With proper implementation, aggregation of EVs as controllable loads can support the grid by providing such ancillary services as frequency regulation and spinning reserve [44].

Frequency regulation is the service provided to ensure constant match between the generation and the load in order to avoid frequency deviation. The response must be within a few seconds to the change in grid frequency [45]. Traditionally, the grid operator performs real-time control regulation in response to load demand by increasing or decreasing generation. Spinning reserve is an additional generation that provides fast response, usually within 10 minutes to compensate for sudden loss of generation [45]. Providing for spinning reserve increases the daily operation cost because additional generators are committed on and other cheaper generators are made to operate less than their optimal output to provide the spinning reserve [46].

In [47], a study which used Fuzzy optimisation method to coordinate charging of fleet of EVs and bid into the electricity market to provide regulation and spinning reserve was described. The ancillary service capacity that the fleet manager/aggregator can provide is based on the extent to which the actual charging rate of each EV in the fleet can be moved either above or below the scheduled charging rate. The fleet manager, therefore, optimises the charging rates of EVs in the fleet between their maximum and minimum points vis-à-vis the ancillary service capacity to be provided such that profits are maximised. With this ability, the fleet manager creates variable

load out of the fleet of EVs being charged. Depending on the signal received from the grid operator, the fleet manager either reduces the net load to provide up regulation (from the perspective of using load to achieve regulation) or increases the net load to provide down regulation.

Other related studies [48], [49] investigated the possibility of aggregation of EVs providing ancillary services to the grid. All the EVs in the fleet that participate in providing the ancillary service would be compensated based on the time duration of their participation [44]. The impact of varying the charging rate of EV batteries was not considered in all the studies reviewed.

2.2.2 EVs As Energy Storage System

When the flow of power between EV and grid is bidirectional then the EV can be considered as a storage entity, and could be managed as dispersed energy storage resource according to the system operators or market players' needs [42]. The bidirectional power flow between grid and EV is denoted here as V2G.

As dispersed energy storage resource, fleet of EVs can provide active power support to the grid [44]. With proper implementation, bidirectional operation of batteries of fleet of EVs can support grid in terms of frequency control, demand response, spinning reserves and energy shifting, smoothening the variable output from renewable electricity generation, and utilising surplus energy when supply exceeds demand [50]. Fig 2.3 illustrates the concept of peak load shaving and load levelling by EV on a hypothetical daily load curve.

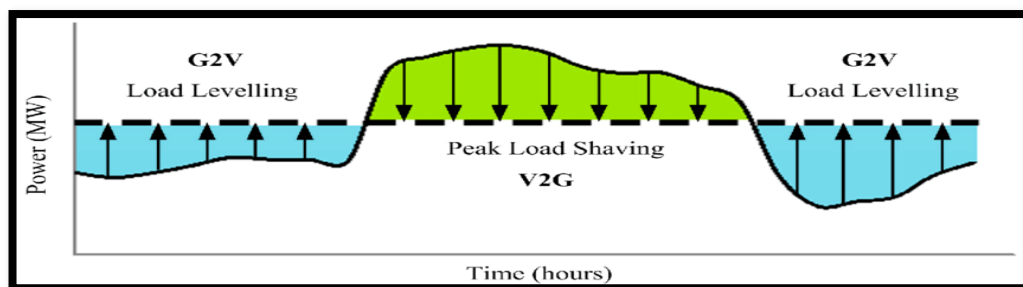


Fig.2.3 Concept of peak load shaving and load levelling by EVs [51]

There are many benefits, technical, economic and environmental, derivable from the bidirectional operation of EVs batteries. Average cost of electricity generation is reduced as EVs help to flatten the load profile of a power system [41]. Power system

is relieved of both technical and financial stress of meeting peak load demand with expensive peaker generating units. Curtailment cost of generation from renewable energy resources is reduced [44]. Reduction in grid emissions, as more low-carbon renewable energy resources are integrated into the system and the less efficient peaker generating units are infrequently used to meet the peak load demand [52].

Many studies in the literature have investigated the V2G capability of EVs in supporting the grid. In [53], load agent, generation agent and energy storage agent (consisting of fixed batteries and EV batteries as mobile storage) were modelled in an optimisation problem with the aim of flattening daily load curve in response to hourly prices. Optimal day-ahead spinning reserve requirements are quantified in an optimisation model that aims at minimising the total costs of generation, expected energy not served and expected energy served by EV in the study described in [46]. In [51], optimisation technique to flatten the grid load by using EV batteries to provide peak load shaving and load levelling was presented.

The ability of EVs as dispersed energy storage resources that support integration of wind energy is presented in [54], where how the use of parking lots for EVs can help independent system operator to reduce generation curtailment from turbines. In [55], aggregation of EVs was formed into a virtual power plant to provide active power regulation for wind integration.

Deployment of EVs as dispersed energy storage resources is contingent on many stochastic factors. Principal amongst the factors is the probability of EVs availability. Other factors are the states of charge of the batteries and the maximum depth of discharge of battery individual EV owner would be willing to allow considering unexpected travel plans.

Table 2.1 presents an evaluation of the suitability of EVs alongside other domestic loads to provide primary and secondary frequency response services, frequency control demand management (FCDM) service and fast reserve service to the grid. Response time, duration and minimum load requirements for these services are given in [56]. The primary frequency response service requires loads (at least 10MW) that can respond to the frequency event with less than 10 seconds and last to a further 20 seconds. For a secondary frequency response service, the load (at least 10MW) should respond within 30 seconds and continue to a further 30 minutes. In the FCDM service,

the domestic load (at least 3MW) should be curtailed within 2 seconds and it should last for longer than 30 minutes. Fast reserve service requires load (50MW) response within 2 minutes and it should last to an extra 15 minutes.

Table 2.1 EV and domestic load suitability to support the grid [56], [57]

Load	Primary frequency response	Secondary frequency response	FCDM	Fast reserve
EV	Partly	Partly	Partly	Partly
Space and water heating	Partly seasonal	Partly seasonal	Partly seasonal	Partly seasonal
Cold appliance	Yes	Yes	Yes	Yes
Cooking	No	No	No	No
Wet appliance	No	Partly	Partly	Yes
Consumer electronics	No	No	No	No
Home computing	No	No	No	No
Lighting	No	No	No	No

Degradation of the EV battery and its economic implications are also important factors for consideration in its bidirectional operation. An investigative experiment into the degradation impacts of bidirectional operation of commercial Li-ion cells, similar to the EV batteries, was presented in [50]. Results of the experiment showed that a V2G operation once a day accelerates both the capacity loss and resistance increase of the battery. V2G implementation could decrease the lifetime of the battery to under 5 years. On the other hand, according to the study, interrupting charging process in G2V had insignificant effect on capacity loss, resistance increase and lifetime of the battery.

2.2.3 EVs As Uncontrollable Loads

EV is considered to be an uncontrollable load when neither its charging process can be interrupted, nor the charging rate be regulated. As uncontrollable load, the flow of power between the grid and the EV battery is unidirectional from the grid to the EV battery. With typical power charger ratings of 3kW (13A) for residential Mode 2 and

3.7kW (16A) for residential Mode 3 [58], a high penetration of EVs as uncontrollable loads will increase the grid load demand during the charging process [59].

This presents both technical challenges and business opportunities in the electricity industry. Technical challenges that may arise include increased peak load demand, violation of statutory voltage limits, harmonic problems, increased grid losses and overloading of grid assets especially if the charging of EVs coincides with the peak load demand of the grid [60]. Business opportunities arising from high penetration of EVs includes increased electricity generation and a boost in economic activities for players in the electricity industry, as attention gradually shifts from the gas and oil industry [39].

To understand the worst-case scenario of the impacts of charging requirements of high penetration of EVs on the existing grid infrastructure, EVs must be considered as uncontrollable loads. The charging patterns and uptake level of EVs is likely to have significant impacts on electricity demand, affecting the technologies needed to meet the demand and grid performance [61]. The dispatch of generating technologies to meet demand is a complex task based on the balance of economics, contractual agreement, regulations and environmental consciousness. Many studies on the impacts of charging of EVs on power systems usually based the dispatch of generating technologies on optimisation techniques, aiming at least cost unit commitment [62]–[66]. In [62], a numerical optimisation model that simultaneously optimises power plant dispatch and charging of EVs on the German power system was performed. PLEXOS, a commercial optimisation software was used to investigate the impacts of charging of EVs on the Irish power system and electricity market in [63].

In [67], the dispatch of generating technologies was not based on optimisation, but on subsisting operational philosophy of the power system operators. A dispatch model for western grid of the United States was developed based on the correlation identified between the system load and the capacity factors of generating units. The model was used to dispatch generating units to meet system load demand under two charging patterns of EVs and analyses were carried out of the impacts of the charging patterns on the system scheduling and GHG emissions.

2.3 IMPACTS OF LOAD DEMAND OF EVS AND HPs ON LV DISTRIBUTION NETWORK

Policies and regulations were adopted at the United Nations to reduce the GHG emissions and the effect of the climate change [68]. The UK has a policy target of 80% reduction of GHG emissions with respect to the 1990 level by the year 2050 [69]. The realization of the target will involve a transition from fossil fuel based to low carbon-based electricity generation and usage. Decarbonisation of road transport and heat take centre stage considering that in 2016 GHG emissions from transport and domestic sectors accounted for 26% and 14% respectively of the total UK GHG emissions [5].

The main source of the GHG emissions in the transport sector is the road transport, in particular passenger cars [5]. In the domestic sector, the use of natural gas for heating is the most significant source GHG emissions in the sector [5]. About 81% of heating demand is basically met by natural gas boilers in the UK [70], [71]. Therefore, there is considerable potential for cutting down on GHG emissions with increasing share of renewable energy sources in the electricity generation, increasing uptake of HPs for residential heating and EVs for road transportation.

Studies have been carried out on the benefit of electrifying the domestic heating demand. Possible energy and GHG emissions savings achievable by using HPs for residential heating in Italy was estimated in [72]. Results highlight that if a fourth of the existing residential buildings are heated by means of ASHPs, a saving of about 20% of natural gas can be achieved in 2024, with a corresponding reduction of about 1.7Mt of GHG emissions [72]. Different technologies for satisfying heat demand in residential buildings were compared in [73] in terms of primary energy consumption. Results showed that electric resistance is practically less favourable than HPs, and the primary energy savings provided by HPs compared to natural gas boilers is about 30% on average [73].

According to [74], replacing 80% of current gas-fired boilers with HPs would enable the UK to meet its target of 80% emissions reduction in the domestic sector by 2050. The caveat according to [74] is that the replacement of gas boilers with HPs must be accompanied by simultaneous decarbonisation of the electricity supply.

To reduce emissions in the transport sector, EVs are expected to play a dominant role. The UK Government's ambition is that nearly all cars and vans on the roads are zero emission by 2040 [75]. Government says as this number grows EVs will become a "*resource for a smart electricity*" bringing benefits for drivers and creating a more flexible and efficient energy system [75].

Widespread uptake of EVs and HPs will introduce new load patterns, and may lead to much higher peak demand. The higher peak demand may impact local LV distribution networks, particularly at clustered locations [76]. The way in which conventional electricity networks have operated in the past is unlikely to manage these new challenges without much higher system costs and perhaps reduction in the overall system reliability [77], [78].

In [79], reinforcement cost for the UK's distribution networks was estimated to reach up to £36bn between the year 2010 and 2050 if passive distribution networks and passive demand approaches are maintained. The reinforcement is driven by thermal ratings of equipment and network voltage constraints. In the study, single-speed ASHP was modelled to mimic the operation of a boiler, charging of EVs was modelled using Monte Carlo and the UK distribution network topologies at different voltage levels were synthesised using fractal theory.

A probabilistic impact assessment methodology using Monte Carlo to simulate daily profiles for photovoltaic panels, EVs, HPs and micro CHP was described in [80]. The method was tested on 128 real UK LV feeders. From the results, lookup tables to estimate the hosting capacity of feeders for each integrated technology was developed by correlation analysis between the first occurrence of problem and the parameters (length, number of households) of the feeder [80].

Many other works considered the separate impacts of EVs and HPs on the LV distribution network [81]–[86]. In [81], LV distribution network operation security-risk information, such as over-current and under-voltage due to the uptake of EVs, was obtained from three-phase distribution load flow studies that use stochastic parameters drawn from Monte Carlo. The capability of providing security risk information by deterministic and stochastic analytical approaches was compared and impacts due to controlled and uncontrolled charging were analysed. The work concluded that

stochastic approach gives better information and that controlled charging could mitigate network problems.

In [82], probabilistic methodology (Monte Carlo) and OpenDSS power flow software were used to assess the impact of HPs (ASHP and GSHP) on LV distribution network. The results from the studies showed that thermal problems are likely to arise at much earlier uptake levels of HPs than for voltage problems, and moving from upstream components (transformers) to downstream ones (feeders).

2.4 MANAGEMENT OF LOAD DEMAND OF EVS AND HPs IN LV DISTRIBUTION NETWORKS

The uptake of low carbon technologies, particularly EVs and HPs, at LV distribution networks, in the quest of cutting down on GHG emissions in the transportation and residential sectors, has the potential to cause general load increase and may lead to higher and longer peak load demand [87], [88]. This development can, as hinted in previous studies [88], [89], pose a real challenge of capacity overloading to transformers at the LV distribution network of electricity system.

Transformer is one of the most critical equipment in the power system [90]. Although, transformers are usually designed to withstand certain margin of overload, prolonged periods of transformer overloading could lead to premature transformer failure and shorter transformer life expectancy [91]. Amongst the impacts of an unplanned outage of a transformer are reduction in system reliability and economic losses to DNOs [92], [93].

2.4.1 Loading of Transformer

Deterioration and cumulative aging of winding insulation of transformers are the basis in loading of transformers [94]. Winding insulation of transformers deteriorates as a function of temperature and time. The deterioration effect caused by the hottest-spot temperature (HST) of the winding is considered for the transformer since the temperature distribution inside most transformers is not uniform. The HST has a direct relationship with the size of the load on the transformer, the temperature of the insulation oil and the ambient temperature. For normal life expectancy of the transformer, the HST must not exceed 110°C for transformers using thermally

upgraded insulation paper and 98°C for transformers using non-thermally upgraded insulation paper [94], [95].

The four reference loading levels of the IEEE Standard C57.91-2011 are paraphrased here [94].

- i) **Normal life expectancy loading (NLEL)** is loading for which the HST and the top oil temperature usually do not exceed the permitted maximum temperatures that ensure normal life expectancy of the transformer. However, the transformer could be operated at HST above 110°C but not exceeding 120°C for limited periods with a caveat that the transformer must be operated for much longer periods at HST below 110°C within any 24-hour period. This loading can be continued indefinitely without any risk. To remain in NLEL, it is suggested that the HST be kept in the range of 110°C – 120°C and the top-oil temperature should not exceed 105°C at any time.

- ii) **Planned loading beyond nameplate rating (PLBNR)** is loading for which the HST or top oil temperature exceeds the levels suggested for NLEL. It is accepted by the user as an anticipated, normal, reoccurring loading. This loading is allowed with all components in service. PLBNR is a scenario wherein a transformer is so loaded that its HST is in the temperature range of 120°C – 130°C. The length of time for a transformer to operate in the 120°C – 130°C range should be determined by loss of insulation life calculations, considering the specific load cycle, but usually not exceeding four hours per day.

- iii) **Long-time emergency loading (LTEL)** is loading for which the HST or top oil temperature exceeds those permitted for PLBNR. It is usually allowed only under conditions of prolonged outage of some system elements. The length of time for a transformer to operate in the 120°C – 140°C range should be determined by loss of insulation life calculations, considering the specific load cycle. However, it is suggested one 24-hour period contains no more than six hours operation when the HST is in the range of 130°C – 140°C, together with no more than four hours operation when the HST is in the range of 120°C – 130°C.

iv) **Short-time emergency loading** (STEL) is loading for which the HST or top oil temperature exceeds the limits given for PLBNR. It is an unusually severe condition typically acceptable only after the occurrence of one or more unlikely events that seriously disturb normal system loading. STEL is a scenario wherein a transformer is so loaded that its HST is as high as 180°C for a short time. The length of time for a transformer to operate in the 120°C – 180°C range should be determined by loss of insulation life calculations, considering the specific load cycle. It is suggested that one 24-hour period contains no more than one hour operation when the HST is in the range of 130°C – 180°C, together with no more than six hours operation when the HST is in the range of 13°C – 140°C and no more than four hours operation when the HST is in the range of 120°C – 130°C.

2.4.2 Immediate, Short-Term and Long-Term Effects of Transformer Overloading

The immediate, short-term, and long-term effects of transformer overloading according to IEC Standard 60076-7:2005 are paraphrased here [95].

Immediate effects of overloading a transformer include:

- The temperatures of windings, cables, insulation and oil will rise, and may reach abnormal unacceptable levels.
- Moisture and gas content in the insulation and in the oil will change as the temperature rises.
- Increased flux leakage outside the core, causing additional eddy-current heating in metallic parts linked by the flux.
- Bushings, tap-changers, cable connection joints and other accessories may be subjected to higher stress level than their design.

Short-term effects of overloading a transformer include:

- Reduction in dielectric strength due to the possible presence of gas bubbles in the windings and leads. At HST between 140°C and 160°C, bubbles may develop in the insulation paper. However, bubbles formation can also occur at temperature below 140°C as the moisture concentration increases. Bare metal parts in contact with the oil in the transformer may rapidly rise to high temperature.
- Temporary deterioration of the mechanical properties at higher temperatures could reduce the short-circuit strength.
- Pressure build-up in the bushings may result in a failure due to oil leakage. Gassing in the bushings may also occur if the temperature of the insulation exceeds about 140°C.
- Expansion of the oil could cause overflow of the oil in the conservator.

Long-term effects of overloading a transformer include:

- The gasket materials in the transformer may become more brittle.
- Insulation materials, structural parts and conductors could suffer more deterioration.
- Cumulative thermal deterioration of the mechanical properties of the conductor insulation will accelerate. This may reduce the effective life of the transformer, if the deterioration proceeds far enough and the transformer is subjected to short-circuits.

Traditional solution to addressing distribution transformer overloading due to widespread and high uptake of EVs and HPs would have been upgrading of transformer capacity. However, the number of LV distribution transformers in electricity system to be upgraded, the logistic and the resources involved for such

operation, and in many cases the seasonal nature of the overloads make the solution less desirable to the DNOs [88], [96].

Therefore, alternative smart solution must be the approach. Conclusions from the study completed on behalf of all DNOs in GB, called DS2030, and reported in [97], showed that with suitable adaptation (smart and traditional) the future power network is expected to be technically viable and capable of serving consumers in line with the national standards for security and quality that are applied today.

A research team in the European project, hyper-Network for electro**M**obility (NeMo), developed a tool suite applicable for analysing the design of the grid infrastructure in the face of increasing penetration levels of EVs and DGs [96]. NeMo tool suite analyses the operations of the distribution grids, comparing different techno-economic options and checks the compliance of grid infrastructure to technical parameters [96]. The expected results of the NeMo tool suite are:

- Forecasts of PV generation and EV charging profiles in a given distribution grid with given household demand profiles.
- Identification of grid issues like overloads (transformer and cable), losses and voltage violations, depending on the EV and DG penetration levels.
- Analysing the variables and in an iterative process find final solutions, being either grid reinforcement, demand side management, reactive power control, fixed energy storage, or a combination of all of these.

Testing NeMo tool suite on LV grids in three countries (Germany, Netherlands and Denmark) showed that storage is a viable option for grid support in distribution grids with high penetration of EVs and DG (e.g. PV, wind) [96]. However, for storage to be a cost-effective option it will need to generate revenue from a number of markets such as the energy market and frequency response [97]. Presently, DNOs are barred from energy trading in GB [97], [98]. Therefore, regulations will need to change if DNOs are to use storage as a viable option for grid support at the LV distribution networks.

In [99], heuristic genetic algorithm was used to optimize the siting, sizing, technology and operation of energy storage systems for DNO applications based on technical and economic value. Following from this, cost- and time-based network planning decisions between network upgrades and network upgrade deferral by energy storage systems can be made. The optimisation, however, did not consider the social and environmental impacts of the proposed solution.

Multiple demand side flexibility schemes such as load shifting, strategic load growth, strategic load conservation, reverse load shifting and flexible load were proposed in [100] to mitigate the impacts of both generating (photovoltaic solar panels, wind generators) and consuming (EVs and HPs) distributed energy resources on the LV distribution network. Results showed for the tested cases that on average a mitigation of about 70% and 34% was achieved in terms of voltage and overload problems respectively. The proposed multiple demand side flexibility schemes are contingent on the full cooperation of residential customers and involve lot of assumptions, “*meaning they are in theory immediately realisable*” [100].

A number of strategies to minimise domestic peak demand by controlling charging of EVs and operation of HPs and consequently mitigate their impacts on LV distribution network were proposed in [101]. The strategies include load shifting, demand limited charging and heating, fast and slow charging and bi-directional EV battery operation. The most successful strategy according to [101] was a combination of bi-directional EV battery operation and demand limited heating and charging. However, the degradation effect and the cost of bi-directional operation of EV battery was not considered.

A methodology was developed in [88] for real-time procurement of flexibility for congestion alleviation in LV distribution networks considering the incurred cost due to congestion. The procured flexibility helps to avoid the costs incurred by the transformer overloading. In this regard, the cost of the procured flexibility plays a crucial role, as the DNO may decide to overload the transformer and bear the monetary losses instead of procuring flexibility at a much higher price. A detailed thermal model of the transformer was developed and used in obtaining the costs incurred by overloading. The overloading cost of the transformer was calculated as the difference between the instantaneous aging cost and the aging cost at rated load of the transformer [88]. A multi-agent based local flexibility market was created from the aggregation of

available flexible domestic appliances – HPs and freezers in this case, and small-scale generating technologies – rooftop photovoltaic solar panels.

In [102], a methodology was introduced to improve the accuracy of IEC thermal model by refining its thermal parameters based on measured temperature data during conducted heat run test. Verification of the methodology under one 1MVA 6.6/0.415 kV distribution transformer showed that the accuracy of determining the hot spot temperature of the transformer was improved and maximum penetration level of EVs was improved by 9%. Results showed that IEC recommended parameters were more conservative than the refined parameters, since IEC parameters tend to overestimate the top-oil temperature, the hot spot temperature and the loss of life values.

However, the refined thermal parameters presented in [102] are thermal design specific, which means they are only suitable for the investigated transformer and transformers with the same thermal design. The refined thermal parameters in [102] only show how different the tested transformer is thermally designed from the standard IEC transformer. Also, it is good for transformer asset managers that IEC recommended parameters are conservative, since their conservative values ensure that transformers lives are not risked for just marginal increase in loadability.

In [103], the smooth integration of EVs and management of their charging load in distribution network was based on the coordinated interactions of four agents demonstrated in a multi-agent system based on the integration of three MAS software programs. The four agents are:

- i) **EV agents** who are the EV owners whose requirements of daily trip schedules and daily charge needs must be satisfied.
- ii) **EV virtual power plant agents** who are responsible for managing the EVs charging process and guarantee the daily trip schedules of EV owners in the face of power system requirements and constraints.
- iii) **Distribution system operator technical agent** who is responsible for congestion verification after obtaining charging requirements and schedules from the EV virtual power plant agents.

- iv) **Distribution system operator market agent** who is responsible for establishing the congestion price using market-based control method.

The low point of the multi-agent system described in [103] is that the interactions and the flow of communication messages between the agents to ensure their coordination are rather complex with huge computational burden. Same approach in [103] of managing congestion in the LV distribution network was described in [89]. In [89], an agent called fleet operator performs similar roles as EV virtual power plant operator in [103].

A web-based day ahead charge scheduling of EVs was proposed in [104] to manage the overloading problem in the LV network. In the proposed method, a price responsive schedule for EVs which calculates distribution locational marginal price (DLMP) was developed based on the previously received travel plan information of EV owners. The DLMP is high during overloading and low during period of low demand [104]. The DLMP information is then shared with EV owners for them to decide on most economic charging slots. The shortcoming of the approach is that it is prone to uncertainties such as change in EV owners' travel plan and real-time traffic. Also, some EV owners might not be willing to divulge information about their travel plans, which they consider as personal security information.

2.5 SUMMARY

Relevant literature used in the thesis were discussed. Literature arguing from the perspective of LCA of EVs and ICE vehicles for and against the concept of burden shift of emissions from the road to the grid as EVs replace conventional ICE vehicles were reviewed. The literature indicates that the electricity generation mix of a country should guide the EV adoption policy of its government.

The potential benefits and supports that EVs as aggregation of controllable loads and dispersed storage energy resources could provide the grid were reviewed. In the literature reviewed, the many stochastic factors associated with EVs and EV owners, together with rapid degradation the EV batteries could suffer while supporting the grid were identified as impediments. The impacts of the charging requirements of EVs as uncontrollable loads and how different charging patterns affect the generating

infrastructure vis a-vis capacity, GHG emissions and emission abatement cost were also reviewed in the literature. The converging view indicates that charging of EVs would increase the grid load demand and could stress the grid infrastructure.

The impacts of the load demand of EVs and HPs on LV distribution networks were discussed. Violation of voltage limits, feeders and transformers overloading, and harmonic problems were variously mentioned in the reviewed literature. However, overloading of distribution transformers was by far the most impact mentioned in the literature.

Finally, load management approaches and methods to mitigate the impacts of overloading due to increasing uptake of EVs and HPs in the LV distribution networks were discussed from the literature.

CHAPTER 3

IMPACTS OF ELECTRIC VEHICLE CHARGING REQUIREMENTS AND CHARGING PATTERNS ON POWER SYSTEM SCHEDULING, GRID EMISSION INTENSITY AND EMISSION ABATEMENT COST

3.1 INTRODUCTION

Unabated release of GHG emissions into the atmosphere and its attendant climate change consequences could adversely affect the present and future generations. In the UK, the energy and the transportation sectors have been identified as the two largest producers of GHG emissions [105]. Deployment of RESs in the electricity generation and integration of EVs in the transportation sector have been suggested as means of reducing the GHGs emissions [106].

There are concerns, however, about burden shift of emissions from the transportation sector to the power sector because of increased generation to meet the additional charging load of EVs [107]. This Chapter therefore, empirically investigates the integration of EVs in the road transportation sector in what is defined as electromobility by [108] and its impacts on the power grid in the UK vis-à-vis GHG emissions reduction.

The study is divided into two parts. Firstly, an algorithm was developed to empirically estimate, from historical data, the annual Real-Emission-Reduction (RER) in the UK road transportation sector due to the integration of EVs from the year 2009 to 2013. Secondly, a dispatch model for power system was developed based on the correlation identified, from historical data of the UK power system, between the system load and the capacity factors of generating units. The model was used to dispatch generating units to meet system load demand under two charging patterns of

EVs and analyses were carried out of the impacts of the charging patterns on the system scheduling, GHG emissions and emissions abatement cost.

3.2 ESTIMATING THE TRUE GHG EMISSIONS REDUCTION DUE TO ELECTRIC VEHICLES INTEGRATION

3.2.1 UK Mobility and Transport Statistics

The modal share of different means of commuting in the UK shown in Fig. 3.1 reveals that at least 80% of the trips are made by vehicles.

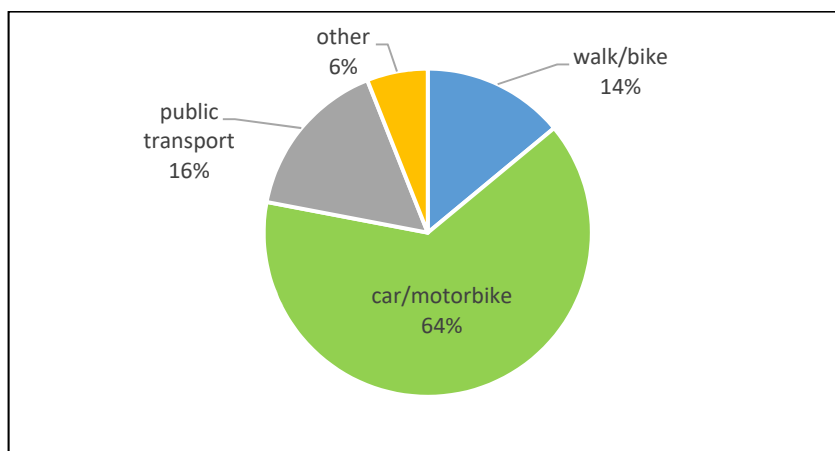


Fig. 3.1 Share of different means of commuting in the UK [109]

In UK, car travel accounts for at least 80% (79% in GB and 81% in NI) of the total annual trips by all vehicle types [110], [111]. Table 3.1 shows the annual motor traffic by vehicle type in GB from 2009 to 2013.

Table 3.1 Motor Traffic by Vehicle Type in Great Britain [112]

Year	Cars & Taxis (10 ⁹ km)	Light vans (10 ⁹ km)	Goods vehicles (10 ⁹ km)	Motor Cycles (10 ⁹ km)	Buses & Coaches (10 ⁹ km)	Total (10 ⁹ km)
2009	394.00	65.50	26.20	5.10	5.00	495.80
2010	385.90	66.10	26.30	4.60	5.00	487.90
2011	387.40	66.60	25.60	4.60	4.70	488.90
2012	386.70	66.40	25.00	4.60	4.40	487.10
2013	386.20	68.50	25.20	4.30	4.50	488.90

Table 3.2 shows the statistics of licensed vehicles by body in GB and Table 3.3 shows the same statistics for NI. From the two tables, the annual number of licensed cars in the UK is more than 80% of the total number of all licensed vehicles by body type in the period under consideration.

Table 3.2 Vehicles Licensed by Body Type in GB [113]

Year	Cars (10 ⁶ units)	Motorcycles (10 ⁶ units)	LGVs (10 ⁶ units)	HGVs (10 ⁶ units)	Buses & Coaches (10 ⁶ units)	Others (10 ⁶ units)	Total (10 ⁶ units)
2009	28.25	1.28	3.18	0.48	0.17	0.60	33.96
2010	28.42	1.23	3.21	0.47	0.17	0.62	34.12
2011	28.47	1.24	3.25	0.47	0.19	0.64	34.26
2012	28.72	1.22	3.28	0.46	0.17	0.67	34.52
2013	29.14	1.22	3.35	0.47	0.16	0.69	35.03

Table 3.3 Vehicles Licensed by Body Type in NI [114]

Year	Cars & Taxis (units)	Motor/ Tri- cycles (units)	LGVs (units)	HGVs (units)	Buses/ Coaches (units)	Agric. Vehicle (units)	Others (units)
2009	862,065	31,403	94,845	24,925	6,033	18,846	5,788
2010	868,867	30,241	94,741	24,222	5,940	20,463	6,007
2011	871,109	28,788	96,117	23,352	5,861	21,896	6,215
2012	878,196	27,253	97,087	22,384	5,835	23,169	6,404
2013	891,063	24,586	NA	NA	5,731	22,411	5,215

In the UK, transportation sector is more than 90% dependent on petroleum for energy [115]. Road transport uses at least 70% of the transport energy and cars are responsible for no less than 45% of the total transport energy [115]. Table 3.4 is presenting the statistics of cars licensed by propulsion and fuel type in NI and Table 3.5 gives similar statistics for GB.

Table 3.4 Cars Licensed by Propulsion/Fuel Type in NI [114]

Year	Petrol (units)	Diesel (units)	EV (units)
2009	279,947	300,249	42
2010	297,732	321,469	31
2011	312,005	340,622	39
2012	324,543	361,313	77
2013	335,895	385,436	150

Table 3.5 Cars Licensed by Propulsion/Fuel Type in GB [116]

Year	Petrol (10 ³ units)	Diesel (10 ³ units)	HEV (10 ³ units)	Gas (10 ³ units)	EV (10 ³ units)	Others (10 ³ units)	Total (10 ³ units)
2009	20,491.20	7,641.40	61.10	50.90	1.50	0.40	28,246.50
2010	20,083.10	8,202.70	82.10	51.00	1.50	0.40	28,420.90
2011	19,548.50	8,763.50	102.30	50.00	2.60	0.40	28,467.30
2012	19,158.80	9,385.10	125.30	48.70	4.10	0.40	28,722.50
2013	18,870.30	10,064.20	153.30	46.30	6.30	0.40	29,140.90

Petrol and diesel-engine cars are approximately 99% of all cars licensed by propulsion/fuel type in the UK (see Table 3.4 and Table 3.5). Consequently, cars contribute largest proportion of the total emissions in the road transport sector and more than 50% of the total emissions in the whole of transportation sector [105].

All these statistics underscore the potential reduction in GHG emissions from the road transport sector if the sector's dependence on fossil fuel is minimised. However, transportation has been consistently accounting for less than 2% of total annual electricity consumption from 2009 to 2013 [115], [117].

3.2.2 The Algorithm for Estimating Real-Emissions-Reduction (RER)

The algorithm begins by first calculating the average daily distance travelled by car in the UK as expressed in equation (3.1).

$$D_d = \frac{D_{yr}}{(365 \times n)} \quad (3.1)$$

Where:

D_d is the average daily distance travelled by a car (km),

D_{yr} is the annual distance travelled by cars (km),

n is the total number of cars.

It is assumed all cars, either EVs or ICE vehicles, travel the same daily distance. With this assumption the annual distance travelled by all EVs can be calculated as expressed in equation (3.2).

$$D_{yrEV} = D_d \times n_{EV} \times 365 \quad (3.2)$$

Where:

D_{yrEV} is the annual distance travelled by EVs (km),

D_d is the average daily distance travelled by an EV (km),

n_{EV} is the total number of EVs.

The annual energy drawn from the power grid by the EVs is then calculated as expressed in equation (3.3).

$$Chrg_{EV} = \eta_{EV} \times D_{yrEV} \quad (3.3)$$

Where:

$Chrg_{EV}$ is the annual energy drawn from the power grid by EVs (kWh),

η_{EV} is the average efficiency of EV (kWh/km),

D_{yrEV} is the annual distance travelled by EVs (km).

The efficiency of Nissan Leaf 2011 model (0.16kWh/km) was used as representative efficiency for EVs [118].

The CO₂ emitted annually at the power grid due to the annual charge energy drawn by the EVs is estimated by equation (3.4).

$$Grid_{EV_CO2} = \left[\left(\frac{Chrg_{EV}}{TAEG} \right) \times (AFUIG \times CO_2 \text{ emitted}/Mtoe) \right] \quad (3.4)$$

Where:

$Grid_{EV_CO2}$ is the CO₂ emitted annually at the power grid due to the annual charge energy drawn by the EVs (gCO₂),

$Chrg_{EV}$ is the annual energy drawn from the power grid by EVs (TWh),

TAEG is the Total Annual Electricity Generated (TWh),

AFUIG is the oil equivalent of Annual Fuel Used In Generation in the UK and net imports (Mtoe),

CO₂ emitted/Mtoe is the CO₂ emitted per Mtoe of AFUIG (g).

In the algorithm, AFUIG was used instead of reported emission intensity of the UK grid because until 2013 reported grid emission intensity figures had been based on 5-year grid-rolling average [119] and were less sensitive to energy mix changes that occurred in electricity generation. AFUIG used in the algorithm included both the Well-To-Tank (WTT) and the Tank-To-Wheel (TTW) factors of the fuel used in the electricity generation [119]. The CO₂ emissions due to AFUIG can be calculated by equation (3.5) according to [120], [121].

$$CO_2 \text{ emitted}/\text{barrel} = \theta_{hc} \times C_{coef} \times C_{oxidised} \times 3.667 \quad (3.5)$$

Where:

θ_{hc} is the heat content of oil (mmbtu/barrel),

C_{coef} is the Carbon coefficient of oil (kgC/mmbtu),

$C_{oxidised}$ is the fraction of Carbon oxidised,

The heat content and the average carbon coefficient of crude oil are 5.80mmbtu/barrel and 20.31kgC/mmbtu respectively [120]. The fraction oxidized is 100% [121]. Substituting these values in equation (3.5) and converting barrel to tonne, we have

$$CO_2 \text{ emitted}/\text{tonne} = 3.08 \times 10^6 \text{ gCO}_2 \quad (3.6)$$

It means for every tonne of oil equivalent used in electricity generation 3.08×10^6 g of CO₂ is emitted. But the AFUIG is in Mtoe. Therefore

$$CO_2 \text{ emitted}/\text{Mtoe} = 3.08 \times 10^{12} \text{ gCO}_2 \quad (3.7)$$

The average CO₂ emission intensity of ICE cars is calculated by equation (3.8)

$$CO_{2ICE} = \frac{MtCO_{2ICE}}{(D_{yr} - D_{yrEV})} \quad (3.8)$$

Where:

$CO_{2_{ICE}}$ is the average CO₂ emission intensity of ICE cars (g/km),

$MtCO_{2_{ICE}}$ is the million tonnes of CO₂ emitted annually by ICE cars

D_{yr} is the annual distance travelled by cars (km),

D_{yrEV} is the annual distance travelled by EVs (km),

The ‘Apparent-Emissions-Reduction’ (AER) in the road transport sector due to the uptake of EVs is given by equation (3.9).

$$AER = CO_{2_{ICE}} \times D_{yrEV} \quad (3.9)$$

Where:

AER is the apparent emissions reduction due to uptake of EVs (g),

$CO_{2_{ICE}}$ is the average CO₂ emission intensity of ICE cars (g/km),

D_{yrEV} is the annual distance travelled by EVs (km).

Therefore, the ‘Real-Emissions-Reduction’ can be estimated by equation (3.10)

$$RER = AER - Grid_{EV_CO2} \quad (3.10)$$

Fig. 3.2 shows the flowchart of the algorithm.

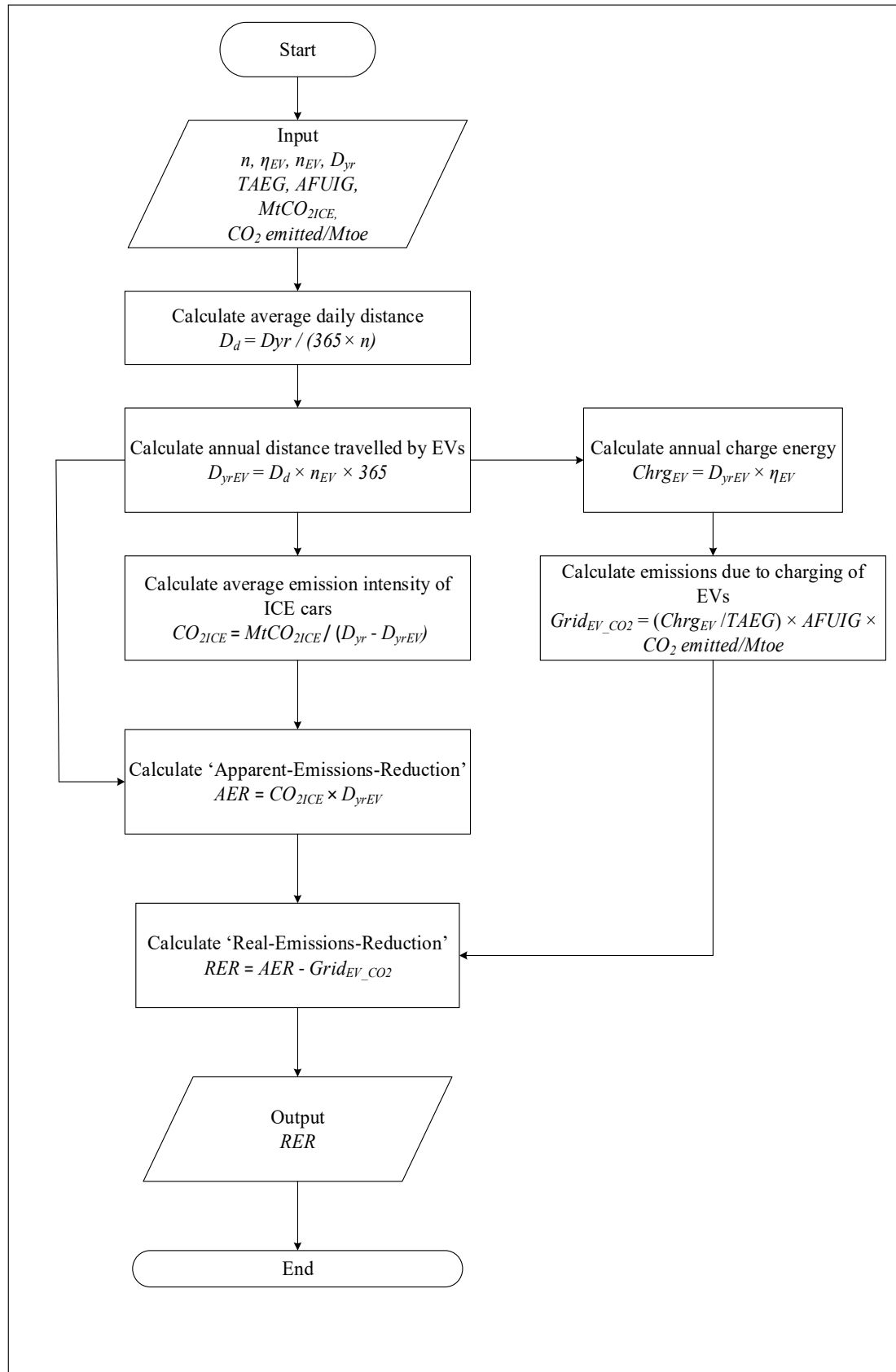


Fig. 3.2 Flowchart of Algorithm for estimating 'Real-Emissions-Reduction'

3.2.3 Application of the Algorithm

The algorithm is applied in the UK based on the data available between 2009 and 2013. Table 3.6 gives information on the electricity generated and the amount of oil equivalent of fuel used in the generation between 2009 and 2013. Table 3.7 provides the information about the CO₂ emissions from ICE cars between 2009 and 2013. Fig. 3.3 is the profile of the UK electricity generation mix between 2009 and 2013.

Table 3.6 Electricity Generated and Fuel used in Generation [122]

Year	Elect. Gen. (TWh)	Fuel used in gen. (Mtoe)
2009	376.72	78.70
2010	381.71	79.29
2011	367.25	76.87
2012	363.41	78.19
2013	359.15	76.44

Table 3.7 Emissions by ICE Cars in UK [123]

Year	Emissions by ICE cars (MtCO ₂)
2009	69.20
2010	66.10
2011	64.80
2012	64.00
2013	62.60

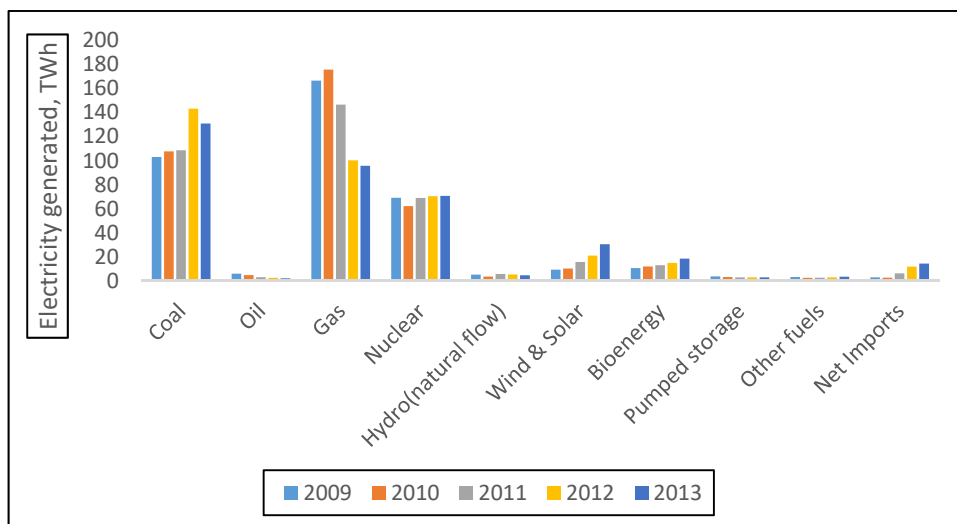


Fig. 3.3 Electricity generation from different sources [124]

3.2.4 Results and Discussion

Fig. 3.4 shows the annual Real-Emissions-Reduction (RER) due to the uptake of EVs from 2009 to 2013, together with the annual Apparent-Emissions-Reduction (AER) and the emissions at the power grid due to the charging of EVs (Grid_{EV_CO2}) as calculated by the algorithm. Also, Table 3.8 gives the results of the emissions intensity of the ICE cars in the UK from 2009 to 2013 as calculated by the algorithm.

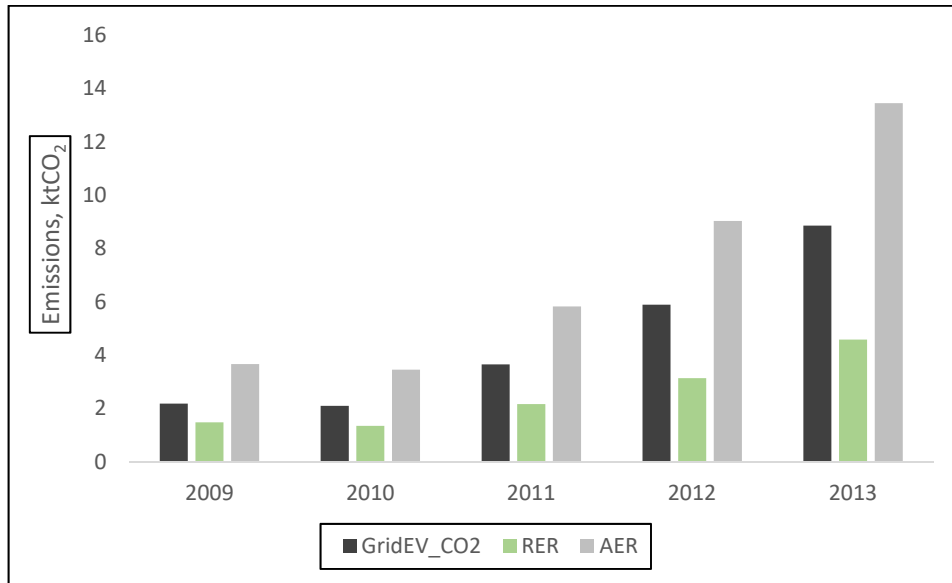


Fig. 3.4 Emissions at the grid due to EVs, RER and AER in the UK, 2009-2013

Table 3.8 Emissions Intensity of ICE Cars in the UK, 2009-2013

Year	Emissions Intensity of ICE cars (g/km)
2009	173
2010	168
2011	164
2012	163
2013	159

The RER dipped in 2010 to **1.3ktCO₂** as against **1.5ktCO₂** in 2009. Amongst plausible reasons for the dip are;

- The increased generation from coal in 2010 relative to 2009 (see Fig. 3.3).
- The lower emissions intensity of ICE cars in 2010 than in 2009 (see Table 3.8).

- The decreased generation from nuclear in 2010 relative to 2009 (see Fig. 3.3).
- The decreased net imports of electricity in 2010 relative to 2009. UK imports electricity from France. France's electricity generation is more low-carbon mix than the UK's one [125]. Therefore, more imports from France lowers the UK grid emission factor and vice-versa.

However, from 2011 to 2013, there was annual increase in RER, **2.2 ktCO₂**, **3.1ktCO₂** and **4.6 ktCO₂** respectively, occasioned by annual increased penetration of RES in electricity generation and annual increase in net imports of electricity.

The difference between the Apparent-Emissions-Reduction and the emissions at the grid due to the charging of EVs gives the Real-Emissions-Reduction. A positive figure indicates a reduction whereas a negative figure indicates an increase. The algorithm is a simple check to tell if the reduction of CO₂ emission due to EVs uptake is increasing, decreasing or an equilibrium point is reached. Equilibrium point is reached when CO₂ emissions at the power grid due to the charging of EVs and the apparent CO₂ emissions saved in the transportation sector due to the uptake of EVs are equal.

The average emission intensity of ICE cars is improving from year to year, dropping from **173g/km** in 2009 to **159g/km** in 2013. Therefore, for EVs to make significant contribution to emission reduction and have comparative advantages over the ICE cars, there must be an increase in RES penetration in the electricity generation mix and improved efficiencies of EVs. Participation of EVs in Demand Response Scheme (DRS) as flexible loads and storage entities in vehicle-to-grid (V2G) operation would also make them desirable in the emerging smart grid.

3.3 DISPATCH MODEL FOR ANALYSING THE IMPACTS OF EVS CHARGING PATTERNS ON POWER SYSTEM SCHEDULING, GRID EMISSIONS INTENSITY AND EMISSIONS ABATEMENT COSTS

Dispatching of generation resources at the Power Station is a complex task based on the balance of economics, contractual agreement, regulations and environmental consciousness in terms of the amount of emissions produced in the course of electricity generation. The complexity of the task could be exacerbated with the integration of large percentage of EVs in the quest to reducing CO₂ emissions.

In this section, a model is described and developed for generation resources dispatch, which is suitable for analysing the impacts of charging patterns of EVs on grid emissions intensity and emissions abatement costs. The dispatch model is based on the correlation between historical system load and capacity factors of generating units as first described in [67]. The dispatch model is tested on data from the UK power system on a typical Winter day in December 2015 with an assumed 50% integration of EVs on the system. However, it must be noted that only generating resources/technologies with transmission entry capacities are considered in the study.

3.3.1 Generation Mix and the System Load

Fig. 3.5 shows the simplified diagram of the Transmission-Entry-Capacity generating resources/technologies that made up the electricity generation mix of the UK as at December 2015 and Table 3.9 gives their capacities [126], [127].

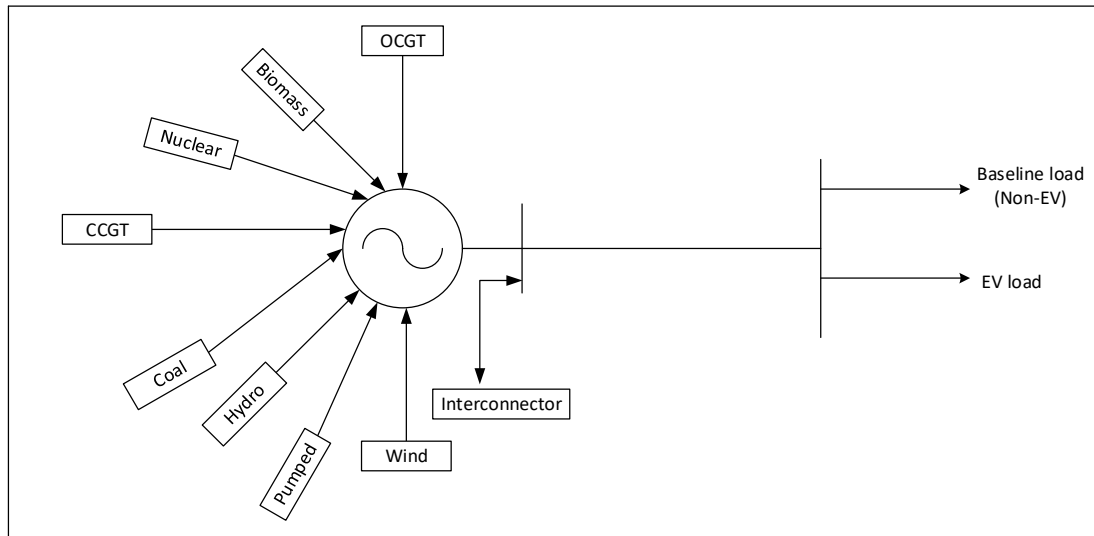


Fig. 3.5 Simplified diagram of UK Power System showing Transmission-Entry-Capacity Generating Technologies as at Dec. 2015

The baseline load indicated in Fig. 3.5 is the normal conventional load on the system, consisting of domestic, commercial and industrial load, before the EV load is added. From Table 3.9, it is seen that RES accounts for 21% while low-carbon technologies account for 56% of the total generating technologies with transmission-entry-capacity.

Table 3.9 UK's Transmission-Entry-Capacity generating technologies as at Dec. 2015

Technology	Transmission-Entry-Capacity (MW)	Percentage of Total (%)
CCGT	31,994	41.5
Coal	13,500	17.5
Hydro	3,836	5.0
Nuclear	9,937	12.9
OCGT	1,470	1.9
Pumped	2,828	3.7
Onshore wind	2,769	3.6
Offshore wind	4,333	5.6
Biomass	2,423	3.1
Interconnector	4,000	5.2
Total	77,090	100

3.3.2 Model Description

Data on system load demand and generation output per technology for each day of December 2015 from [127]–[129] are processed. From the data, average half-hourly load demand and corresponding average half-hourly capacity factors of different generating technologies which met the demand were determined for an average day in December 2015. There were 48 data points each for load demand and capacity factor of each generating technologies. Each data point is the average of data for each day of December 2015. Fig. 3.6 is the average half-hourly load demand curve and average half-hourly output of generating technologies as processed from the data sources.

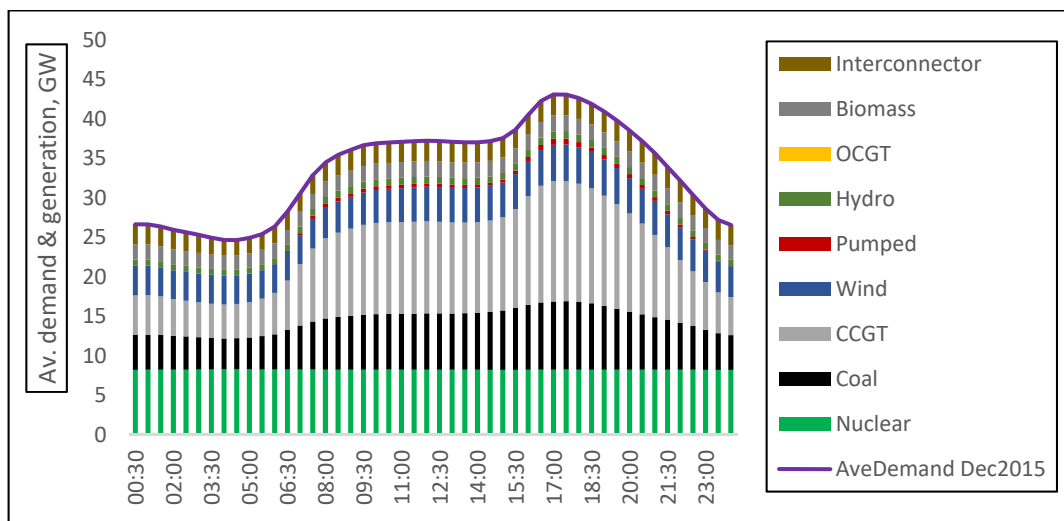


Fig. 3.6 Average half-hourly system load demand and generation dispatch mix, Dec 2015 (Historical data [127]–[129])

Fig.3.7 gives the summary of the average contributions of different generating technologies into the generation mix on a typical day in December 2015 as processed from historical data [127]–[129].

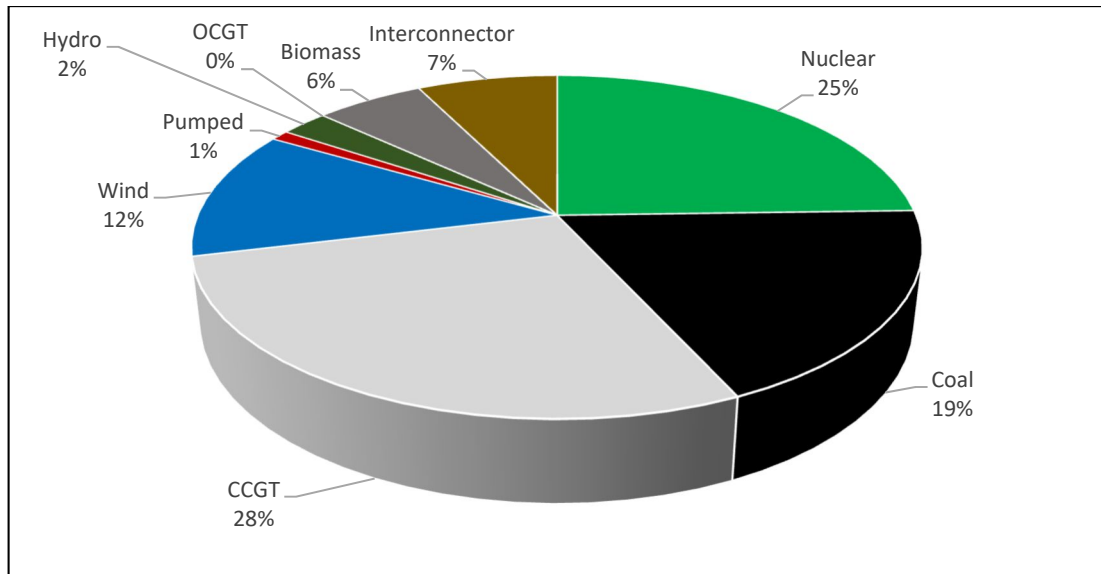


Fig.3.7 Average contribution of different generating technologies into the generation mix, Dec. 2015 (Historical data [127]–[129])

Scatter plots of average load demand and average capacity factor are presented for each generating technology to determine the correlation between them. Fig. 3.8 (a-i) show the correlations of average half-hourly capacity factors versus average half-hourly system load for all the generating technologies.

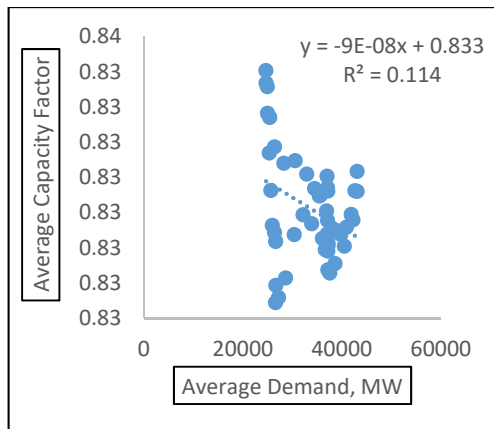


Fig. 3.8 (a) Nuclear

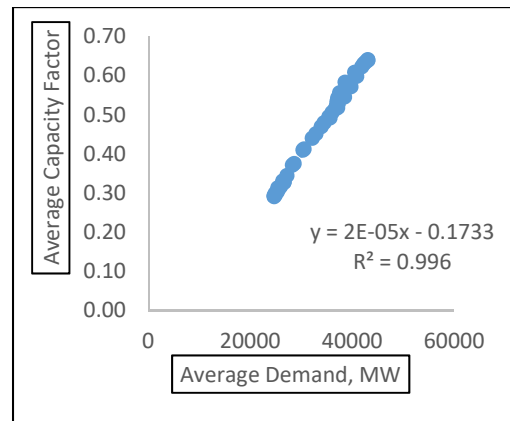


Fig. 3.8 (b) Coal

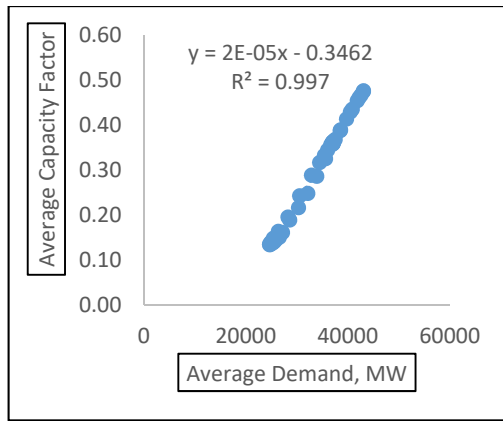


Fig. 3.8 (c) CCGT

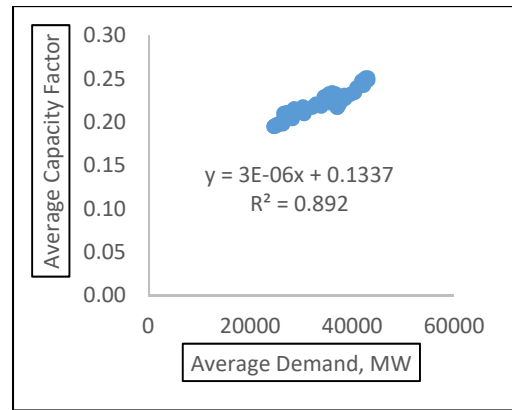


Fig. 3.8 (f) Hydro

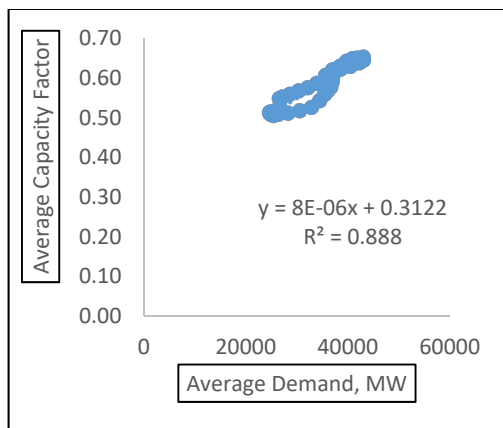


Fig. 3.8 (d) Wind

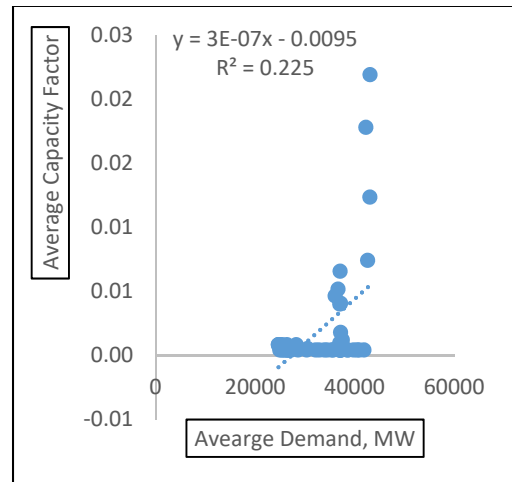


Fig. 3.8 (g) OCGT

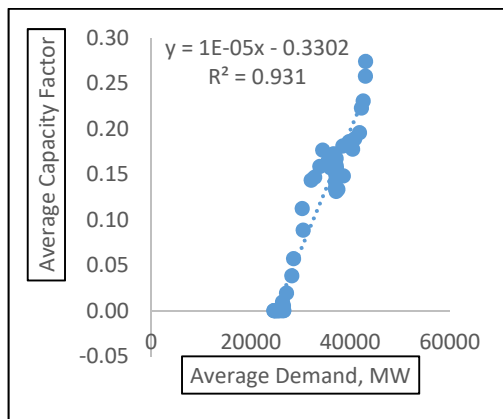


Fig. 3.8 (e) Pumped

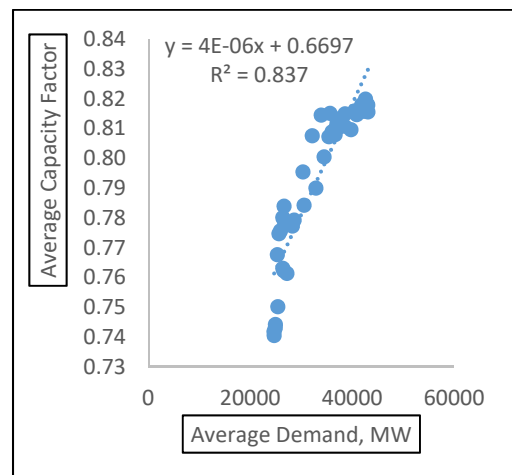


Fig. 3.8 (h) Biomass

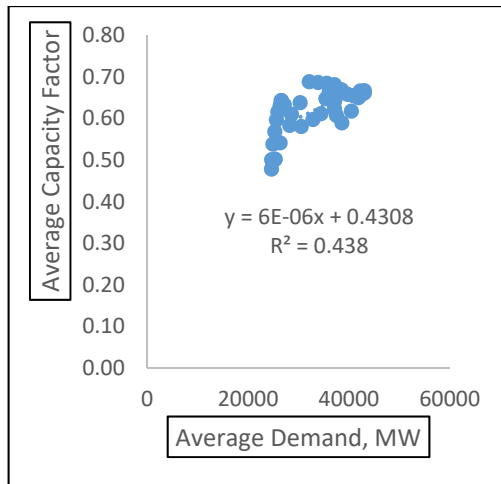


Fig. 3.8 (i) Net Interconnector

Fig. 3.8 (a-i) Average half-hourly capacity factor versus average half-hourly system load

As seen in Fig. 3.8 (a), the Nuclear generating unit shows no correlation between its capacity factor and the load demand. This can be explained as the Nuclear generating unit provides the base load generation and its output is nearly constant at all times irrespective of the load demand.

The Coal, CCGT and Pumped generating units show strong positive correlation between their capacity factors and the load demand as seen in Fig.3.8 (b), (c) and (e) respectively. The coefficient of determination (R^2) of fitness to the regression line of Coal, CCGT and Pumped generating units are 0.996, 0.997 and 0.931 respectively.

The Wind, Hydro and Biomass generating units show fairly strong positive correlation between their capacity factors and the load demand as seen in Fig. 3.8 (d), (f) and (h). Their coefficients of determination (R^2) are 0.888 for Wind, 0.892 for Hydro and 0.837 for Biomass. However, it must be noted that the positive correlation shown by the Wind generating unit between its capacity factor and the load demand is weather related. It has been shown that in Winter, high demand is driven by cold conditions which are due to the strengthening of the easterly winds, and thereby increases average wind power [130].

The OCGT and the Interconnector show weak correlation between their capacity factors and the load demand as seen in Fig. 3.8 (g) and (i). The OCGT is a peaker generating unit which is operated only when the load demand is high. The net output

of the Interconnector on the other hand is dependent not only on the conditions in the system but also on the conditions outside of the system.

3.3.3 Model Formulation

The total electricity generation from the different generating units/technologies to meet the load demand over a certain period of time is the sum product of the capacity factors and the Transmission-Entry-Capacities (TECs) of the generating units/technologies over the period as expressed in equation (3.11).

$$Gen_{Total} = \sum_{i=1}^n \sum_{t=1}^T g_i(t) = \sum_{i=1}^n \left[\left(\sum_{t=1}^T CF_i(t) \right) \times TEC_i \right] \quad (3.11)$$

Where:

Gen_{Total} is the total electricity generation (MW) from all the different generating units/technologies,

i is the identifier index for generating unit/technology,

n is the total number of generating units/technologies,

t is the time interval,

T is the total number of the time intervals,

g_i is the electricity generation (MW) from a particular generating unit/technology,

CF_i is the capacity factor of a particular generating unit/technology,

TEC_i is the transmission-entry-capacity (MW) of a particular generating unit/technology.

The capacity factors of the generating units/technologies can be expressed in terms of their correlations with the load demand as previously established. Thus, equation (3.11) can be expressed in terms of the load demand as given in equation (3.12).

$$Gen_{Total} = \sum_{i=1}^n \sum_{t=1}^T g_i(t) = \sum_{i=1}^n \left[\sum_{t=1}^T ((a_i \times D(t)) \pm b_i) \times TEC_i \right] \quad (3.12)$$

Where:

a_i and b_i are constants of the equation of regression line of the correlation between capacity factor of a particular generating unit/technology and the load demand,

D is the load demand (MW).

The total emissions produced by all the generating units/technologies over a period of time is expressed in equation (3.13).

$$Em_{Total} = \sum_{i=1}^n \sum_{t=1}^T Em_i(t) = \sum_{i=1}^n \left[\left(\frac{EmFac_i}{\eta_i} \right) \times \sum_{t=1}^T g_i(t) \right] \quad (3.13)$$

Where:

Em_{Total} is the total emissions (gCO₂e) produced by all the generating units/technologies,

Em_i is the emissions produced (gCO₂e) by a particular generating unit/technology,

$EmFac_i$ is the emission factor (g/kWh) of a particular generating unit/technology,

η_i is the thermal efficiency (%) of a particular generating unit/technology.

The average grid emissions intensity of the system due to electricity generation from all the generating units/technologies over a period of time can be determined as expressed in equation (3.14).

$$Grid_{EmIntensity} = \frac{1}{T} \sum_{t=1}^T \left(\frac{\sum_{i=1}^n Em_i(t)}{\sum_{i=1}^n g_i(t)} \right) \quad (3.14)$$

Where:

$Grid_{EmIntensity}$ is the average grid emissions intensity of the power system (gCO₂e/kWh).

The total cost of generation by the system is given by equation (3.15).

$$GenCost_{Total} = \sum_{i=1}^n \sum_{t=1}^T gencost_i(t) = \sum_{i=1}^n \left[\sum_{t=1}^T (g_i(t)) \times \mathbb{E}_i \right] \quad (3.15)$$

Where:

$GenCost_{Total}$ is the total cost of electricity generation of the power system over a period of time (£),

$gencost_i$ is the cost of electricity generation of a particular generating unit/technology (£),

\mathbb{E}_i is the variable cost or levelized cost (£/MW) (depending on the focus of the calculation) of operating a particular generating unit /technology to produce electricity.

The opportunity cost of uptake of EVs in terms of emissions savings/avoided on the road can be expressed by equation (3.16).

$$Em_{savings} = EV_{uptake} \times n \times D_d \times CO_{2ICE} \quad (3.16)$$

Where:

$Em_{savings}$ is the emissions savings on the road (ktCO₂e),

EV_{uptake} is the percent uptake of EVs (%),

n is the total number of licensed cars,

D_d is the average daily distance travelled by a car (km),

CO_{2ICE} is the average CO₂ emission intensity of ICE cars (g/km).

The net emissions reduction on the grand scheme is the difference between the emissions savings on the road and the marginal increase of the grid emissions (above the grid baseline emissions) due to EV charging load. The net emissions reduction can thus be expressed by equation (3.17).

$$Em_{Netreduction} = Em_{savings} - Em_{gridincr} \quad (3.17)$$

Where:

$Em_{Netreduction}$ is the net emissions reduction (ktCO₂e),

$Em_{grid_{incr}}$ is the marginal increase of the grid emissions above the baseline grid emissions (ktCO_{2e}),

The marginal increase of the grid emissions above the baseline grid emissions is a function of the magnitude of the EV load, EV charging pattern and how the generating resources are dispatched to meet the load demand. These factors also contribute to the emission abatement cost, which is given by the ratio of the marginal increase in the electricity generation costs (above the baseline generation costs) to the net emissions reduction as expressed in equation (3.18).

$$Em_{abatement_{cost}} = \frac{GenCost_{incr}}{Em_{Net_{reduction}}} \quad (3.18)$$

Where:

$Em_{abatement_{cost}}$ is the emissions abatement cost (£/tCO_{2e}),

$GenCost_{incr}$ is the marginal increase in the electricity generation cost (£).

3.3.4 Model Testing

The dispatch model is tested on data from the UK power system under three scenarios. Electricity generation cost, net emissions reduction and emissions abatement cost are calculated in each scenario. The results of the calculations are compared to analyse how different charging patterns of EVs impact on the power system in terms of dispatch of generating resources, grid emissions intensity and emissions abatement cost. The three scenarios investigated are:

- 1) **Baseline scenario:** The generating units/technologies are dispatched to meet the average load demand on a typical day in December 2015. It is assumed the load demand contains no or insignificant EVs load because the uptake of EVs in the UK as at the end of 2015 was 0.9% [131].
- 2) **Time-Of-Use-Charging scenario (TOUC):** In this scenario, it is assumed that there is 50% uptake of EVs and the EVs are charged based on the Time-Of-Use tariff. The generating units/technologies are thus dispatched to meet the average load demand, which is now augmented by the EVs load.

3) Without-Time-Of-Use-Charging scenario (WTOUC): As in TOUC, 50% uptake of EVs is assumed. But unlike TOUC, the EVs are charged without observing the Time-Of-Use tariff. The generating units/technologies are dispatched to meet the average load demand plus the EVs load.

In 2015, the number of licensed cars in the UK was 30.3 million [131] and annual road traffic made by cars/taxis was 398.6 billion kilometres [132]. The average daily car travel is therefore estimated to be 36km. Average daily EV energy requirement for the charging of EVs on the national grid is thus estimated according to equation (3.19).

$$EV_{MWh_{grid}} = N_{EV} \times dist_{ave} \times \eta_{ave_{EV}} \quad (3.19)$$

Where:

$EV_{MWh_{grid}}$ is the average daily energy requirement of EVs on the grid (MWh),

N_{EV} is the total number of EVs,

$dist_{ave}$ is the daily average distance travelled by car (km),

$\eta_{ave_{EV}}$ is the average of the efficiencies of all the EVs (kWh/km).

Table 3.10 gives the list of the most popular electric cars in the UK in 2015 with their efficiencies and All-Electric-Range [133], [134].

Table 3.10 UK's most popular electric cars in 2015 [133], [134]

Brand [133], [134]	Model	Efficiency (kWh/km) [13]	All-Electric-Range (miles) [13]
Nissan Leaf (24-kWh)	2013/14/15/16	0.184	84
Nissan Leaf (30-kWh)	2016	0.191	107
BMW i	2014/16	0.172	81
Mitsubishi Outlander PHEV	2012/13/14/16	0.191	62
Tesla S (60-kWh)	2014/15/16	0.22	234
Average efficiency		0.192	

The charging patterns for the TOUC and WTOUC scenarios are adapted from [135]. Fig. 3.9 is the average half-hourly EV charging profiles for WTOUC and TOUC average.

Substituting values into equation (3.19), the average daily EV charge requirement on the grid is estimated to be 104.72GWh. This is spread in time over the day according to the charging profile on top of the average load demand. Fig. 3.10 shows the half-hourly system average load profiles for the baseline scenario, TOUC scenario and WTOUC scenario.

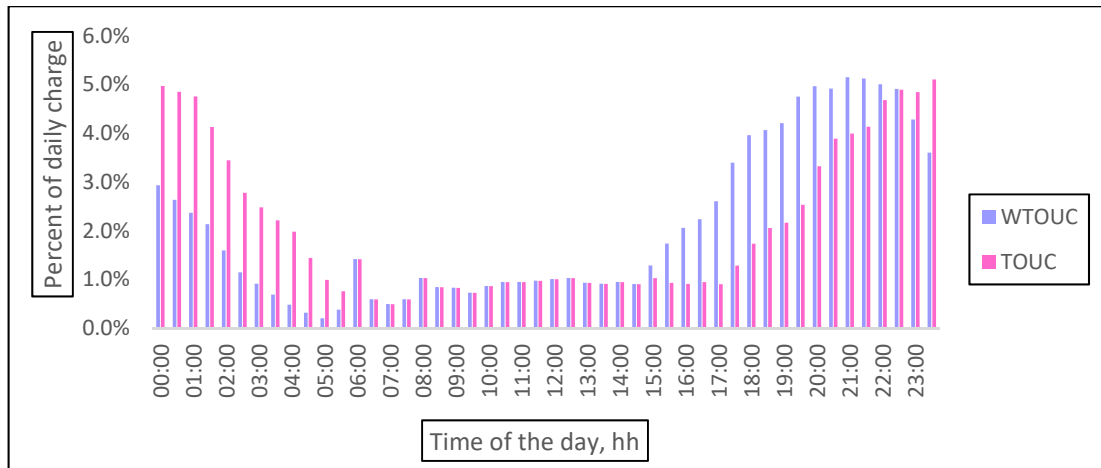


Fig. 3.9 Average half-hourly EV charging profiles: WTOUC and TOUC [135]

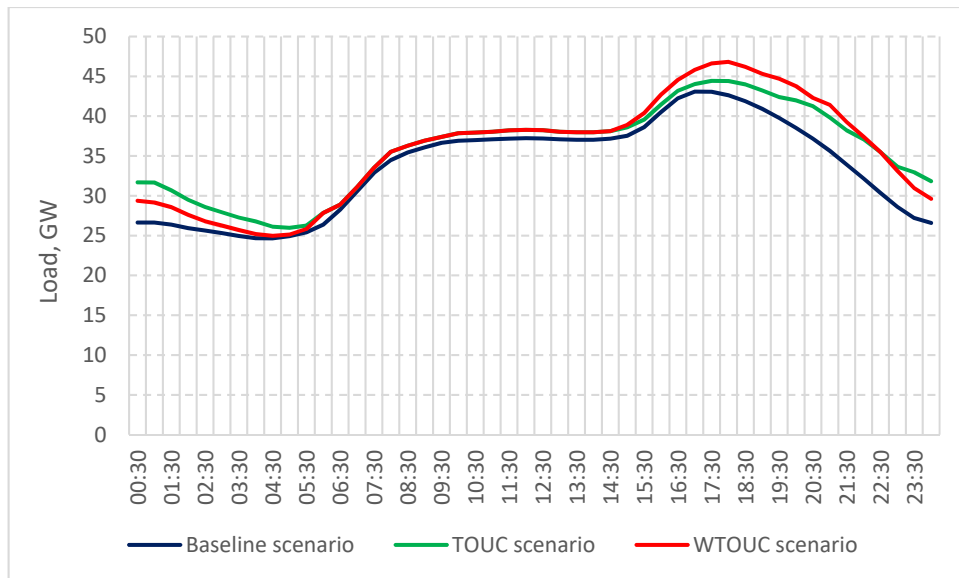


Fig. 3.10 Half-hourly system average load demand

Table 3.11 gives the system parameters in terms of the emission factors, thermal efficiencies and operating costs of the different generating technologies with transmission-entry-capacity that made up the system as at December 2015.

Table 3.11 Parameters of the generating technologies

Generating Technology	Emission factor (CO ₂ kg/kWh) [122], [136]*	Thermal efficiency (%) [122], [137]*	Variable Operating cost (£/MWh) [138]	Levelised Operating cost (£/MWh) [138]
CCGT	0.23	47	64.30	80.00
Coal	0.39	36	62.40	104.00
Hydro	-	-	-	83.00
Nuclear	-	40	7.40	99.00
OCGT	0.18	42	80.30	90.50
Pumped	-	-	-	118.00
Onshore wind	-	-	-	94.00
Offshore wind	-	-	-	161.00
Biomass	0.19*	29*	33.70	93.20
Interconnector	-	-	60.00	60.00

3.3.5 Results and Discussion

The results of the model deployment are presented on scenario basis. Thereafter, comparison and analysis of the results are made.

3.3.5.1 Results for Baseline scenario

Fig. 3.11 shows the half-hourly electricity generation from different generating technologies as dispatched in the Baseline scenario according to the model. Fig. 3.12 is the detail of the daily average contributions of different generating technologies in the Baseline scenario.

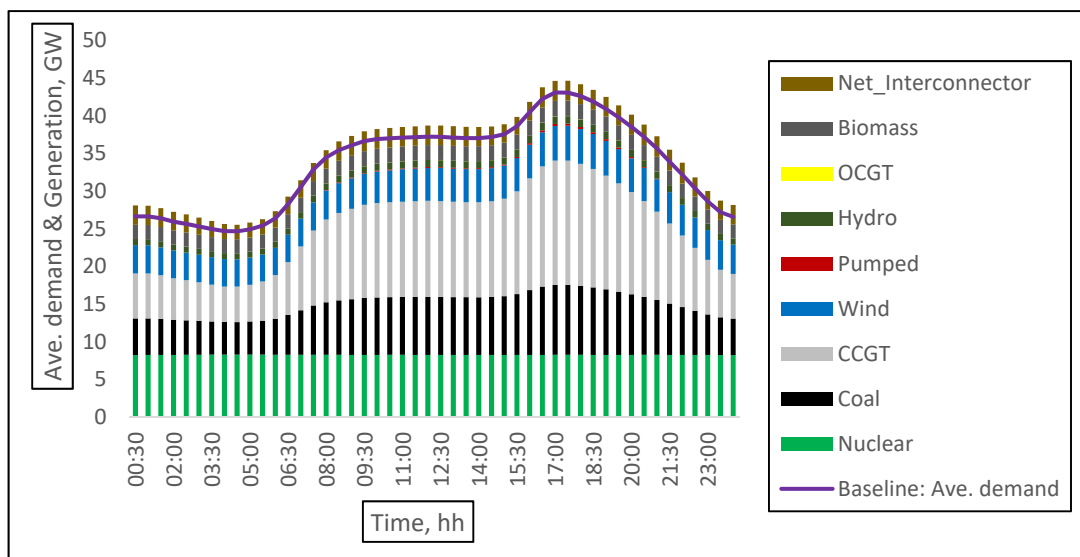


Fig. 3.11 Baseline: Half-hourly generation from different generating technologies (modelled)

Both Fig. 3.11 and Fig. 3.12 respectively are very much comparable to **Fig. 3.6** and **Fig. 3.7** of **Section 3.3.2**. Fig. 3.6 and Fig. 3.7 were produced from historical data and their compatibility with Fig 3.11 and Fig. 3.12, which are products of the proposed dispatch model, gives confidence in the model.

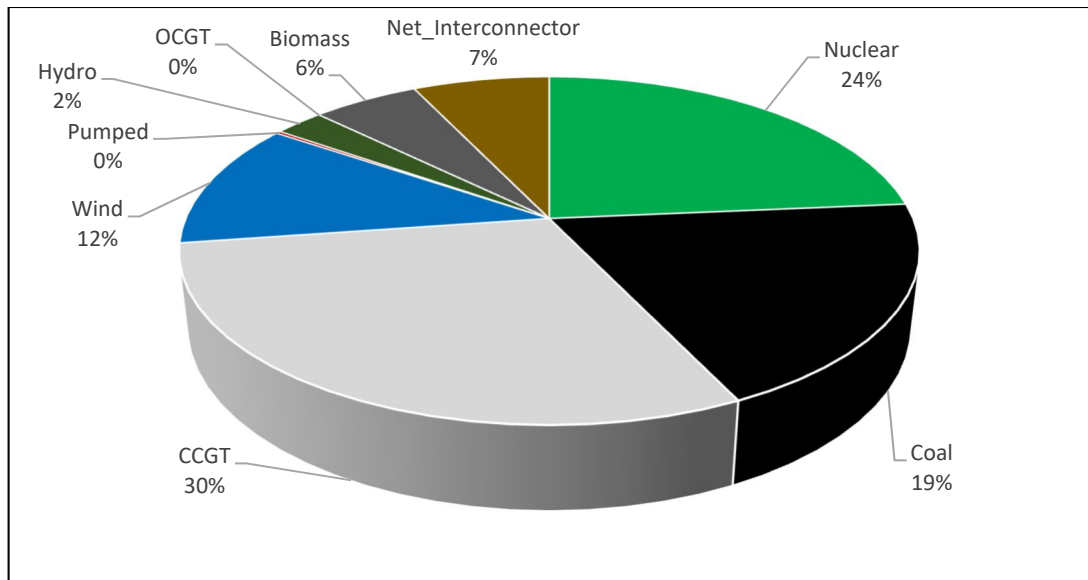


Fig. 3.12 Baseline: Daily average contributions from different generating technologies (modelled)

The marked observation between Fig. 3.11 and Fig. 3.6 is that whereas in Fig. 3.6, there is no mismatch between the average load demand and the generation but in Fig. 3.11 there is a mismatch of surplus generation of about 3% (total for a whole day) over the load demand.

In terms of contribution to the electricity mix, individual generating technology in Fig. 3.12 compares well with Fig. 3.7.

3.3.5.2 Results for TOUC scenario

Fig. 3.13 and Fig. 3.14 show the half-hourly electricity generation from different generating technologies as dispatched according to the model and the summary of the daily average contributions of different generating technologies respectively for the TOUC scenario. There is surplus generation of about 3% (total for a whole day) over the load demand.

The maximum average load demand is 44GGW with CCGT contributing 32% of the total electricity generation. Pumped and OCGT contributed less than 1% at 5.55GW and 0.11GW respectively.

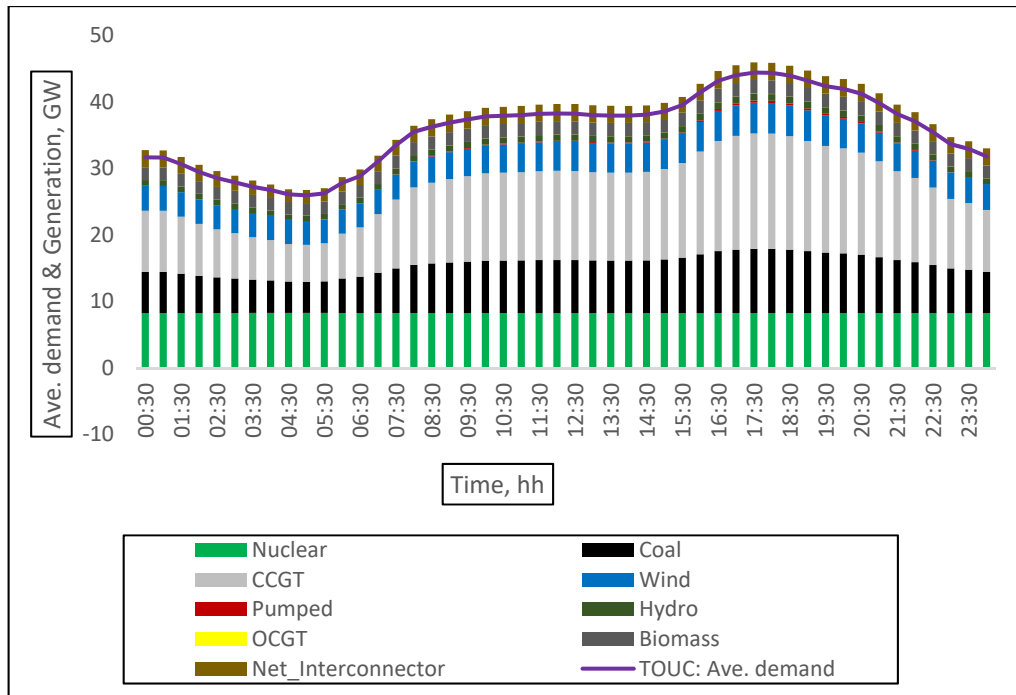


Fig. 3.13 TOUC: Half-hourly generation from different generating technologies (modelled)

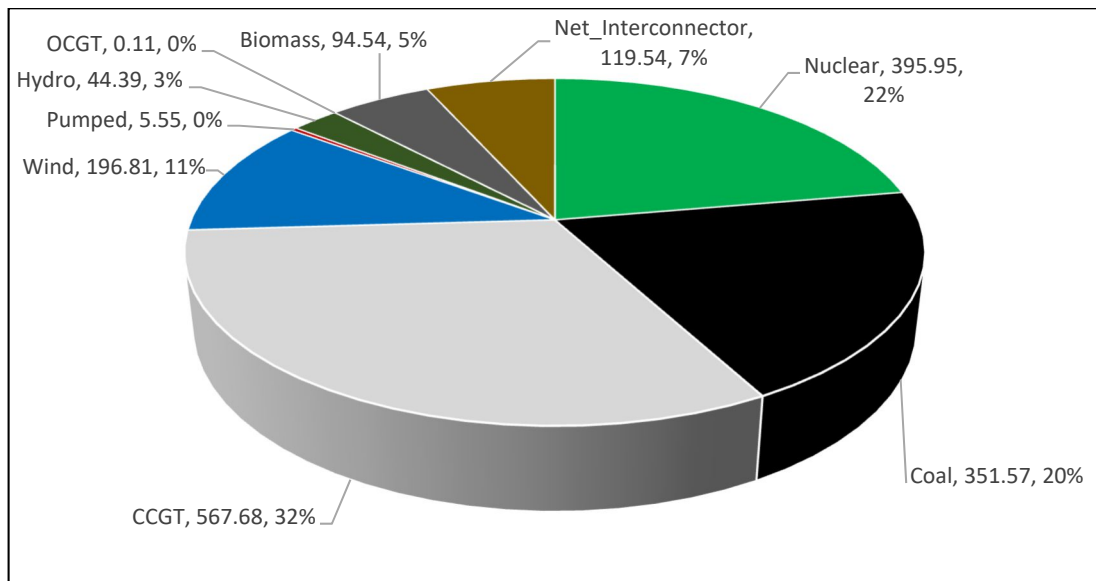


Fig. 3.14 TOUC: Daily average contributions from different generating technologies (modelled)

3.3.5.3 Results for WTOUC scenario

Fig. 3.15 and Fig. 3.16 show the half-hourly electricity generation from different generating technologies as dispatched according to the model and the summary of the daily average contributions of different generating technologies respectively for the WTOUC scenario. There is also in this scenario a surplus generation of about 3% (total for a whole day) over the load demand.

The maximum average load demand is 47GW. The percentage contributions of the different generating technologies are almost the same as in the TOUC scenario. However, electricity generation from Pumped and OCGT increased in this scenario to 6.18GW and 0.12GW respectively, but is still less than 1% of the total electricity generation.

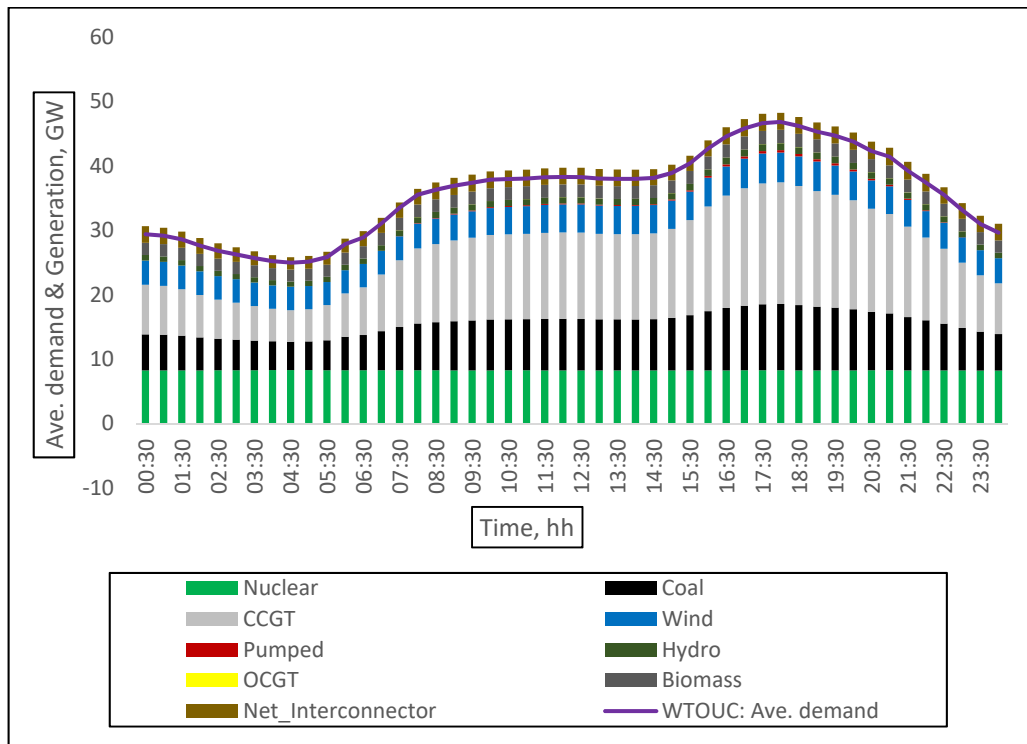


Fig. 3.15 WTOUC: Half-hourly generation from different generating technologies (modelled)

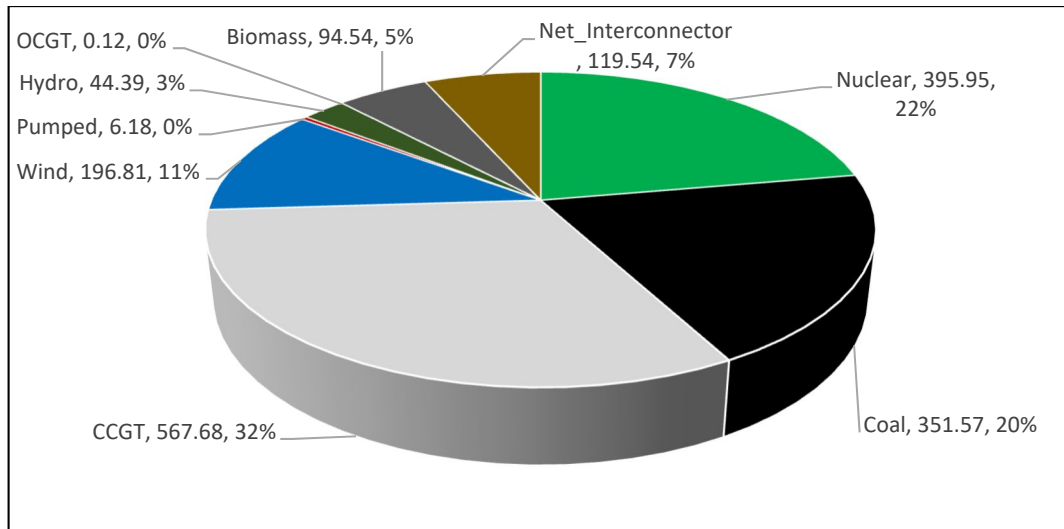


Fig. 3.16 WTOUC: Daily average contributions from different generating technologies (modelled)

3.3.5.4 Comparison and Analysis of results

For each of the scenario, the volume of emissions produced, average grid emissions intensity and electricity generation costs (both levelised cost and variable cost) are calculated. These are presented in Table 3.12.

Table 3.12 Emissions, average grid intensity and generating costs for all scenarios

Scenario	Emissions produced (ktCO ₂)	Average grid emissions intensity (gCO ₂ /kWh)	Variable generating cost (£M)	Levelised generating cost (£M)
Baseline	321.79	406	32.81	78.91
TOUC	353.64	422	35.87	83.25
WTOUC	353.65	419	35.87	83.29

The emissions produced in both TOUC and WTOUC scenarios are almost the same at a value of **354ktCO₂**. This is because the contributions of the emissions-producing generating technologies to the electricity mix are almost the same in both TOUC and WTOUC scenarios except for OCGT which slightly contributed more (by **0.01GW**) in WTOUC as seen in Fig. 3.14 and Fig. 3.16 respectively. The marginal increase in grid emissions above the baseline in both TOUC and WTOUC is therefore **32ktCO₂**.

The Baseline average grid emissions intensity is **406gCO₂/kWh**. However, notwithstanding the fact that almost the same the volume of emissions was produced in both TOUC and WTOUC scenarios, the average grid emissions intensities of the

TOUC and WTOUC scenarios are **422gCO₂/kWh** and **419gCO₂/kWh** respectively. The disparity between the average grid emissions intensities of TOUC and WTOUC is because of the difference in aggregated mix outputs of the generating technologies at some instances. Fig. 3.17 shows the grid emissions intensity profiles of all the scenarios over a 24-hour period. The average grid emissions intensity of the WTOUC is, however, lower than that of TOUC because the Pumped hydro technology slightly contributed more (by 0.63GW) in WTOUC than in TOUC, (see Figs. 3.14 and 3.16).

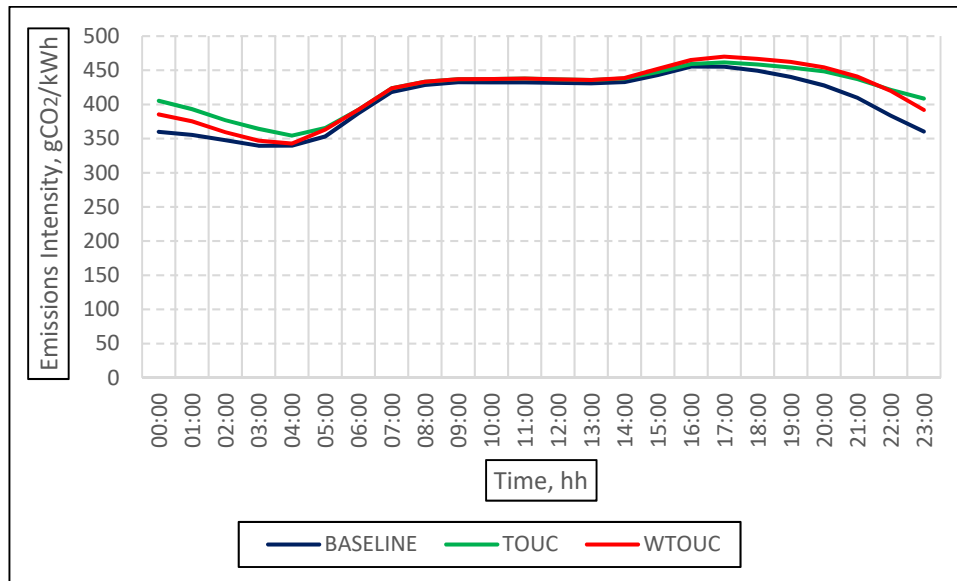


Fig. 3.17 Grid emissions intensities of the scenarios

Using the reported 2015 average new car CO₂ emissions of 121.4g/km [139], the emissions savings on the road, on a day in December 2015, due to 50% uptake of EVs is calculated according to equation (3.16) to be **66.29ktCO₂**. The net emissions reduction in both TOUC and WTOUC is therefore calculated to be **34.29ktCO₂** according to equation (3.17).

The variable generating cost in the Baseline scenario is £32.81M. While the variable generating costs in both TOUC and WTOUC are the same at £35.87M. This is so because the contributions of the generating technologies in both TOUC and WTOUC are almost the same except for OCGT and Pumped hydro technologies which slightly contributed more in WTOUC. However, the extra contribution of OCGT in WTOUC is insignificant (0.01GW) to affect the total cost. Also, the extra contribution of the Pumped hydro in WTOUC is at no variable cost since the variable generating cost of the Pumped hydro is assumed to be zero in this work. Therefore, the marginal increase in the variable generating cost above the baseline is **£3.06M** in both TOUC

and WTOUC. The emissions abatement cost in terms of the variable generating cost in both TOUC and WTOUC is calculated to be **£89.24/tCO₂** according to equation (3.18).

Marginal increase in the levelised generating costs above the baseline in both TOUC and WTOUC are **£4.34M** and **£4.38M** respectively. This is because the levelised generating cost in WTOUC is higher due to the extra contribution of the Pumped hydro technology. Therefore, the emissions abatement costs in terms of the levelised generating costs in both TOUC and WTOUC are **£126.57/tCO₂** and **£127.73/tCO₂** respectively. Table 3.13 summarises the comparison of the TOUC and WTOUC scenarios.

Table 3.13 Comparison of TOUC and WTOUC scenarios

Scenario	Net emissions reduction (ktCO ₂)	Marginal increase in generating cost (£M)		Emissions abatement cost (£/tCO ₂)	
		Variable	Levelised	Variable	Levelised
TOUC	34.29	3.06	4.34	89.24	126.57
WTOUC	34.29	3.06	4.38	89.24	127.73

3.4 SUMMARY

In this Chapter, two studies were carried out to empirically investigate the integration of EVs in the road transportation sector and its impacts on the UK power grid as it relates to GHG emissions reduction.

In the first study, an algorithm was developed to empirically estimate, from historical data, the annual ‘Real-Emissions-Reduction’ (RER) in the UK road transportation sector due to the integration of EVs from 2009 to 2013. The algorithm considered the extra electricity due to the charging of the EVs on the grid without particular interest on the charging pattern.

The CO₂ emissions was estimated on the basis of converting total annual fuel used in electricity generation to their tonnes of oil equivalent (toe). Results of the algorithm showed the following:

- RER decreased in 2010 to 1.3ktCO₂ from 1.5ktCO₂ in 2009.
- RER increased steadily from 2.2ktCO₂ in 2011 to 4.6ktCO₂ in 2013.

- Average emissions intensity of ICE cars decreased steadily from 173gCO₂/km in 2009 to 159gCO₂/km in 2013.

In the second study, a dispatch model for generating technologies/resources was developed based on the correlation between historical system load demand and capacity factors of the generating technologies/resources.

The model was deployed to dispatch generating technologies/resources under two charging patterns of EVs. In one charging pattern designated as TOUC (Time-Of-Use-Charging), the charging pattern was based on the time of use tariff. And the other charging pattern designated as WTOUC (Without-Time-Of-Use-Charging), was not patterned after time of use tariff but instead assumed the EV owners charged their cars at their own will.

Analyses were then carried out on the impacts of the charging patterns on the scheduling of the generating technologies/resources, net emissions reduction and the emissions abatement costs. The results of the study showed the following:

- The contributions of the generating technologies/resources into the total electricity generated were almost the same in both TOUC and WTOUC except for the slight extra contributions of Pumped (0.63GW) and OCGT (0.01GW) in the WTOUC scenario.
- Emissions produced in both TOUC and WTOUC scenarios were almost the same at 354ktCO₂. Therefore, net emissions reduction in both scenarios was almost the same at 34.29ktCO₂.
- Average grid emissions intensity was lower in WTOUC at 419gCO₂/kWh than in TOUC at 422gCO₂/kWh.
- Both TOUC and WTOUC had same variable generating cost of £35.87M. But WTOUC had higher levelised generating cost £83.29M than TOUC of £83.25M.
- Emissions abatement cost based on variable generating cost in both scenarios were the same at £89.24/CO₂. However, emissions abatement cost based on levelised generating cost was higher in WTOUC at £127.73/tCO₂ than in TOUC at £126.57/tCO₂.

CHAPTER 4

LOW CARBON TECHNOLOGIES INTEGRATION IN LOW VOLTAGE DISTRIBUTION NETWORK

4.1 INTRODUCTION

This chapter investigates and analyses the impacts of integration of LCTs, with focus on EVs and HPs, on the LV distribution network. The UK has a policy target of 80% reduction of GHG emissions with respect to the 1990 level by the year 2050 [69]. The realization of the target will involve a transition from fossil fuel based to low carbon-based electricity generation and consumption. Data from [140] revealed considerable potential that could be leveraged on in cutting down GHGs emissions in the UK, if more HPs are replacing gas-boilers for residential heating and more EVs replacing conventional ICE cars for transportation. Therefore, the uptake of HPs and EVs are expected to increase in the drive to reducing the GHGs emissions. Increasing uptake of HPs and EVs would constitute additional electricity load demand at the LV distribution network.

It is assumed that most EV owners will charge their cars at home [141], [142]. For this reason, the focus of the investigation and analysis is on LV distribution network serving residential area. National projection figures of different uptake scenarios of EVs and HPs as presented in the National Grid's Future Energy Scenarios document [143] were scaled down to the level of the real and typical residential LV network used as case study. National Grid's Future Energy Scenarios is presenting a number of "*plausible and credible pathways for the future of energy, from today out to 2050*". These scenarios are developed based on the energy trilemma of security, affordability and sustainability.

Average typical winter weekday and summer weekday demand profiles of HP and average daily charge requirement of EV were modelled. Gridlab-D, an agent-based power system simulation software [144]–[146], was employed to perform a power flow simulation study of the LV network. The simulation was run for four different scenarios considering seasonal load profiles and projected EVs and HPs uptakes for

each of the year 2020, 2030, 2040 and 2050 respectively. The results were analyzed in terms of transformer loading, voltage profiles of the feeders, and the ampacity loading of the cables for the different scenarios of the years.

4.2 DESCRIPTION OF SCENARIOS

Four scenarios were created each for the year 2020, 2030, 2040 and 2050. The scenarios are based on two factors:

- i) **Uptake of HPs and EVs:** Two uptake scenarios are considered - Steady State (SS) scenario and Two Degrees (TD) scenario. Both scenarios are adapted from [143]. SS scenario depicts a business-as-usual scenario with less prosperous economic growth, little innovation in renewable energy resources (RESs) and LCTs and limited political drive to encourage the populace to embrace greener LCTs. In SS scenario, technological innovation and investment are business as usual characterized by low risk and short-term value approach, which focus on security of supply at affordable cost. The scenario name ‘Two Degrees’ is culled from the Article 2 of the Paris Agreement [68] and it indicates the target of holding the increase in the global average temperature to well below 2°C above the pre-industrial levels. The TD depicts a scenario of prosperous economic growth, increased focus on RESs and LCTs, and strong political drive to achieve the renewable integration and all of UK’s 2050 emissions reduction targets. It is a scenario in which technology and investment are focused on innovation in RESs (solar and wind) and low carbon (nuclear) generation.
- ii) **Season of the year:** Two seasonal load profiles are considered under this factor – typical Summer weekday (SmrWd) and typical Winter weekday (WtrWd) load profiles.

The four scenarios are therefore:

- (1) Steady State Summer Weekday (SSSmrWd)
- (2) Steady State Winter Weekday (SSWtrWd)
- (3) Two Degrees Summer Weekday (TDSmrWd) and

(4) Two Degrees Winter Weekday (TDWtrWd)

4.3 DETAILS OF THE CASE STUDY LV NETWORK

In this study, a real and typical urban LV network in Cardiff area from the project in [147] is used as the case study. The area is supplied by a 500-kVA, 11/0.415-kV (no load), 50-Hz, Dyn11, ONAN mineral oil filled, free breathing, ground mounted transformer. The transformer supplies 298 buildings in four feeders. Fig. 4.1 is the simplified diagram of the LV network and Table 4.1 gives the analysis of the number of buildings per feeder, annual baseline load of the feeders in 2014 and the length of the feeders.

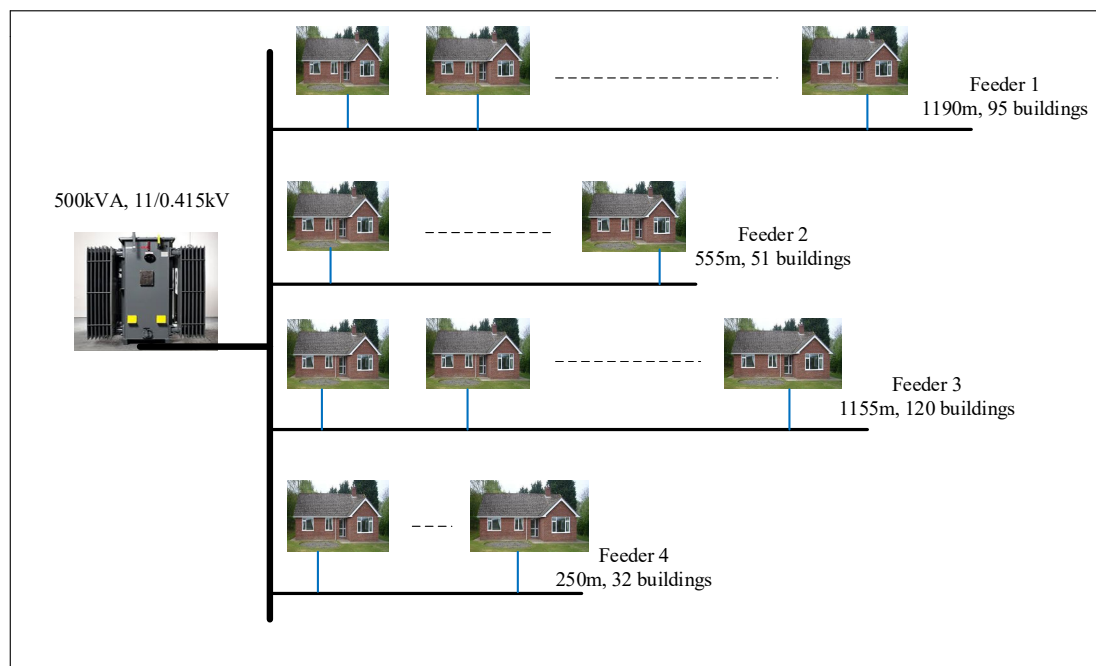


Fig. 4.1 Simplified diagram of the case study LV network

Analysis of the feeders indicates that both Feeders 1 and 2 have feeder density of approximately 8 and 9 buildings per 100m length of the feeder respectively. Feeders 3 and 4, on the other hand, both have feeder density of approximately 11 and 13 buildings per 100m length of the feeder respectively.

Table 4.1 Feeders Analysis [147]

Feeder	2014 Annual load (kWh)	Length (m)	Number of Buildings (Units)
1	360,782.4	1190	95
2	202,291.8	555	51
3	402,697.1	1155	120
4	108,936.0	250	32
	1,074,707.30		298

4.4 CALCULATION TO DETERMINE FUTURE BASELINE ELECTRICITY DEMAND PROJECTION FOR THE LV NETWORK

Here, residential baseline electricity demand is described as that which excludes the electricity demand of EVs and HPs. Projected residential annual baseline electricity demand in the GB for 2020, 2030, 2040 and 2050 are estimated from the breakdown analysis of annual demand in [143]. Residential annual electricity demand in the GB in 2014, which is the reference year in this work, was 109TWh [122]. In 2014, the uptake levels of both EVs and HPs were insignificant, and their combined electricity demand was not visible in the total residential annual electricity demand presented in [143] and [122]. Therefore, residential annual electricity demand in 2014 is regarded as ‘reference baseline’ in the context of this work. Residential relative baseline electricity demands for 2020, 2030, 2040 and 2050 with respect to 2014 are calculated. Table 4.2 gives the summary of the residential annual baseline demands for 2014, projected residential annual baseline demand for 2020, 2030, 2040 and 2050 with their respective relative baseline demand with respect to 2014 residential annual baseline demand in the GB.

Table 4.2 GB Residential Annual Baseline Demand and Relative Baseline Demand

Year	Annual Baseline Demand (TWh) [143]	Relative Baseline Demand (calculated with respect to year 2014)
2014	109	1.00
2020	112	1.03
2030	113	1.04
2040	118	1.08
2050	129	1.18

Given the 2014 residential annual electricity demand of the case study LV network, then its projected future annual baseline electricity demand can be obtained by equation (4.1)

$$LV_{baseline_dmd(yr)} = LV_{baseline_dmd(2014)} \times Rel_{(yr)} \quad (4.1)$$

Where:

$LV_{baseline_dmd(yr)}$ is the projected LV network annual baseline electricity demand (MWh) of a particular year.

$LV_{baseline_dmd(2014)}$ is the baseline electricity demand (MWh) of the case study LV network in 2014.

$Rel_{(yr)}$ is the relative baseline demand of a particular year with respect to 2014 and

yr is the year identifier index.

With equation (4.1), the projected future annual baseline electricity demand of the case study LV network in 2020, 2030, 2040 and 2050 are calculated. Table 4.3 gives the results of this calculation.

Table 4.3 Calculated Projected Annual Baseline Demand of the LV Network

Year	Annual Baseline Load Demand (MWh)
2020	1,107
2030	1,118
2040	1,161
2050	1,268

Based on the normalisation of load profiles from [148], projected annual baseline demand of the LV network for the respective years are converted to half-hourly seasonal (summer weekday and winter weekday) daily profiles.

The relative baseline demand figures in Table 4.2 above indicate changes in the future residential electricity demand. Over the 10 years from 2020 to 2030, the residential electricity demand barely increases. The Compound Annual Growth Rate (CAGR) of residential annual baseline electricity demand during the period is 0.1% as calculated by equation (4.2).

$$Baseline_{CAGR} = \left[\left(\frac{Baseline_{end}}{Baseline_{start}} \right)^{1/n} - 1 \right] \times 100\% \quad (4.2)$$

Where:

$Baseline_{CAGR}$ is the compound annual growth rate of the baseline electricity demand.

$Baseline_{end}$ is the baseline electricity demand (MWh) at the end of the period.

$Baseline_{start}$ is baseline electricity demand (MWh) at the start of the period and

n is the time duration of the period in years.

The two counter acting factors responsible for the trend are increase in number of households [149] and declining electricity demand in the residential sector [150].

Factors responsible for the declining electricity demand in the residential sector are decrease in average household size [149], increase in ownership of new and more energy efficient appliances [151], improved building insulation [151] and increase in electricity retail prices [152]. The CAGR of residential baseline electricity demand in the periods 2030–2040 and 2040–2050 are 0.4% and 0.9% respectively. Over the two-decade interval, number of households keeps increasing [149] whereas average household size and ownership of new and more energy efficient appliances figures are settling [149], [151]. This explains the rise in the CAGR from 0.4% to 0.9% during the periods.

The implication of low CAGR (0.1%), in spite of the increase in the number of households between 2020 and 2030 [149], is that more customers would need to be served by the Distribution Network Operators (DNOs) for disproportional and marginal increase in electricity demand in the residential sector. This condition is not business friendly and the DNOs may review residential electricity retail price upward to cover for additional resources committed to serving the increasing customers. However, with uptake of EVs and HPs the electricity demand from the residential sector is expected to increase considerably. This is because most EV owners, more than 80%, find their homes to be the most convenient locations to recharge their EVs [153], [142]. With the anticipated increasing uptake of EVs and HPs over the coming years up onto 2050, the CAGR of electricity demand from the residential sector is expected to increase rapidly over that period. Rapid increase of residential electricity demand due to uptake of EVs and HPs presents the DNOs with both technical challenges and business opportunities. Technical challenges because of the concern that distribution system might be stressed and business opportunities because consumers' energy spending is shifting from the oil and gas to the electricity industry.

4.5 CALCULATION TO DETERMINE EVS UPTAKE PROJECTIONS FOR THE LV NETWORK

The projected future number of cars in the GB up unto 2050 is first calculated. The calculation of the projected future number of cars in the GB is based on extrapolation from historical data of the number of cars in the GB [154], population of the GB [155], and the number of households in the GB [149], [156]. Fig. 4.2 and Fig. 4.3 show the

trend in average household size, cars per household and cars per head of population in the GB between 1994 and 2017.

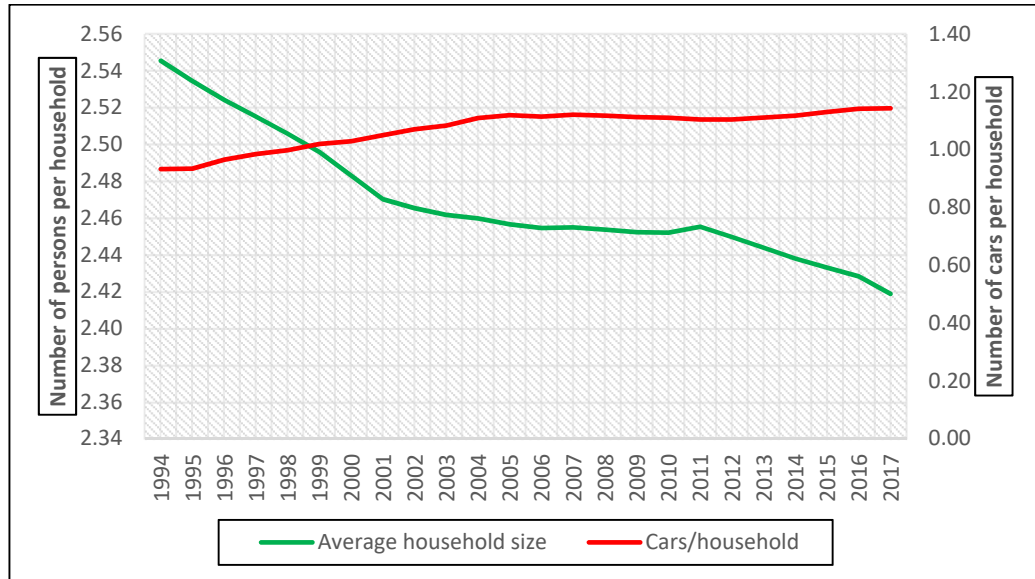


Fig. 4.2 Average household size and cars per household in GB, 1994-2017

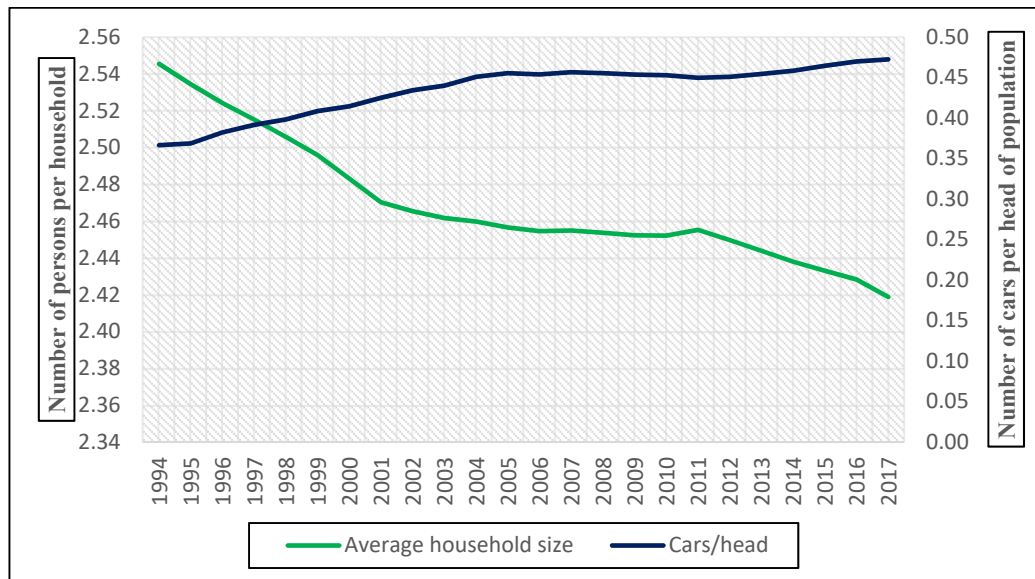


Fig. 4.3 Average household size and cars per head of population in GB, 1994-2017

As seen from Fig. 4.2 and Fig. 4.3 both cars per household and cars per head of population share similar trend in their relationship with the average household size. In both cases as the average household size in GB decreased by approximately 0.4% between 1994 and 2004, cars per household and cars per head both increased by almost 2.0% in the same period. Many economic and social factors, which are outside the

scope of the present work, could be responsible for declining trend in the average household size. However, the somewhat inverse relation between average household size and cars per household could be explained thus; two persons of the same household sharing a car may end up with two cars if one person goes out to form another household. Therefore, in GB, car ownership (hence number of cars) is associated with number of households and household size. In the last 10 years (2007-2017), the average household size changed slightly by an annual decrease of 0.1%. Similarly, over the same period, both cars per household and cars per head figures increased at an annual rate of 0.2% each. For the rest of this work, it is assumed that the average household size decreases by 0.1% annually, while cars per household and cars per head figures both increase by 0.2% annually up unto 2050.

Average household size, cars per household and cars per head of the population are calculated up unto 2050 based on this assumption. Then from projected number of households in GB [149], [156] and the projected population [155], [157], projected number of cars are calculated by either equation (4.3) or (4.4).

$$Cars_{projected(yr)} = Cars_{perHH(yr)} \times HH_{projected(yr)} \quad (4.3)$$

$$Cars_{projected(yr)} = Cars_{perH(yr)} \times Population_{projected(yr)} \quad (4.4)$$

Where:

$Cars_{projected(yr)}$ is the projected number of cars (Millions) in a particular year.

$Cars_{perHH(yr)}$ is the number of cars per household in a particular year

$HH_{projected(yr)}$ is the projected number of households (Millions) in a particular year.

$Cars_{perH(yr)}$ is the number of cars per head of population in a particular year.

$Population_{projected(yr)}$ is the projected population (Millions) in a particular year.

The results of the calculations are shown in Table 4.4

Table 4.4 Average household size, cars/household, cars/head and number of cars GB, 2020-2050

Year	Ave. Household size (calculated)	Cars per Household (calculated)	Cars per Head (calculated)	Population (Millions) [155], [157]	Number of households (Millions) [149], [156]	Number of cars (Millions) (calculated)
2020	2.41	1.15	0.47	67	28	32
2030	2.39	1.17	0.48	71	30	35
2040	2.36	1.19	0.49	75	32	38
2050	2.34	1.21	0.50	78	33	40

The percentage error between the average household size calculated based on the assumption earlier made from the its relationship with cars per household and the average household size calculated from the projected population and projected number of households is less than 1% in 2020, 2030, 2040 and 2050. The low percentage error figure justifies the assumption.

Projected percentage of future uptake of EVs in TD and SS scenarios are now calculated. The calculation is based on the projected number of EVs in GB in each scenario up unto 2050 as reported in [143] and the calculated projected future number of cars up unto 2050. Table 4.5 shows the results of the calculation for the percentage of future uptake of EVs.

Table 4.5 Percentage uptake of EVs GB, 2020-2050

Year	Number of cars (Millions) (calculated)	Number of EVs (Millions) [143]		Percentage EV uptake (%) (calculated)	
		TD	SS	TD	SS
2020	32.0	2.0	0.4	6.3	1.3
2030	35.0	9.0	2.0	25.7	5.7
2040	38.0	17.0	4.0	44.7	10.5
2050	40.0	25.0	7.0	62.5	17.5

Presently, typical household annual average electricity consumption in GB as revised in 2017 is estimated to be 3100kWh [158]. Typical household annual average electricity consumption has been on a declining trend since 2005 [158]–[161]. However, for this study, it is assumed constant at the 2017 revised value. Therefore, total number of households in the LV network can be determined by dividing its annual electricity demand (see Table 4.3) by typical household annual average electricity consumption as expressed in equation (4.5).

$$LV_{NoHH(yr)} = \frac{LV_{baseline_dmd(yr)}}{HH_{typical_dmd(yr)}} \quad (4.5)$$

Where:

$LV_{NoHH(yr)}$ is the number of households in the LV network in a particular year

$LV_{baseline_dmd(yr)}$ is the projected LV network annual baseline electricity demand (MWh) of a particular year.

$HH_{typical_dmd(yr)}$ is the typical household annual average electricity demand (MWh) in a particular year and

yr is the year identifier index.

With the assumption of at least one car per household, the number of future uptake of EVs in each of TD and SS scenario in the LV network for a particular year is the product of the number of households in the LV network and the percentage uptake of EVs for the corresponding year as expressed by equation (4.6).

$$LV_{NoEV(yr)} = LV_{NoHH(yr)} \times EV_{\%uptake(yr)} \quad (4.6)$$

Where:

$LV_{NoEV(yr)}$ is the number of EVs in the LV network in a particular year

$LV_{NoHH(yr)}$ is the number of households in the LV network in a particular year

$EV_{\%uptake(yr)}$ is the percentage uptake of EVs in a particular year and

yr is the year identifier index.

Table 4.6 shows the results of calculation of equations (4.5) and (4.6) for the number of households and number of EVs in TD and SS scenarios.

Table 4.6 Calculated Number of Households and number of EVs per scenario in the LV network, 2020-2050

Year	Number of Households (Units)	Number of EVs (Units)	
		TD	SS
2020	357	23	5
2030	360	93	21
2040	374	167	39
2050	409	256	72

4.6 EVS CHARGING LOAD REQUIREMENT IN THE LV NETWORK

Average daily energy requirement of EVs in the LV network is estimated. In this work, average daily energy requirement of an EV is defined as that amount of kWh by which the battery is depleted at the end of all the day's trips and by which the battery

must be replenished before the start of the next day's trips. Average daily energy requirement of an EV can be quickly estimated by the product of average daily travel distance of the EV and the battery efficiency of the EV as expressed in equation (4.7).

$$EV_{kWh_{daily}} = distance_{daily} \times \eta_{EV} \quad (4.7)$$

Where:

$EV_{kWh_{daily}}$ is the average daily energy requirement (kWh) of an EV.

$distance_{daily}$ is the average daily travel distance (km) of an EV.

η_{EV} is the battery efficiency (kWh/km) of EV.

In this work 2015 Nissan Leaf 24kWh model is chosen as the representative EV. Nissan Leaf is the most popular pure electric car in the UK [27]. 2015 Nissan Leaf 24kWh has a combined city and highway efficiency of approximately 0.2kWh/km and a range of at least 120km on full battery charge [162]. From the National Travel Survey [163], average daily car travel distance in the UK is estimated to be 36km. Therefore, with EV efficiency and average daily car travel distance already established, an EV will need 7.2kWh, which is 30% of the full state of charge (SoC) of the battery, as its average daily energy requirement. In the LV network, the total average daily energy requirement will be the number of EVs in the network multiplied by 7.2kWh as expressed in equation (4.8).

$$LV_{EV_{kWh_{daily}}} = \sum_{i=1}^n EV_i \times 7.2 \quad (4.8)$$

Where:

$LV_{EV_{kWh_{daily}}}$ is the average daily EVs charge requirement (kWh) of the

LV network.

n is the number of EVs in the LV network.

i is the identifier index for EVs.

The constant 7.2 presented in (4.8) is the average daily energy requirement (kWh) of an EV. Equation (4.8) only gives the minimum average daily EVs charge requirement of the LV network, since it assumes 7.2kWh as daily charge requirement for all EVs. In reality, this cannot be the case and can give a misleading optimistic

result of the impact study. Therefore, a more realistic daily EVs charge requirement is proposed. It is assumed that the EV battery should not be depleted below 7.2kWh (30% SoC), the minimum required to guarantee daily average travel distance. This gives the range of daily charge requirement of an EV to be between minimum of 7.2kWh (30% SoC) and maximum of 16.8kWh (70% SoC). A probability distribution function (PDF) of daily charge requirement of 100 EVs (representing 100% for easy normalization) was created with a mean of 12kWh and standard deviation of 3kWh between the minimum of 7kWh and maximum of 17kWh. Fig. 4.4 shows the daily charge requirement distribution.

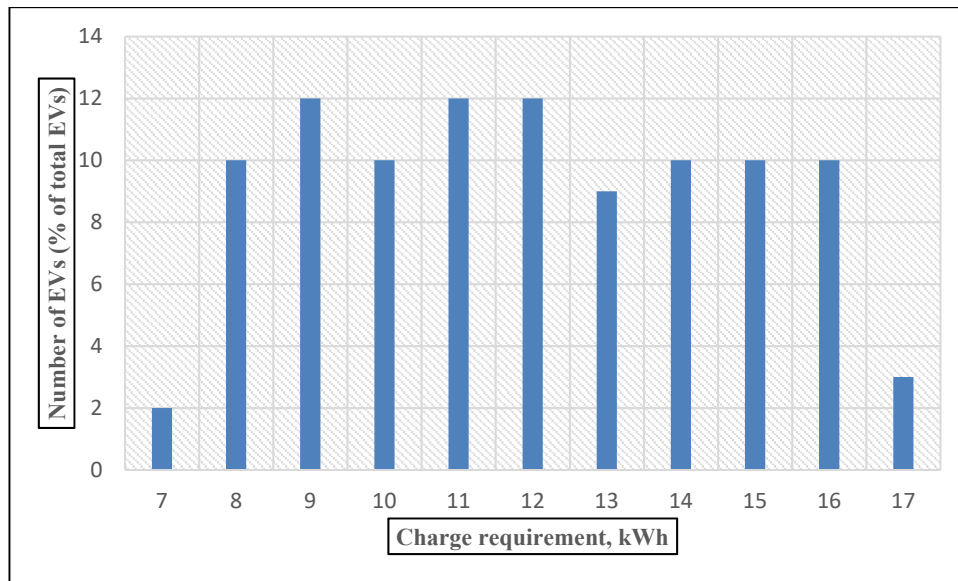


Fig. 4.4 EVs daily charge requirement distribution

From Fig. 4.4, the more realistic daily charge requirement of EVs in the LV network is the sum product of the values of the x and y axes of the bars as expressed by equation (4.9).

$$LV_{EV_{kWh_{daily}}} = \sum_{k=1}^K x_k y_k \quad (4.9)$$

Where:

$LV_{EV_{kWh_{daily}}}$ is the average daily EVs charge requirement (kWh) of the

LV network.

K is the total number of bars.

x is the number of EVs.

y is the charge requirement (kWh).

k is the identifier index for the bars.

The half-hourly percent of average daily charge in [135] is adopted in this work to generate the actual average half-hourly EV charging profile. Data such as number of trips, start and end times of trips, average distance travelled, arrival times at homes, etc. generated from the National Travel Survey and Time Use Survey formed the basis of this charging profile [135]. Fig. 4.5 shows the average half-hourly EV charging profile used in this study.

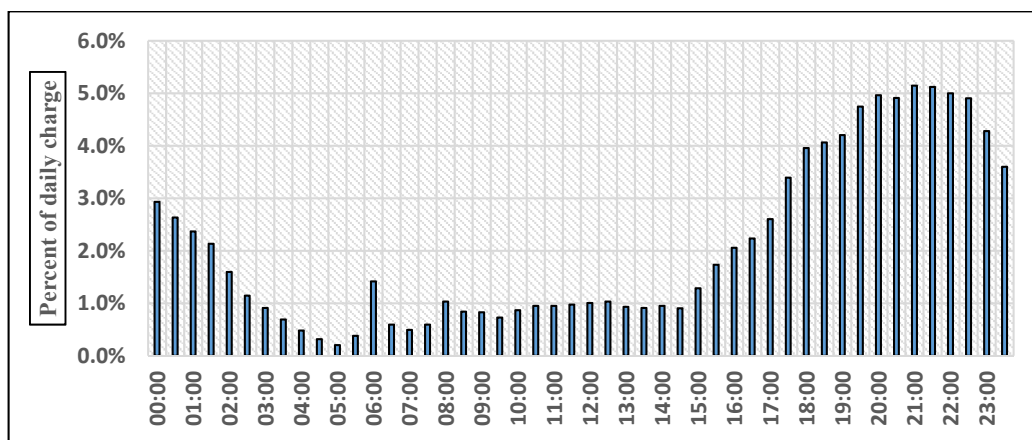


Fig. 4.5 Average half-hourly EV charging profile [135]

From the charging profile of Fig. 4.5, it is seen that the bulk of the charging demand takes place between 16:00 and 00:00 hours. The average peak demand for EV charging, 5.1% of average daily energy requirement, occurs at 21:00 hours.

4.7 CALCULATION TO DETERMINE HPS UPTAKE PROJECTIONS FOR THE LV NETWORK

Projected percentage of future uptake of HPs in TD and SS scenarios are first calculated based on the projected number of HPs uptake in each scenario according to [143] and the number of households as earlier calculated in Table 4.4. Table 4.7 shows the results of the calculation for the percentage of future uptake of HPs.

Table 4.7 Percentage uptake of HPs GB, 2020-2050

Year	Number of Households (Millions) (calculated)	Number of HPs (Millions) [143]		Percentage HP uptake (%) (calculated)	
		TD	SS	TD	SS
2020	28	0.43	0.24	1.5	0.9
2030	30	3.74	0.72	12.5	2.4
2040	32	8.09	0.86	25.3	2.7
2050	33	16.69	0.91	50.6	2.8

With the previous estimate of the number households in the LV network area (see Table 4.6), the uptake number of HPs in each scenario can be determined. The number of future uptake of HPs in each of TD and SS scenario in the LV network for a particular year is the product of the number of households in the LV network and the percentage uptake of HPs for the corresponding year as expressed in equation (4.10).

$$LV_{NoHP(yr)} = LV_{NoHH(yr)} \times HP_{\%uptake(yr)} \quad (4.10)$$

Where:

$LV_{NoHP(yr)}$ is the number of HPs in the LV network in a particular year

$LV_{NoHH(yr)}$ is the number of households in the LV network in a particular year

$HP_{\%uptake(yr)}$ is the percentage uptake of HPs in a particular year and

yr is the year identifier index.

Table 4.8 shows the results of the calculation for the number of future uptake of HPs in TD and SS scenarios.

Table 4.8 Calculated Number of Households and number of HPs per scenario in the LV network, 2020-2050

Year	Number of Households (Units)	Number of HPs (Units)	
		TD	SS
2020	357	5	3
2030	360	45	9
2040	374	95	10
2050	409	207	12

4.8 MODELLING THE HP OPERATION

The operation of variable speed Air Source Heat Pump (ASHP) providing both space heating (SH) and domestic hot water (DHW) is modelled. The operation of variable speed ASHP is dynamic in that the heat output and the coefficient of performance (COP) of the HP vary with the heating demand of the building it is installed in and the external temperature respectively. Fig. 4.6, adapted from [164], illustrates the block diagram of HP system configuration modelled in this work. The HP system configuration is such that the provision for DHW and SH are mutually exclusive. The DHW provision has priority control in the event of DHW demand and SH demand occurring at the same time. In this event, the DHW demand is met first and then the SH demand. This design configuration is the most common in the market [164]–[166].

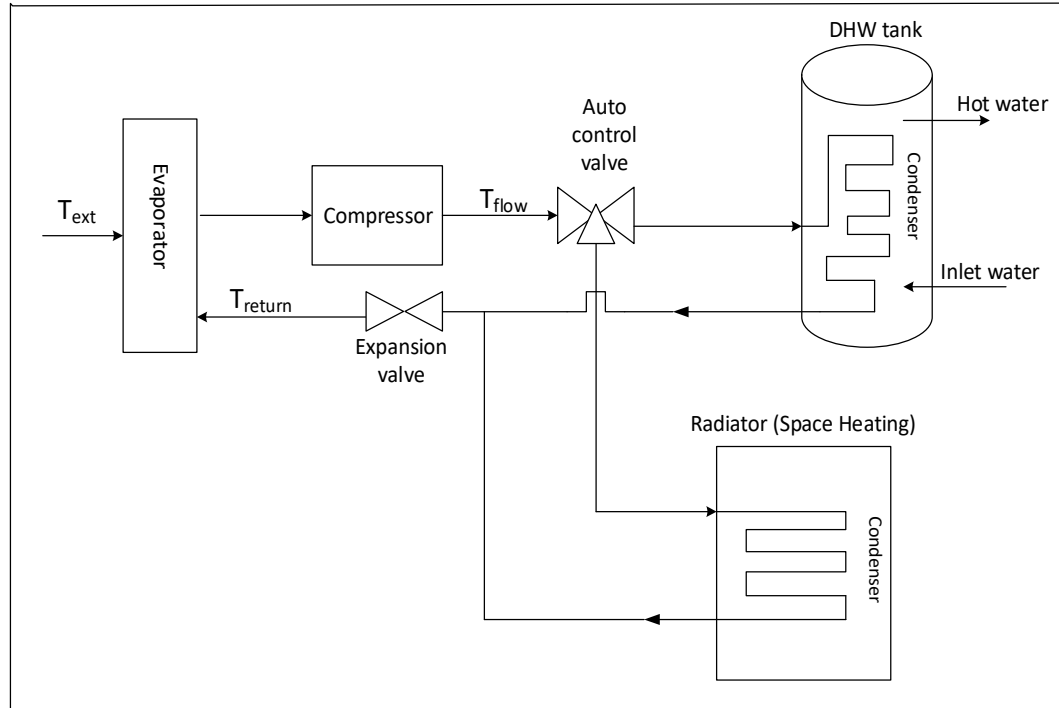


Fig. 4.6 Block diagram of HP System Configuration (adapted from [164])

4.9 MODEL FORMULATION OF HP OPERATION IN SH MODE

The formula, as adapted from [167], for the internal air temperature of the building after a time slot t is given as by equation (4.11):

$$T_{int(t+1)} = T_{int(t)} - (Q_{loss(t)} - Q_{gain(t)} - HP_{SH(t)} \cdot y(t)) \frac{\Delta t}{\Delta q} \quad (4.11)$$

Where:

$T_{int(t+1)}$ is the internal air temperature ($^{\circ}C$ or K) of the building after a time slot t .

$T_{int(t)}$ is the internal air temperature ($^{\circ}C$ or K) of the building in time slot t .

$Q_{loss(t)}$ and $Q_{gain(t)}$ are the heat loss (W) and heat gain (W) of the building in time slot t .

$HP_{SH(t)}$ is the heat output (W) of the HP in SH mode in time slot t .

$y(t)$ is binary variable which determines the operational status (ON = 1 or

OFF = 0) of the HP in SH mode in time slot t .

Δt is the duration of the time slot in (s).

Δq is the energy needed to change the internal air temperature of the building by $1^\circ C$ $\left(\frac{J}{^\circ C}\right)$.

The heat loss of a building is the sum of heat loss through the fabric of the building (floors, walls, roof, windows and doors) and the heat loss due to ventilation/infiltration [168]. The heat loss, $Q_{loss(t)}$, of the building in time slot t is given by equation (4.12):

$$Q_{loss(t)} = (\sum(AU) + 0.3N_{ac}V) \times (T_{int(t)} - T_{ext(t)}) \quad (4.12)$$

Where:

U is thermal transmittance $\left(\frac{W}{m^2K}\right)$.

A is surface area through which heat transfer occurs (m^2).

N_{ac} is the number of air changes per hour $\left(\frac{ac}{h}\right)$.

V is the volume of the building (m^3).

$T_{int(t)}$ is the internal air temperature ($^\circ C$ or K) of the building in time slot t .

$T_{ext(t)}$ is external air temperature ($^\circ C$ or K) in time slot t .

The heat gain, $Q_{gain(t)}$, of the building in time slot t is given by equation (4.13):

$$Q_{gain(t)} = (Q_p \times N_p) + (A_{SW} \times SHGC \times S_{rad(t)}) \quad (4.13)$$

Where:

Q_p is heat gain from one person (W).

N_p is number of occupants.

A_{SW} is area of window facing south (m^2).

$SHGC$ is solar heat gain coefficient of window.

$S_{rad(t)}$ is solar irradiance $\left(\frac{W}{m^2}\right)$ in time slot t .

The energy needed to change the internal air temperature of the building is given by equation (4.14):

$$\Delta q = C_{air} \times \rho_{air} \times V \quad (4.14)$$

Where:

C_{air} is specific heat capacity of air for typical room condition $\left(\frac{J}{Kg^{\circ}C}\right)$.

ρ_{air} is density of air $\left(\frac{Kg}{m^3}\right)$.

V is the volume of the building (m^3).

The operational status, $y_{(t)}$, of the HP in SH mode is represented by equation (4.15):

$$y_{(t)} = \begin{cases} 1 = ON, & T_{int(t)} < T_{set} - T_{sg} \\ 0 = OFF, & T_{int(t)} > T_{set} + T_{sg} \\ y_{(t-1)}, & T_{set} - T_{sg} \leq T_{int(t)} \leq T_{set} + T_{sg} \end{cases} \quad (4.15)$$

Where:

$T_{int(t)}$ is the internal air temperature ($^{\circ}C$ or K) of the building in time slot t .

T_{set} is the set-point temperature of the internal air ($^{\circ}C$ or K).

T_{sg} is the swing temperature ($^{\circ}C$ or K).

$y_{(t-1)}$ is the operational status of the HP in previous time slot.

In equation (4.15), T_{set} is the desired internal air temperature and therefore the thermostat set-point. If the actual internal air temperature, $T_{int(t)}$, drops below the temperature lower limit, T_{low} , which is the difference between T_{set} and T_{sg} , then the HP is switched ON to raise the internal air temperature. Conversely, when the internal air temperature rises above the temperature upper limit T_{up} , which is the sum of T_{set} and T_{sg} , the HP switches OFF. However, the operational status of the HP remains unchanged if the internal air temperature is between T_{low} and T_{up} .

Ignoring losses, the heat output of the HP in SH mode is equal to the radiator output which is also equal to the condenser output. That is:

$$HP_{SH(t)} = Q_{condenser(t)} = Q_{radiator(t)} \quad (4.16)$$

Where:

$HP_{SH(t)}$ is the heat output (W) of the HP in SH mode in time slot t .

$Q_{condenser(t)}$ is the condenser heat output (W) in time slot t

$Q_{radiator(t)}$ is the radiator heat output (W) in time slot t .

The heat flux inside the condenser of the HP can be expressed as:

$$Q_{condenser(t)} = mc(T_{flow} - T_{return(t)}) \quad (4.17)$$

Where:

m is the mass flow rate ($\frac{kg}{s}$) of water.

c is the specific heat capacity ($\frac{J}{kg^{\circ}C}$) of water.

T_{flow} is the operating temperature ($^{\circ}C$ or K) of the working fluid reaching the condenser and

$T_{return(t)}$ is the temperature ($^{\circ}C$ or K) of the working fluid leaving the condenser.

The heat output of the radiator can be expressed as:

$$Q_{radiator(t)} = U_{rad}A_{rad}(T_{rad(t)} - T_{int(t)}) \quad (4.18)$$

Where:

U_{rad} is the heat transmission coefficient ($\frac{W}{m^2K}$) of the radiator.

A_{rad} is the surface area (m^2) of the radiator.

$T_{int(t)}$ is the internal air temperature ($^{\circ}C$ or K) of the building in time slot t .

$T_{rad(t)}$ is the radiator temperature ($^{\circ}C$ or K).

The radiator temperature, $T_{rad(t)}$, is the average of the temperature of the working fluid reaching the condenser (T_{flow}) and the temperature of the working fluid leaving the condenser ($T_{return(t)}$). That is:

$$T_{rad(t)} = \frac{T_{flow} + T_{return(t)}}{2} \quad (4.19)$$

From equations (4.16) to ((4.19) the return temperature, $T_{return(t)}$, can be expressed as:

$$T_{return(t)} = \frac{T_{flow}(2mc - U_{rad}A_{rad}) + 2U_{rad}A_{rad}T_{int(t)}}{U_{rad}A_{rad} + 2mc} \quad (4.20)$$

Based on test data, from the Heat Pump Test Centre WPZ, of 30 different models of ASHPs [21], the expression for the Coefficient of Performance (COP) of HP can be deduced from the plot of COP against ' $T_{return} - T_{ext}$ ' with a coefficient of determination (R^2 value) of 0.9797 by equation (4.21):

$$COP_{(t)} = 7.90471e^{-0,024(T_{return(t)}-T_{ext(t)})} \quad (4.21)$$

Where:

$COP_{(t)}$ is the coefficient of performance of the HP at time slot t .

$T_{ext(t)}$ is the external air temperature ($^{\circ}C$ or K) at time slot t .

The COP-curve, which is here defined as the plot of COP against ' $T_{return} - T_{ext}$ ' derived from the test data, is shown in Fig. 4.7 In Fig. 4.7, there are 9 test points and the COP at a point is the average of COPs of 30 ASHPs at that point.

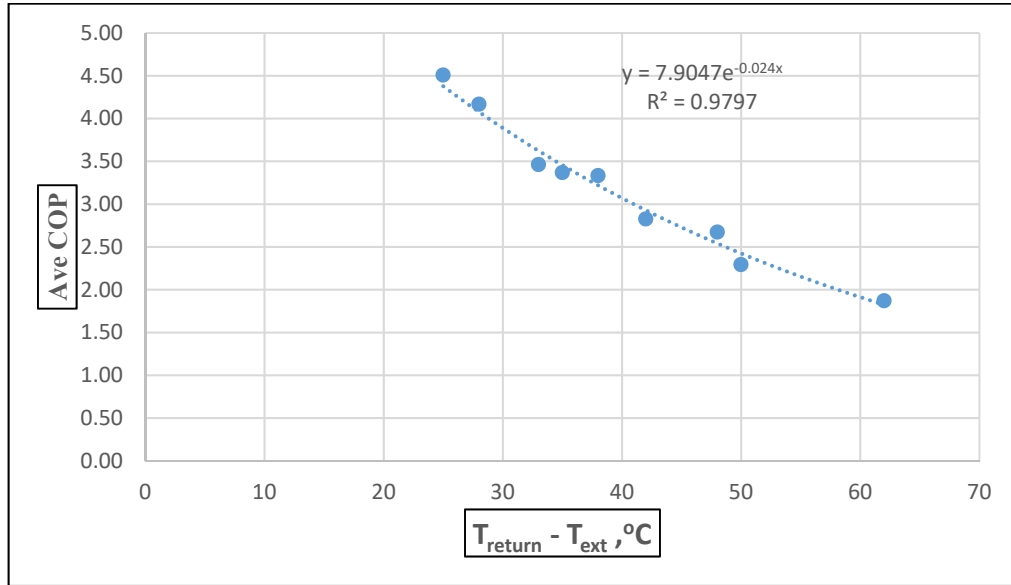


Fig. 4.7 The COP -curve adapted from test data at HP Test Centre WPZ [21]

The actual electrical input, $P_{SH_{elect}(t)}$ (W), for the operation of the HP in SH mode is therefore given by equation (4.22):

$$P_{SH_{elect}(t)} = \frac{HP_{SH(t)}}{COP_{(t)}} \quad (4.22)$$

Two temperature regimes were used in the modelling. The set-point temperature, T_{set} , of the HP between 00:00 hours and 10:30 hours is 18°C with a swing temperature, T_{sg} , of 2°C . Whereas T_{set} between 11:00 hours and 23:30 hours is 20.5°C with a T_{sg} of 3°C .

4.10 MODEL FORMULATION OF HP OPERATION IN DHW MODE

Here, the formulation of the model that describes the heat balance and temperature flow inside the hot water tank is developed. In the model formulation, single-node state is assumed since there is no occurrence of draw event large enough to trigger the transition from single-node state into two-node state. A hot water tank remains in single-node state and only changes into two-node state when a considerable volume of water is drawn in a usage event which occurs in a short interval of time [169]. In single-node state, the water in the tank is considered as a single mass of body with the heat and temperature of the water uniformly distributed. Therefore, the water in the tank is not stratified after a draw event into upper layer warm water and lower layer cold water from the inlet that replaces the drawn water. Fig. 4.8 shows the DHW tank in single-node state as modelled in this work.

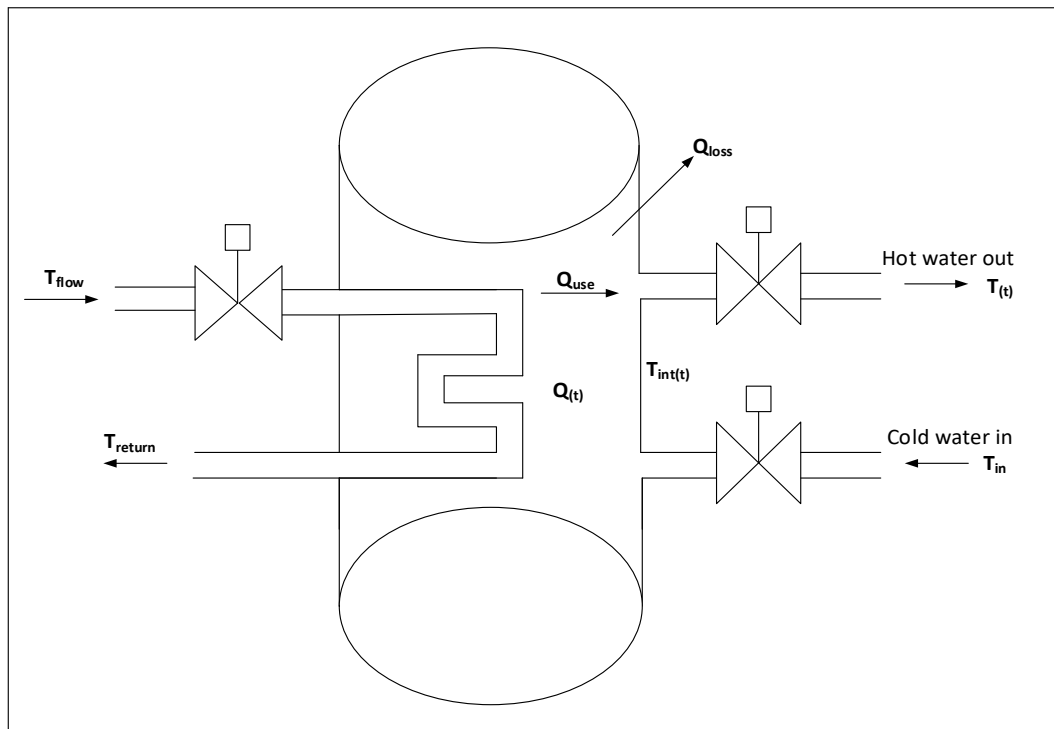


Fig. 4.8 DHW tank in single-node state (adapted from [169])

The temperature, $T_{(t)}$, of the water leaving the tank is the average temperature of the hot water inside the tank. The tank is refilled with inlet water at temperature, T_{in} , to replace the drawn water. The inlet water mixes with the hot water inside the tank and a new average temperature, $T_{(t+1)}$, is formed for the next water draw event. The heat (W) available inside the tank after a water draw event in time slot t can be expressed in terms of heat balance equation as follows:

$$Q_{(t+1)} = Q_{(t)} - Q_{use(t)} - Q_{aml(t)} + HP_{DHW(t)} \cdot z_{(t)} \quad (4.23)$$

Where:

$Q_{(t+1)}$ is the heat (W) remaining after a water draw event.

$Q_{(t)}$ is the heat (W) available before the water draw event.

$Q_{use(t)}$ is the heat (W) loss due to the water draw event.

$Q_{aml(t)}$ is the heat (W) loss to the ambience due to heat dissipation from the tank the to the environment.

$HP_{DHW(t)}$ is the heat output (W) of the HP in DHW mode in time slot t .

$z_{(t)}$ is binary variable which determines the operational status (ON = 1 or

OFF = 0) of the HP in DHW mode in time slot t .

The heat balance equation in (4.23) can be written in terms of volume and change in temperature as follows:

$$\begin{aligned} & \frac{Vc(T_{(t+1)} - T_{in})}{60t} \\ &= \frac{Vc(T_{(t)} - T_{in})}{60t} - \frac{V_{use(t)}c(T_{(t+1)} - T_{in})}{60t} - U_{ta}A_{ta}(T_{(t)} - T_{int(t)}) \\ &+ \frac{Vc(T_{flow} - T_{return(t)})}{60t} \cdot z_{(t)} \end{aligned} \quad (4.24)$$

Where:

V is the volume (l) of the tank.

$V_{use(t)}$ is the volume (l) of the hot water used in time slot t .

$T_{(t)}$ is the temperature ($^{\circ}C$ or K) of hot water inside the tank in time slot t .

$T_{(t)}$ is also equal to the return temperature, $T_{return(t)}$, of the working fluid.

$T_{(t+1)}$ is the temperature ($^{\circ}C$ or K) of hot water inside the tank after the water draw event.

T_{in} is the temperature ($^{\circ}C$ or K) of the inlet cold water.

U_{ta} is the heat transmission coefficient ($\frac{W}{m^2K}$) of the tank.

A_{ta} is the surface area (m^2) of the tank.

c is the specific heat capacity of water in $\frac{kJ}{kg^{\circ}C}$ i.e. $4.184 \frac{kJ}{kg^{\circ}C}$.

$T_{int(t)}$ is the internal air ($^{\circ}C$ or K) of the building in time slot t .

T_{flow} is the operating temperature ($^{\circ}C$ or K) of the working fluid.

t is the duration of the time slot in minutes.

The operational status, $z_{(t)}$, of the HP in DHW mode is represented as follows:

$$z_{(t)} = \begin{cases} 1 = ON, & T_{(t)} < T_{set(W)} - T_{sg(W)} \\ 0 = OFF, & T_{(t)} > T_{set(W)} + T_{sg(W)} \\ z_{(t-1)}, T_{set(W)} - T_{sg(W)} \leq T_{(t)} \leq T_{set(W)} + T_{sg(W)} \end{cases} \quad (4.25)$$

Where:

$T_{(t)}$ is the temperature ($^{\circ}C$ or K) of hot water inside the tank time slot t .

$T_{set(W)}$ is the set-point temperature ($^{\circ}C$ or K) of hot water inside the tank.

T_{sg} is the swing temperature ($^{\circ}C$ or K).

$z_{(t-1)}$ is the operational status of the HP in previous time slot.

Substituting for constant and solving for $T_{(t+1)}$ in equation (4.23) yields:

$$T_{(t+1)} = \frac{VT_{(t)} + V_{use(t)}T_{in} - 0.0143tU_{ta}A_{ta}(T_{(t)} - T_{int(t)}) + V(T_{flow} - T_{(t)}) \cdot z_{(t)}}{(V + V_{use(t)})} \quad (4.26)$$

The set-point temperature, $T_{set(W)}$, of the HP for DHW is $50^{\circ}C$ with a swing temperature, $T_{sg(W)}$, of $5^{\circ}C$. The hot water set-point temperature and the swing temperature are such that will prevent the growth of Legionella bacteria inside the tank. Legionella bacteria mostly thrives in the temperature range between $20^{\circ}C$ and $45^{\circ}C$ [170].

The COP of the HP while working in DHW mode is as expressed in equation (4.21) with $T_{return(t)}$ substituted by $T_{(t)}$. The actual electrical input, $P_{DWH_{elect}(t)}$ (W), for the operation of the HP in DHW mode is given by:

$$P_{DWH_{elect}(t)} = \frac{HP_{DHW(t)}}{COP_{(t)}} \quad (4.27)$$

4.11 IMPLEMENTATION OF THE HP OPERATIONAL MODEL

A 6-kW heat output capacity, variable-speed ASHP with a COP of 2.7 at test condition A-7/W35 and R407C as refrigerant [21] was modelled. The HP operational model as SH and DHW provider was implemented in MATLAB for a typical winter week day and a typical summer week day. Fig. 4.9 shows the block diagram of the implementation process of the model. Inputs to the model in the SH mode are time series external air temperature, time series solar radiation, thermostat set-point for the desired internal air temperature, SH swing temperature and the time series internal air temperature which is fed back from the output. These input parameters interact with intrinsic properties of the building (such as size of building, areas of building fabrics and U-values of building fabrics), number of occupants and the COP-curve of the HP to produce outputs in the SH mode.

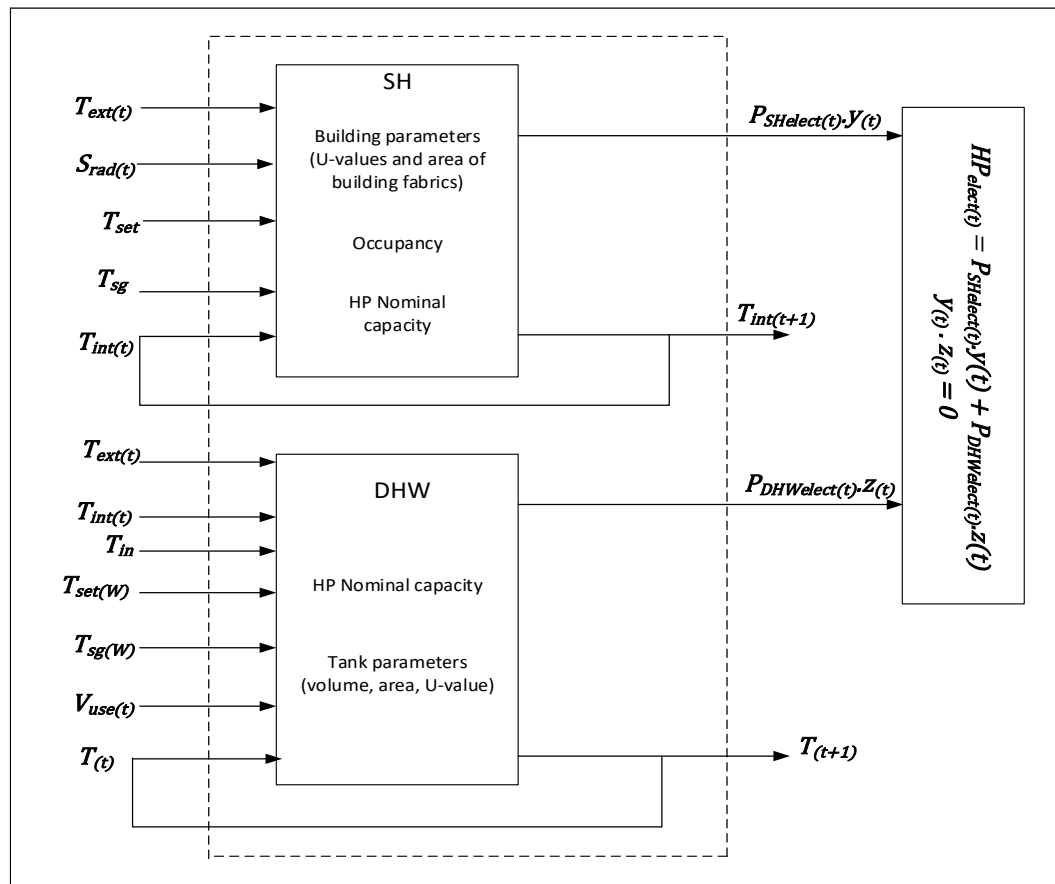


Fig. 4.9 Block diagram of implementation process of HP operation

In the DHW mode, the inputs are time series external air temperature, time series internal air temperature, temperature of inlet water, thermostat set-point for the desired hot water temperature, DHW swing temperature, time series water usage profile and the hot water temperature which is fed back from the output. The tank parameters like volume, surface area and heat transmission coefficient interact with the input parameters to produce outputs in the DHW mode.

Input data about parameters of buildings used in the model are available in appendix A.1. Parameters of DHW tank and radiator used in the model are provided in appendices A.2 and A.3 respectively. Weather data and water draw events are available in appendix A.4.

The outputs of the model depend on the mode of the HP (SH mode or DHW mode) which is active in a time slot. The outputs of the model in SH mode are internal air temperature and the electricity consumption of the HP in that mode while the outputs in DHW mode are hot water temperature and the electricity consumption of the HP in

that mode. The electricity consumption of the HP in a time slot t is given by equation (4.28):

$$HP_{elect(t)} = P_{SH_{elect(t)}} \cdot y(t) + P_{DWH_{elect(t)}} \cdot z(t) \quad (4.28)$$

Equation (4.29) ensures that the HP can only operate either in SH mode or DHW mode at a given time slot.

$$y(t) \times z(t) = 0 \quad (4.29)$$

The model is run with 100 buildings. Each building is considered as a single zone in the modelling process. In order to achieve diversity in the operation of the HPs in different buildings, the following input parameters of the model are randomized: building size, U-values of building fabrics, number of occupants, SHGC of windows, number of air change, initial internal air temperature and initial hot water temperature.

Fig. 4.10 is presenting the average of the HPs electricity demand on a typical winter week day and a typical summer week day. Peaks are observed at about 7:30 and 9:30 in the morning for both typical winter week day and typical summer week day average electricity demand of the HPs.

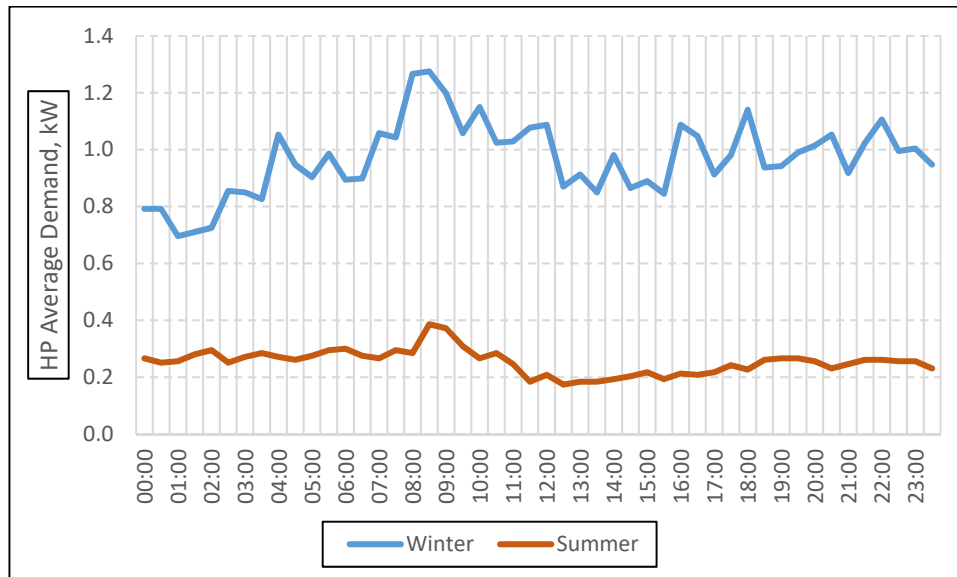


Fig. 4.10 HP daily average demand

4.12 HP MODEL VALIDATION

To validate the developed HP operational model, empirical data from credible sources were used as inputs to run the model. The model outputs, typical winter week day and typical summer week day average electricity demand of HPs expressed in half-hourly intervals, were compared with the measured daily average electricity demand of HPs in the Carbon, Control and Comfort (CCC) project [171].

The comparison between the model outputs and the actual measured outputs of the CCC project showed close similarity in trends and kW values of the HPs daily average electricity demand profile. This gives reasonable credence to the usefulness of the developed model. Fig. 4.11 is the screenshot from CCC Project of average HP demand. The midnight peak observed in Fig. 4.11 but not in Fig. 4.10 is due to the fact that the HPs in the CCC project operate a weekly pasteurization cycle (raising the DHW temperature above 60°C to kill Legionella bacteria) which always takes place at midnight [171].

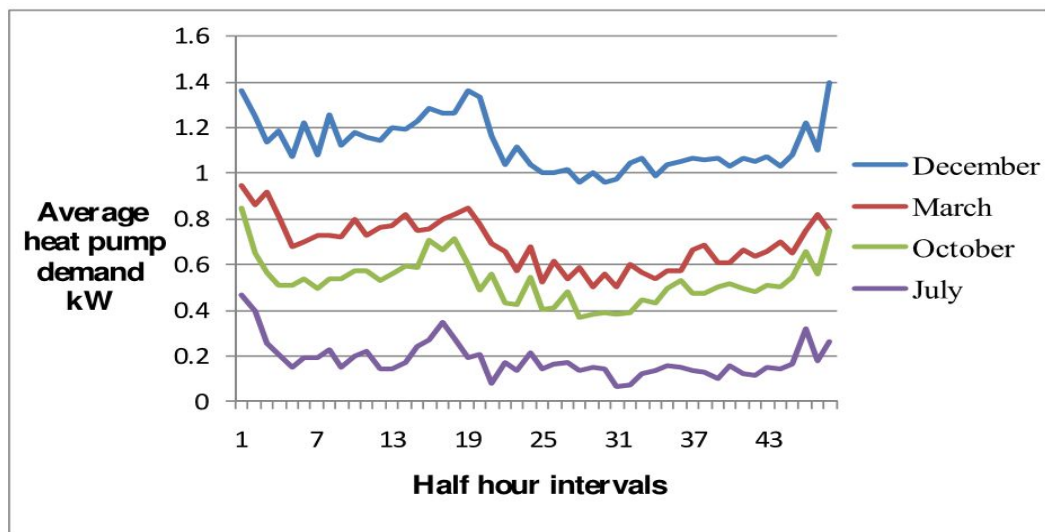


Fig. 4.11 Screenshot from CCC Project of average HP demand [171]

4.13 DATA SOURCES

Empirical data of the input variables used in the modelling of HP operation were carefully sourced for. Decision on the number of occupants per household was based on [156]. Average daily DHW requirement of household in litres/day was estimated in line with technical guidelines from [172] and it is given by equation (4.30):

$$HH_{daily_{DHW}} = 25N_p + 36 \quad (4.30)$$

Where:

$HH_{daily_{DHW}}$ is the average daily household DHW requirement in litres.

N_p is the number of occupants in the household.

Normalized DHW tapping profile from [173] was used to estimate the actual DHW draw at any time of the day. Fig. 4.12 illustrates the normalized DHW tapping profile. Data on geometric and constructional characteristics of the hot water tank came from [174]. Data about buildings parameters which consist of building type and size and U-values of building elements were from [175] and [176] respectively. Weather data were from [177].

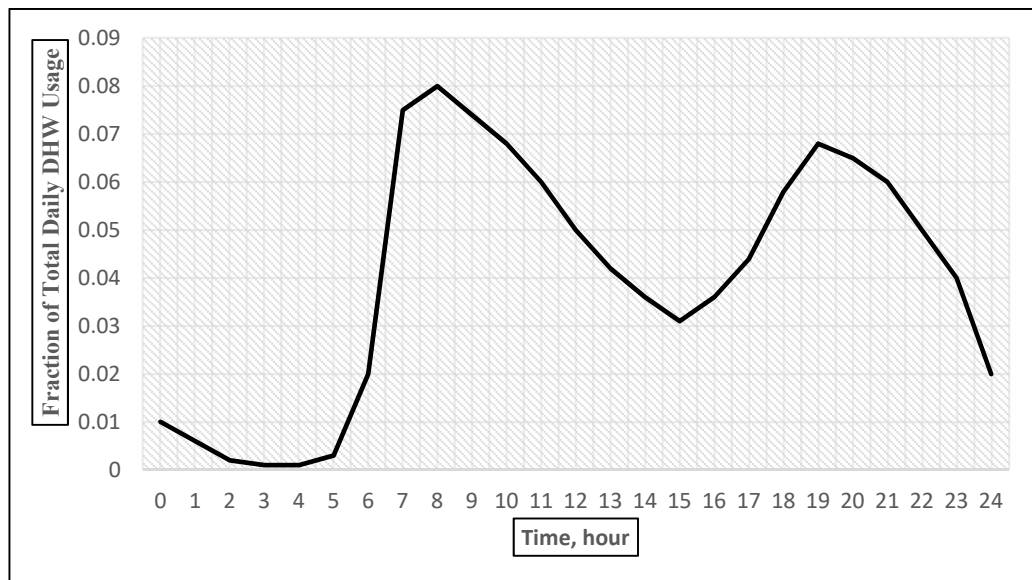


Fig. 4.12 Normalised DHW tapping profile [173]

4.14 LV NETWORK MODELLING AND SIMULATION IMPLEMENTATION

The loads were modelled using the ‘exact lumped load model’ as described in [178]. This model is useful in situation where the locations and sizes of the loads are unknown, providing reasonable results for the line losses and voltage drop along a feeder. In exact lumped load model, one-third of the load is placed at the end of the line and two-thirds of the load is placed one-fourth of the way from the source end. The EVs and the HPs are distributed amongst the feeders based on the ratio of the number of buildings per feeder. Table 4.9 below shows the EVs and HPs distribution.

The components (lines and transformer) of the LV network were modelled in GridLAB-D power system simulation software.

Table 4.9 Distribution of EVs and HPs amongst the feeders

Year	Feeder 1				Feeder 2				Feeder 3				Feeder 4			
	EVs		HPs		EVs		HPs		EVs		HPs		EVs		HPs	
	TD	SS	TD	SS	TD	SS	TD	SS	TD	SS	TD	SS	TD	SS	TD	SS
2020	7	1	1	1	5	1	1	1	9	2	2	1	2	1	1	-
2030	28	6	14	3	19	4	9	2	37	9	18	4	9	2	5	1
2040	50	12	29	3	33	8	19	2	67	16	38	4	17	4	10	1
2050	77	22	62	4	51	14	41	2	102	29	83	5	26	7	21	1

Power flow calculations of the LV network were performed using the power flow module of the GridLAB-D software. The GridLAB-D power flow simulation was run for twenty-four hours with half-hourly resolution for a typical winter week day and a typical summer week day for the years 2020, 2030, 2040 and 2050 under the TD and SS scenarios. For the simulation, Newton-Raphson power flow solver was chosen, and the results were output in comma separated values (CSV) format for further analysis.

4.15 SIMULATION RESULTS

The impacts of integration of EVs and HPs on transformer loading, voltage profiles of the feeders and ampacity loading of the cables were evaluated in the power flow simulation of the LV network under study. The results of the transformer loading profiles of the LV network for the four scenarios for the years 2020, 2030, 2040 and 2050 are as presented in Fig. 4.13 (a-d) with the solid bold red line indicating the nominal capacity of the transformer in percentage.

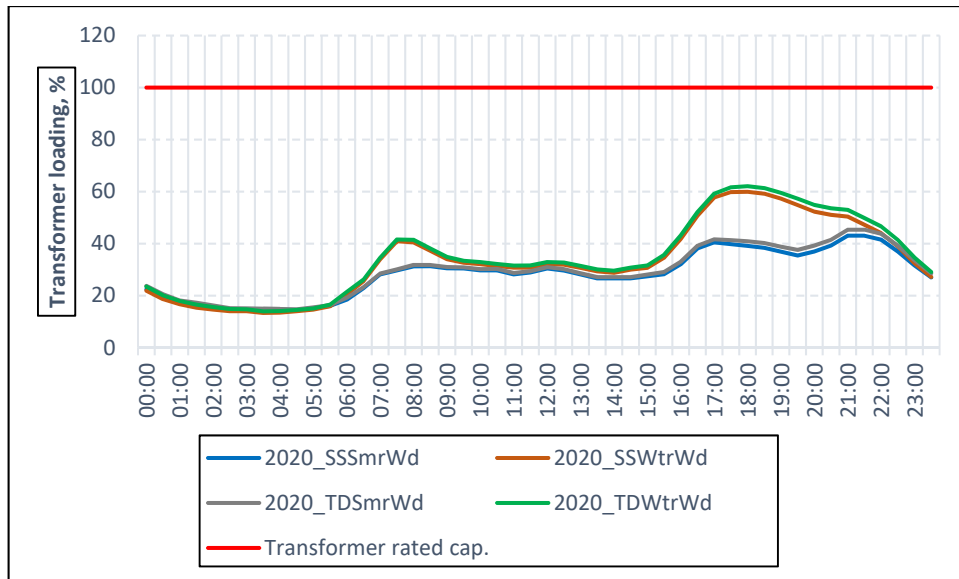


Fig. 4.13(a) Half-hourly Percentage Transformer Loading of the LV network, 2020

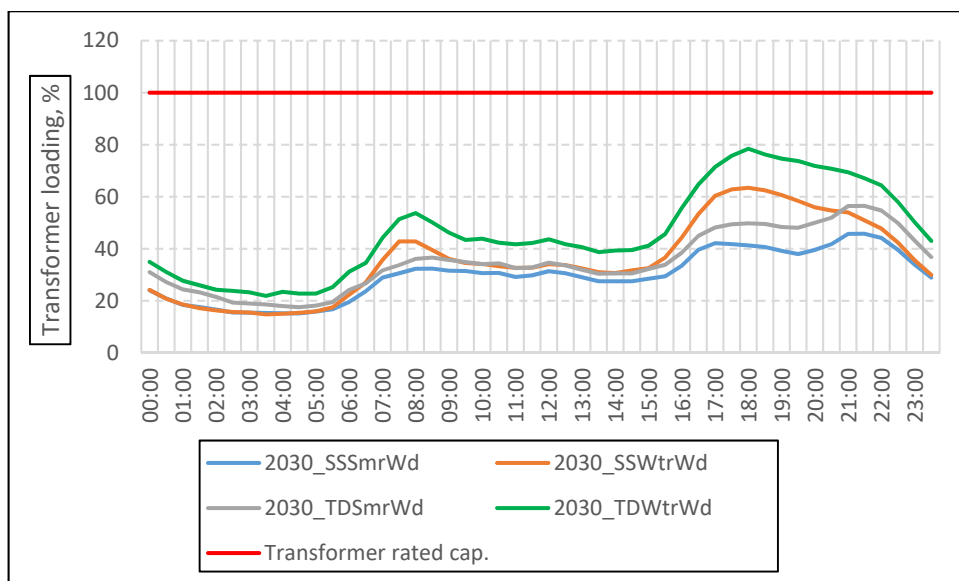


Fig. 4.13(b) Half-hourly Percentage Transformer Loading of the LV network, 2030

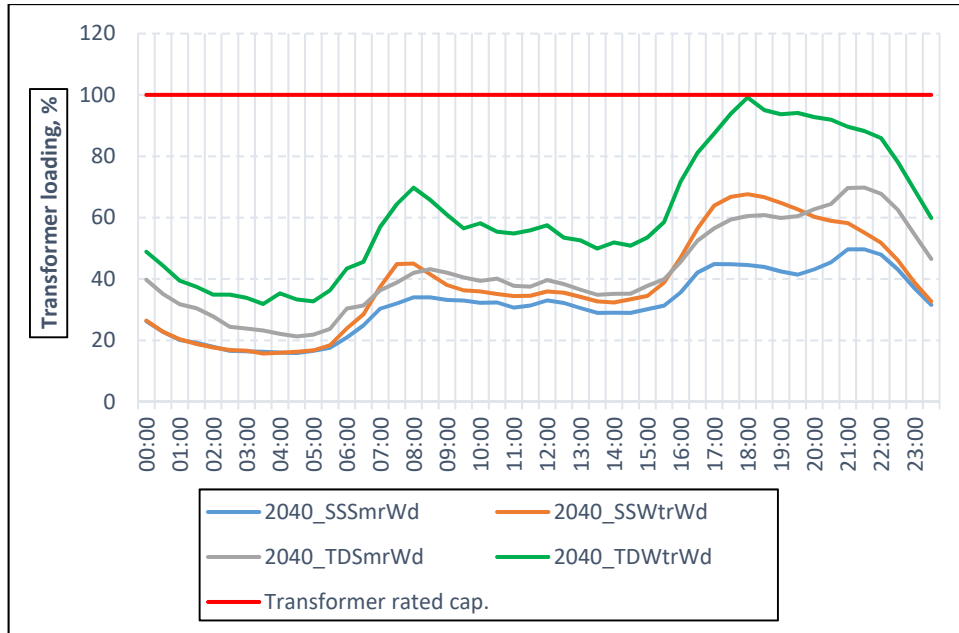


Fig. 4.13(c) Half-hourly Percentage Transformer Loading of the LV network, 2040

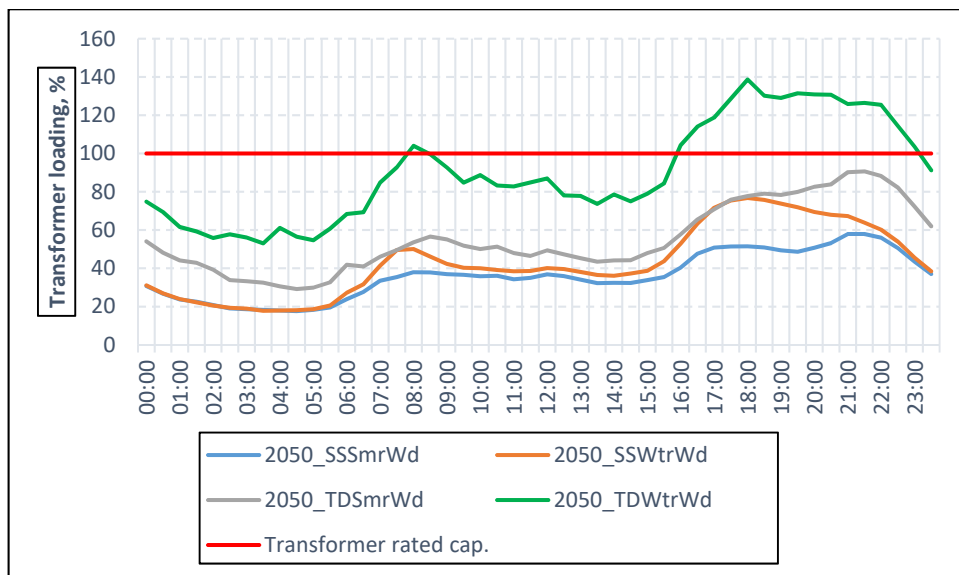


Fig. 4.13(d) Half-hourly Percentage Transformer Loading of the LV network, 2050

In all the scenarios for all the years considered, there is a common trend of load build up in the early morning and in the early evening. The trend is, however, more pronounced in the WtrWd scenarios than in the SmrWd scenarios. The early morning load build up crests between 08:00 AM and 09:00 AM, while the early evening load build up crests between 18:00 PM and 19:00 PM. The early morning load build up can be explained due to the increased usage of hot water and hence more operation of HPs

at that time of the day. **Fig. 4.10** and **Fig. 4.12** allude to this plausible explanation. However, the more pronounced early evening load build up can be attributed to the combination of increasing EV charging as people are returning home from work and increased HPs demand triggered by the slightly increased hot water usage at that time of the day. **Fig. 4.5**, **Fig. 4.10** and **Fig. 4.12** support this explanation.

Up until 2040, the transformer can withstand the load requirement of the LV area network in all scenarios as seen in Fig. 4.13 (a) – (c). However, a continual increase in the transformer loading is observed from 2020 through 2040. The increase is most evident in the TDWtrWd scenario; increasing from **62%** of the transformer nominal capacity at 18:00 PM in 2020 to **100%** of the transformer nominal capacity at 18:00 PM in 2040. By 2050, as seen in Fig. 4.13(d), the overloading of the transformer in the TDWtrWd scenario is significant. In this scenario, the nominal capacity of the transformer is exceeded on two instances. The transformer is first slightly overloaded by about 4% between 08:00 AM and 09:00 AM. Then from 17:30 PM the transformer is subjected to a sustained overload of about **30%** for not less than five hours. This is the most critical scenario and it is going to be the focus of interest henceforth.

In Fig. 4.14 the voltage profiles at the farthest end of all the feeders in 2050-TDWtrWd scenario are presented with the solid bold red line indicating the statutory limit for voltage drop in per unit. There is no violation of voltage drop limit in any of the feeders. The voltage profiles of the feeders follow the same trend with two notable dips at 08:00 AM and 18:00 PM. The greatest dip in voltage of value **0.96 p.u.** occurs at the far end of Feeder number 1 at 18:00 PM.

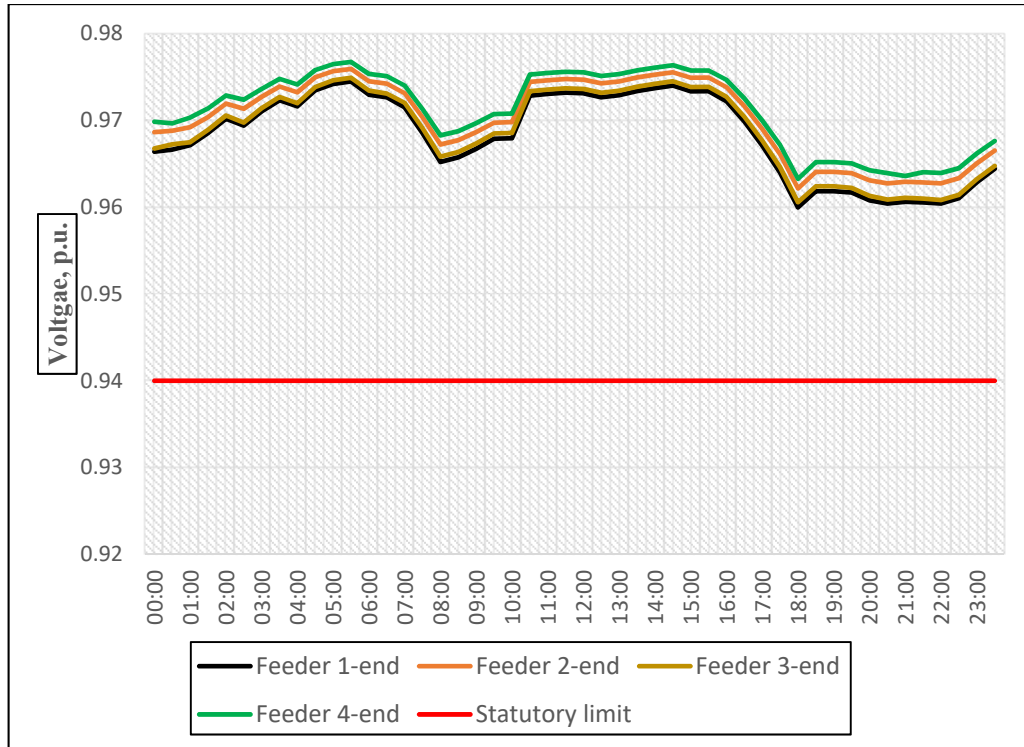


Fig. 4.14 Voltage profiles at the farthest end of feeders in 2050_TDWtrWd

To observe the impact of integration of LCTs on thermal loading capacity of cables, percentage ampacity loading of the first cable of the four feeders in 2050_TDWtrWd scenario is examined. Fig. 4.15 shows the percentage ampacity loading of the first cable of the feeders in 2050_TDWtrWd scenario with the solid bold red line indicating the nominal ampacity of the cables in percentage.

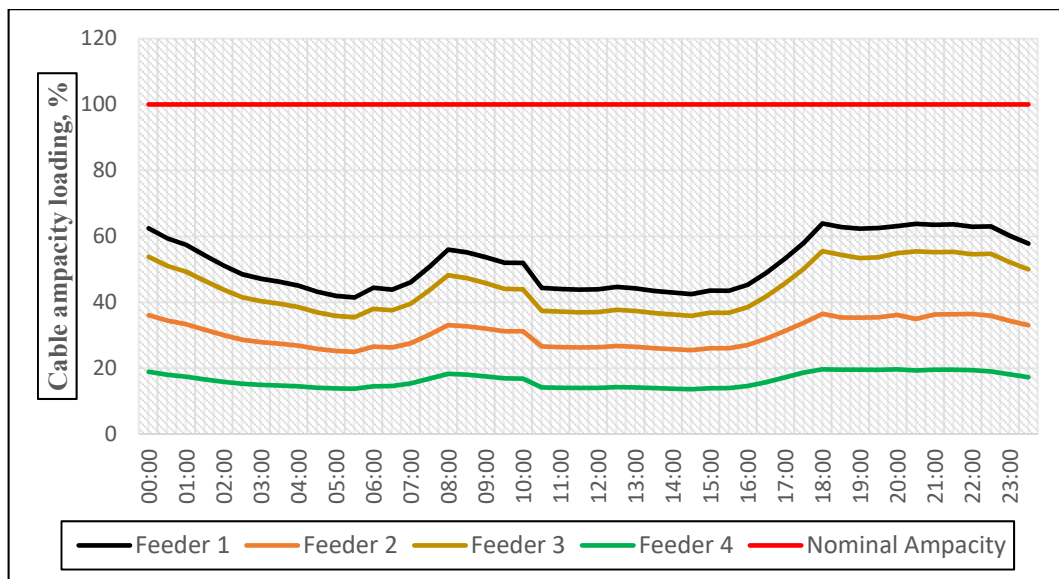


Fig. 4.15 Percentage ampacity loading of feeders in 2050_TDWtrWd

There is no cable that is loaded beyond its ampacity rating. The most loaded cable is the first cable in Feeder number 1; reaching approximately **64%** of its nominal ampacity at 18:00 PM.

4.16 SUMMARY

The impacts of adoption of EVs for road transportation and HPs for domestic heating on transformer loading, voltage profiles of feeders and cable thermal loading in residential LV network were investigated. The impact study was done in four scenarios for the years 2020, 2030, 2040 and 2050. The scenarios were based on two factors;

- i) Uptake level of EVs and HPs
 - Two Degree scenario (TD)
 - Steady State scenario (SS)
- ii) Season of the year
 - Winter weekday (WtrWd)
 - Summer weekday (SmrWd)

Calculations were made by scaling down the national projected number of EVs and HPs to estimate the uptake of EVs and HPs in the typical residential LV area distribution network used as the case in the years 2020, 2030, 2040 and 2050. Average minimum daily energy requirement of an EV in the LV network was estimated based on daily average travel distance, capacity and efficiency of the EV battery. And based on the knowledge of the average minimum daily energy requirement of an EV, the possible maximum daily energy requirement was determined. Average electricity demand profiles of HP for a typical winter weekday and a typical summer weekday were created by modelling the operation of HP and implementing the model in MATLAB. The modelled operation of the HP was validated against Carbon, Control and Comfort (CCC) field trial project. Power flow of the LV network was run using GridLAB-D, an agent-based power system simulation software.

From the simulation results, the following were discovered:

- i) The transformer could withstand the load requirement of the LV network in all scenarios up until 2040.
- ii) By 2050, under the TDWtrWd scenario, the transformer was subjected to a sustained overload of about **30%** above its nominal rating from early evening for about five hours.
- iii) There was no violation of voltage drop limit in any of the feeders in all the scenarios and in all the years considered. The greatest dip in voltage was **0.96 p.u.** at 18:00 PM in 2050 under the TDWtrWd scenario.
- iv) No cable was thermally overloaded in all the scenarios and in all the years considered. The highest cable loading was about **64%** of its nominal thermal capacity at 18:00 PM in 2050 under the TDWtrWd scenario.

CHAPTER 5

ADAPTIVE THERMAL MODEL FOR LOADING OF DISTRIBUTION TRANSFORMERS IN LOW CARBON LV DISTRIBUTION NETWORKS

5.1 INTRODUCTION

In this chapter, a method of adaptive thermal loading of distribution transformer serving a LV area distribution network characterised by significant uptake of EVs and HPs is presented. In the context of this work, adaptive thermal loading of transformer is defined as the process of loading a transformer based on real and present operating environment conditions rather than on static load rating of the transformer. The aim is to investigate to what extent the transformer capacity headroom for the accommodation of more EVs and HPs load on the LV distribution network could be raised while asset reinforcement deferral is enforced.

As established in Chapter 4, a significant uptake of EVs and HPs at LV distribution network, in the quest of cutting down on GHG emissions in the transportation and residential sectors, has the potential to cause general load increase and may lead to higher and longer peak load demand. This development could pose a real challenge of capacity overloading to distribution transformers at the LV distribution network of electricity system. Prolonged and/or accumulated periods of overloading could shorten transformer's life expectancy and leads to premature failure [179]. Thus, restricting the further uptake of HPs and EVs.

Transformers are amongst the most critical equipment in the power system [90] and their unplanned outages could cause reduction in system reliability [92], [93] and economic losses to the DNOs in terms of penalties and compensations to be paid to The Office of Gas and Electricity Markets (Ofgem) and customers [180]. At LV distribution network level, distribution transformers usually do not operate in parallel. Therefore, failure of one transformer due to overloading will cause power outage of

all feeders associated with the transformer and consequently all the areas being supplied by the feeders would be disconnected.

A direct solution to addressing distribution transformer overloading is the upgrading of the transformer capacity. However, the number of LV distribution transformers in electricity system that may require upgrading, as there are a total estimate of 684,000 units of distribution transformers in the UK [181], and the resources needed for such operation make the solution less desirable to the DNOs. Therefore, it is important to develop cost-effective solutions for the optimal utilization of the existing transformer capacity. Adaptive thermal loading of transformer is one of such solutions.

5.2 ASSUMPTION

The transformer is of oil-filled construction with thermally upgraded insulation paper. The cooling method is oil natural air natural (ONAN). Associated transformer equipment such as tap changers, switchgears, bushings, protection and metering instruments, busbars, etc., can withstand the additional stress that comes with the excess load above the transformer nameplate rating.

5.3 ADAPTIVE THERMAL LOADING VERSUS STATIC LOADING OF TRANSFORMER

The aging process and hence the expected life of an oil-immersed transformer are principally determined by the aging of the paper insulation of its winding [182]. The paper insulation degradation is a function of temperature, moisture content, oxygen content and time [183]. Moisture and oxygen contents of the insulation paper can be minimized with modern preservation techniques [184], [185]. Temperature and time therefore remain as the major factors determining the degradation rate of paper insulation and therefore the expected life of the transformer [186]. The temperature of the hottest spot within the transformer winding, known as the ‘Hot Spot Temperature’ (HST) is reckoned as the operating temperature of the paper insulation [187]. The higher the HST, the quicker the winding insulation degrades and the faster the transformer ages. The degradation rate of insulation paper doubles for every 6°C rise above the rated HST [95]. The HST is a function of ambient air temperature, oil temperature, and transformer design amongst others [188].

Static load rating is specified by the manufacturers to limit the operating temperature to less than 110°C, for a thermally upgraded insulation paper, based on ambient temperature of 30°C to ensure normal life expectancy of the transformer [95]. However, the ambient temperature in UK rarely reaches 30°C and the transformers are operating, most of the time, below their temperature limits, i.e. thermally low loaded. This condition can be exploited to safely maximize the use of existing transformer capacity based on real conditions in which the transformer operates. Transformers can therefore be adaptive thermally loaded based on real environmental conditions and HST rather than on static load rating. The use of static load rating does not fully capture the real and present thermal conditions and can lead to false indication of capacity reinforcements and/or strategic measures to reduce load due to false indication of full capacity being exhausted.

In adaptive thermal loading of the transformer, load data is combined with meteorological measurements. Using these pieces of information, transformers can be loaded in such a way to gain variable capacity headroom by leveraging on environmental cooling. This implies that adaptive thermal rating may exceed the nameplate rating when environmental conditions are favourable. However, under harsh environmental conditions, adaptive thermal rating may be lower than the nameplate rating of the transformer. The rationale behind adaptive thermal loading of transformer is to enable the DNOs use more optimally the distribution transformers and possibly achieve capacity reinforcement deferral following load increase due to the uptake of HPs and EVs in homes.

5.4 TRANSFORMER THERMAL MODELLING

IEC 60076-7:2005 stipulates how oil-immersed transformer can be operated under different ambient temperature and time-varying load. Fig. 5.1 is the transformer thermal diagram per [95] which explains the temperature distribution inside the transformer.

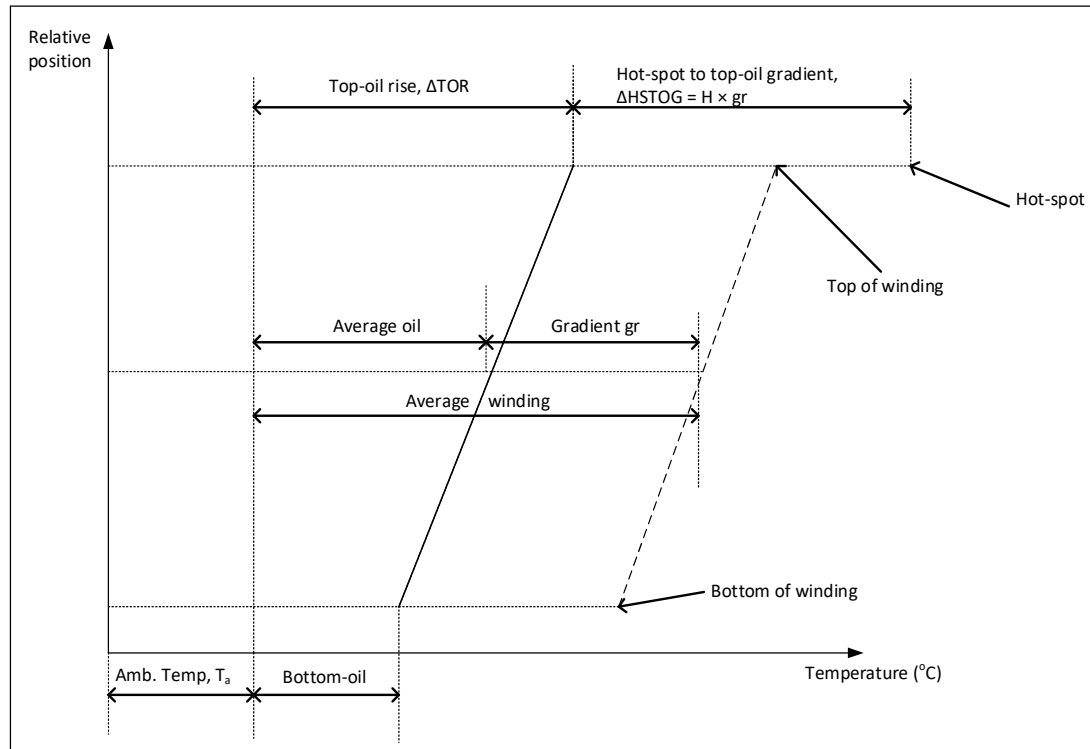


Fig. 5.1 Transformer thermal diagram [95]

From Fig. 5.1, it is seen that the Hot Spot Temperature $HST(t)$ is a sum of three components: the ambient temperature $T_a(t)$, top-oil temperature rise $\Delta TOR(t)$ and the hot-spot to top-oil gradient $\Delta HSTOG(t)$.

$$HST(t) = T_a(t) + \Delta TOR(t) + \Delta HSTOG(t) \quad (5.1)$$

The $HST(t)$ during a transient period, i.e., load change from one steady state to another can be modelled by functions of the exponential forms of top-oil temperature and hot-spot to top-oil gradient as follows:

For load increase:

$$\Delta TOR(t) = \Delta TOR(i) + [\Delta TOR(f) - \Delta TOR(i)] \times f_1(t) \quad (5.2)$$

$$\Delta HSTOG(t) = \Delta HSTOG(i) + [\Delta HSTOG(f) - \Delta HSTOG(i)] \times f_2(t) \quad (5.3)$$

Where:

$\Delta TOR(i)$ and $\Delta TOR(f)$ are the initial and final top-oil temperature rise ($^{\circ}\text{C}$) at the beginning and the end of the load change respectively.

$\Delta HSTOG(i)$ and $\Delta HSTOG(f)$ are the initial and final hot-spot to top-oil gradient ($^{\circ}\text{C}$) at the beginning and the end of the load change respectively.

$f_1(t)$ and $f_2(t)$ are exponential functions that describe the relative increase of top-oil temperature rise and hot-spot to top-oil gradient per unit of the steady state value respectively.

$$f_1(t) = 1 - e^{-\frac{t}{k_{11} \times \tau_o}} \quad (5.4)$$

$$f_2(t) = \left[k_{21} \times \left(1 - e^{-\frac{t}{(k_{22} \times \tau_w)}} \right) - (k_{21} - 1) \times \left(1 - e^{-\frac{t}{(\tau_o/k_{22})}} \right) \right] \quad (5.5)$$

Where:

k_{11} , k_{21} and k_{22} are thermal constants of the transformer.

τ_o , τ_w and t are oil time-constant (mins), winding time-constant (mins) and duration of the load change (mins) respectively.

For load decrease:

$$\Delta TOR(t) = \Delta TOR(f) + [\Delta TOR(i) - \Delta TOR(f)] \times f_3(t) \quad (5.6)$$

$$\Delta HSTOG(t) = \Delta HSTOG(f) + [\Delta HSTOG(i) - \Delta HSTOG(f)] \times f_4(t) \quad (5.7)$$

$f_3(t)$ and $f_4(t)$ are exponential functions that describe the relative decrease of top-oil temperature rise and hot-spot to top-oil gradient per unit of the steady state value respectively.

$$f_3(t) = e^{-\frac{t}{k_{11} \times \tau_o}} \quad (5.8)$$

$$f_4(t) = \left[k_{21} \times \left(e^{-\frac{t}{(k_{22} \times \tau_w)}} \right) - (k_{21} - 1) \times \left(e^{-\frac{t}{(\tau_o/k_{22})}} \right) \right] \quad (5.9)$$

In equations (5.5) and (5.9), if k_{21} is unity and τ_w is negligible, then equations (5.3) and (5.7) become:

$$\Delta HSTOG(t) = \Delta HSTOG(f) \quad (5.10)$$

The initial and final top-oil temperature rise after a load change over a period t are given by equations (5.11) and (5.12) respectively;

$$\Delta TOR(i) = \Delta TOR_{(R)} \times \left(\frac{(K_i^2 \times R) + 1}{(R + 1)} \right) \times \quad (5.11)$$

$$\Delta TOR(f) = \Delta TOR_{(R)} \times \left(\frac{(K_f^2 \times R) + 1}{(R + 1)} \right)^x \quad (5.12)$$

Where:

$\Delta TOR_{(R)}$ is the top-oil temperature rise ($^{\circ}\text{C}$) at rated load.

R is the ratio of loss at rated load to no-load loss.

K_i is the ratio of initial load to the rated load.

K_f is the ratio of final load to the rated load.

x is the oil exponent constant.

Similarly, the initial and final hot-spot to top-oil gradient after load change are given by equations (5.13) and (5.14) respectively:

$$\Delta HSTOG(i) = \Delta HSTOG_{(R)} \times (K_i)^y \quad (5.13)$$

$$\Delta HSTOG(f) = \Delta HSTOG_{(R)} \times (K_f)^y \quad (5.14)$$

Where:

$\Delta HSTOG_{(R)}$ is the hot-spot to top-oil gradient ($^{\circ}\text{C}$) at rated load.

y is the winding exponent constant.

The degradation rate of the transformer winding insulation obeys the Arrhenius reaction rate theory [189]. Therefore, the per-unit life (PUL) of transformer is given by:

$$PUL(t) = 9.8 \times 10^{-18} \times e^{\left(\frac{15000}{HST(t)+273} \right)} \quad (5.15)$$

The inverse of the PUL is the Aging Acceleration Factor (AAF).

$$AAF(t) = \frac{1}{PUL(t)} \quad (5.16)$$

From (5.15) and (5.16), for HST of 110°C both PUL and AAF are unity. For HST greater than 110°C , PUL is less than unity and AAF is higher than unity. Conversely, for HST less than 110°C , PUL is higher than unity and AAF is less than unity.

The estimate of the transformer loss life in percentage of normal life expectancy after a 24-hour operating period can be determined by equation (5.17).

$$LoL_{(24hr)} = \frac{\sum_{t=1}^T (AAF(t) \times T_s(t))}{\sum_{t=1}^T T_s(t)} \times \frac{24}{N_{life}} \times 100\% \quad (5.17)$$

Where:

t is the index of time interval.

T is the total number of time intervals.

T_s is the duration of time interval in hours.

N_{life} is the normal life expectancy of the transformer in hours.

5.5 MATHEMATICAL FORMULATION OF THE ADAPTIVE THERMAL MODELLING OF TRANSFORMER

Transformers are important components, in terms of both capital investment and reliability of the power system. High capacity utilisation factor of transformers and good returns on investments are therefore the expectations of the DNOs. The adaptive thermal loading of transformer is formulated as a non-linear programming function that optimises the capacity utilisation factor of the transformer in accordance with the real and present operating and environmental conditions by maximising daily return on the transformer utilisation. Constraints to the optimisation problem are the thermal and load conditions that ensure the normal life expectancy of the transformer is not jeopardised. The objective function is formulated as follows:

$$DRU = \max \sum_{t=1}^T [(L_{(t)} \times EP_{(t)}) - (TOC_{(t)} \times LoL_{(t)})] \quad (5.18)$$

Where:

DRU is the ‘Daily Return on transformer Utilisation’ in £.

$L_{(t)}$ is the load (kW) on transformer at time t .

$EP_{(t)}$ is the ‘Energy Price’ (£/kWh) at time t .

$TOC_{(t)}$ is the ‘Total Owning Cost’ (£) of the transformer at time t .

$LoL_{(t)}$ is the loss of life of the transformer at time t in per unit.

t is the index of time interval.

T is the total number of time intervals.

Total owning cost $TOC_{(t)}$ not only takes the initial cost of buying the transformer into account but also the cost to operate and maintain the transformer [190]. TOC can be determined as the sum of the initial cost price C_p , the cost of no-load C_{NL} , and the cost of load-loss C_{LL} [190] as expressed in equation (5.19).

$$TOC_{(t)} = C_p + C_{NL} + C_{LL(t)} \quad (5.19)$$

The objective function in equation (5.18) is subject to the following constraints:

$$K(t) \leq 1.8 \quad (5.20)$$

$$\Delta TOR(t) \leq 110^\circ\text{C} \quad (5.21)$$

$$HST(t) \leq 140^\circ\text{C} \quad (5.22)$$

$$LoL_{(24hr)} \leq 0.0133\% \quad (5.23)$$

The constraint expressed in equation (5.20) limits the transformer loading to 1.8 per unit of its rated capacity. In equation (5.21), the top-oil temperature rise is limited to 110°C to manage pressure build-up. This is to prevent expansion of oil which could lead to overflow of the oil in the tank. The HST is kept under 140°C in equation (5.22) to prevent formation of gas bubbles in the oil and paper insulation. Equation (5.23) ensures that the daily cumulative loss of life of the transformer insulation does not exceed that of normal operation of the transformer at HST of 110°C for 24 hours.

Fig. 5.2 shows the algorithm for adaptive thermal loading of transformer and optimal DRU .

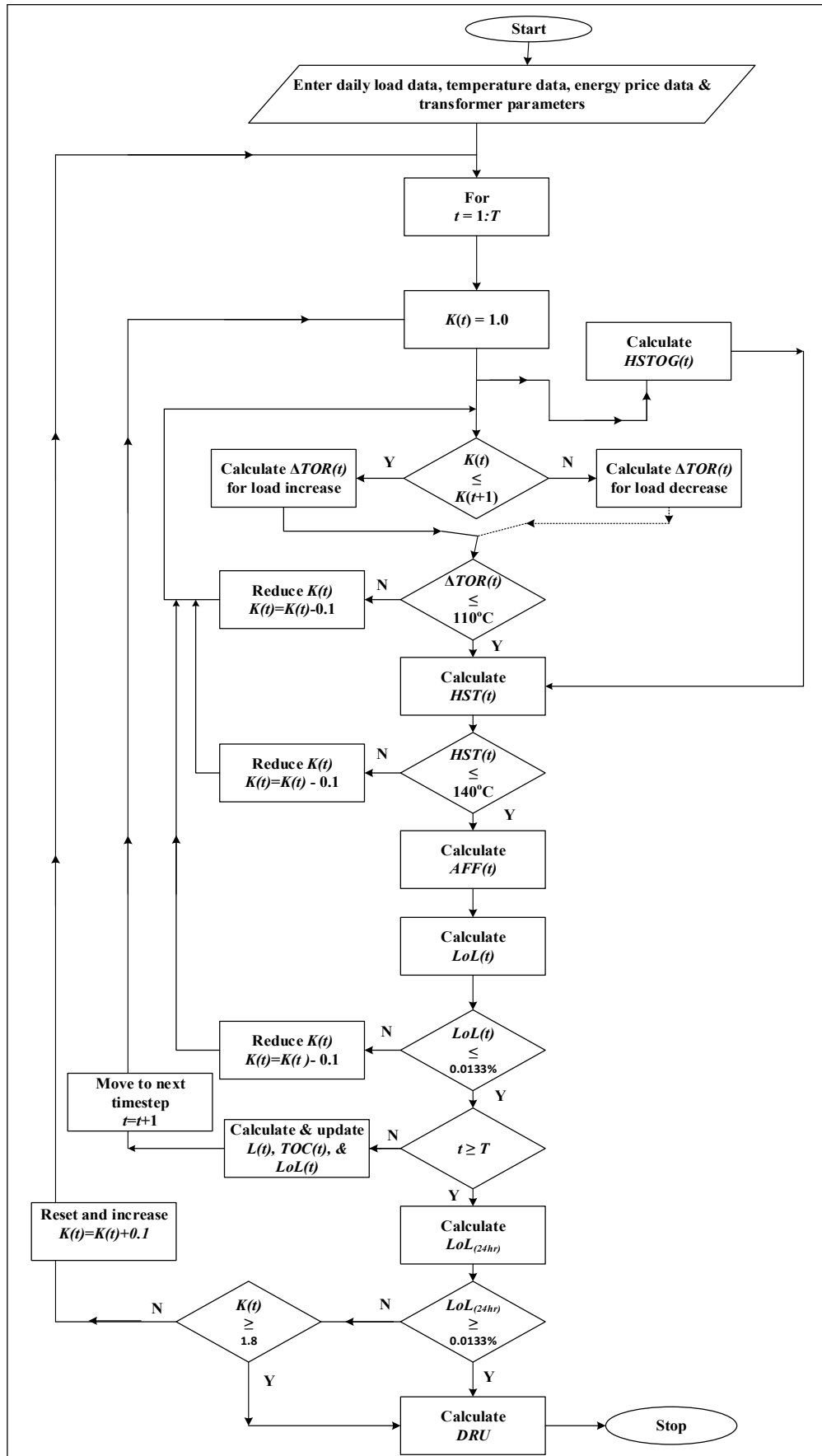


Fig. 5.2 Algorithm for adaptive thermal loading of transformer and optimal DRU

5.6 CASE STUDY

The case study transformer is the 500-kVA, 11/0.415-kV (no load), 50-Hz, Dyn11, ONAN mineral oil filled, free breathing, ground mounted distribution transformer serving a real and typical LV area distribution network in Cardiff previously described in **Section 4.3**.

Power flow simulation of the LV area distribution network was performed for the years 2020, 2030, 2040 and 2050 following the integration of EVs and HPs in the network. By 2050, the LV area could be characterised as one hosting a considerable number of EVs and HPs as seen in **Tables 4.6** and **4.8** of **Sections 4.5** and **4.7** respectively. **Fig. 4.13(d)** of **Section 4.15** is the transformer loading profiles of the LV area in 2050 on typical Winter weekday and typical Summer weekday under the EVs and HPs uptake scenarios previously described in **Section 4.2**. In the **TDWtrWd** scenario, beginning from early evening the transformer is subjected to a sustained overload of more than 30% for not less than five hours.

The task is how to manage the transformer overloading cost-effectively and create more headroom for further integration of EVs and HPs. The transformer was studied, and its thermal behaviours analysed when carrying the load demand of the LV area under both **TDWtrWd** and **TDSmrWd** scenarios in **2050**. Three situations were investigated:

- 1) **Dumb loading (DL)**: The transformer is allowed to carry the load demand of the LV area without any intervention. This is a do-nothing situation.
- 2) **Capacity enhancement (CE)**: The capacity of the transformer is upgraded to a higher rating, i.e. replace the transformer with one of higher rating.
- 3) **Adaptive loading (AL)**: The transformer is allowed to carry the load demand of the LV area based on the proposed adaptive thermal loading method.

In each of the three situations, the following plots of the transformer were obtained and compared to prove the merit of adaptive thermal loading of transformer.

- Transformer loading profile
- Daily *HST* plot
- Daily cumulative *LoL* plot
- Daily cumulative *DRU* plot

The parameters of the transformer in the case study are given in Table 5.1 below.

Table 5.1 Thermal Parameters of distribution transformer

Parameters	Values
Rating	11/0.4kV,500kVA
Cooling type	ONAN
x	0.8
y	1.6
k_{11}	1.0
k_{21}	1.0
k_{22}	2.0
$\Delta TOR_{(R)}$	65°C
$\Delta HSTOG_{(R)}$	23.0°C
N_{life}	180,000hours
τ_O	180minutes
τ_W	10minutes
R	5
Rated load current (L_r)	722.5A

The rated load loss of the transformer was determined from the power flow simulation of LV area. Fig. 5.3 is the plot of the transformer loading against load losses for thirteen randomly chosen transformer loading values. From the plot of Fig. 5.3, the winding resistance of the secondary is estimated to be **0.02Ω**.

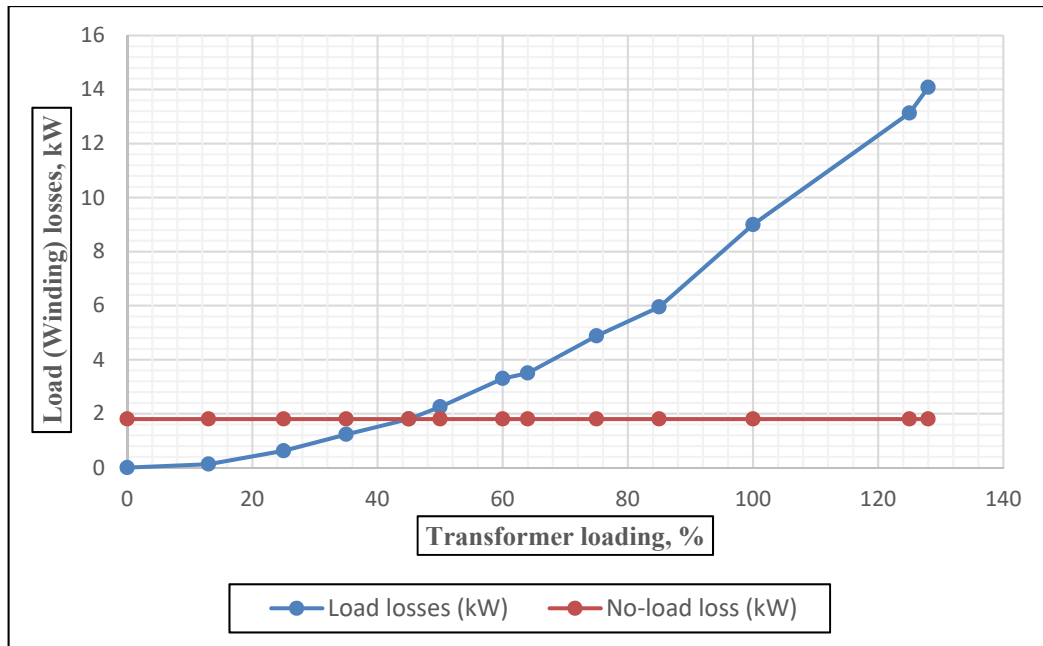


Fig. 5.3 Transformer Loading and load losses

5.6.1 Dumb Loading (DL)

The transformer is loaded to carry the load demand of the LV area without any consideration to its thermal capacity. To simulate the situation, equation (5.18) is applied on the transformer without imposing the constraints of equations (5.20) to (5.23) while the thermal conditions of the transformer is evaluated. Ambient temperature data for a typical winter day and a typical summer day used in the simulation are from the MET Office [177]. The UK day-ahead wholesale electricity price from N2EX [191] divided by a factor of 0.363 to reflect the total electricity price, in line with the Office of gas and electricity markets (Ofgem) electricity bill breakdown [192] gives the energy price used in equation (5.18). The cost price of transformers was supplied by a UK-based power equipment marketing company on a non-disclosure agreement.

5.6.2 Capacity Enhancement (CE)

The capacity of transformer under study is upgraded to 800kVA and then allowed to carry the load demand of the LV area without any further intervention. After the

capacity upgrading, Equation (5.18) is then applied on the transformer without imposing the constraints of equations (5.20) to (5.23).

5.6.3 Adaptive Loading (AL)

The transformer is allowed to carry the load demand of the LV area based on the proposed adaptive thermal loading method. The objective function of equation (5.18) was implemented on the transformer subject to the constraints of equations (5.20) to (5.23). Analytical Solver[®] – a commercial optimization software package from the Frontline Solvers [193] was used to solve the optimization problem. The problem model was diagnosed as Non-Convex Non-Linear Programme (NonCvx NLP) and it was solved with KNITRO (V10.3.0.0) Solver Engine. For TDWtrWd and TDSmrWd load scenarios, solutions were found in 0.55 seconds at the 35th iteration and in 0.61 seconds at the 57th iteration respectively with all the constraints and optimality conditions satisfied on a 3-GHz, 8-GB, 64-bit Windows 10 personal computer.

5.7 RESULTS OF THE CASE STUDY

5.7.1 Typical Winter Weekday Results

Fig. 5.4(a) shows the load demand of the LV area and the transformer loading profiles of the three investigated situations on a typical Winter weekday and Fig. 5.4(b) shows the transformer utilisation factors for the three investigated situations.

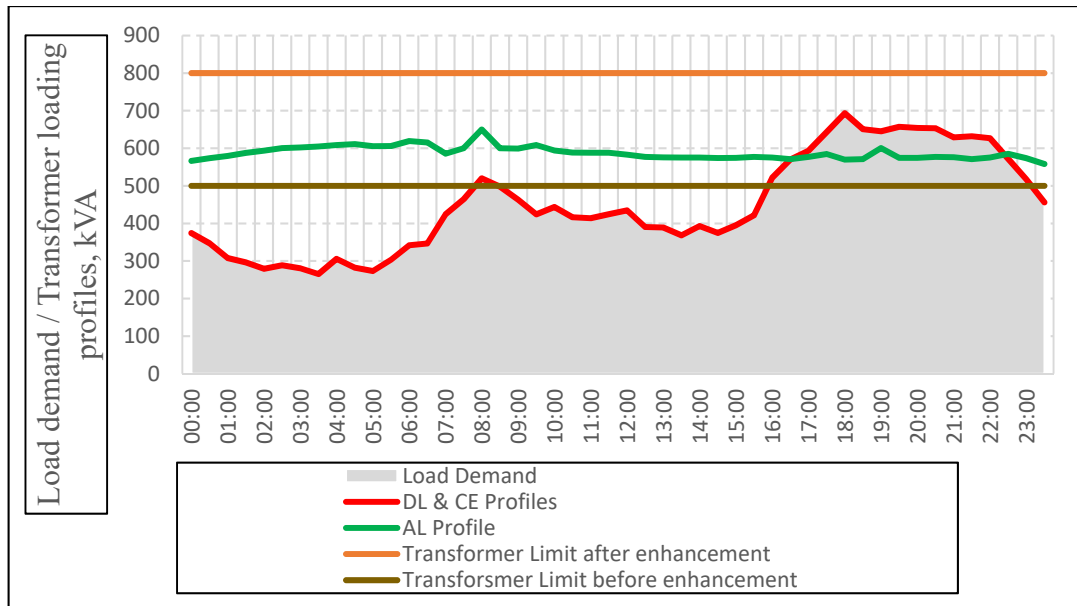


Fig. 5.4(a) Transformer Loading profiles on a Winter weekday

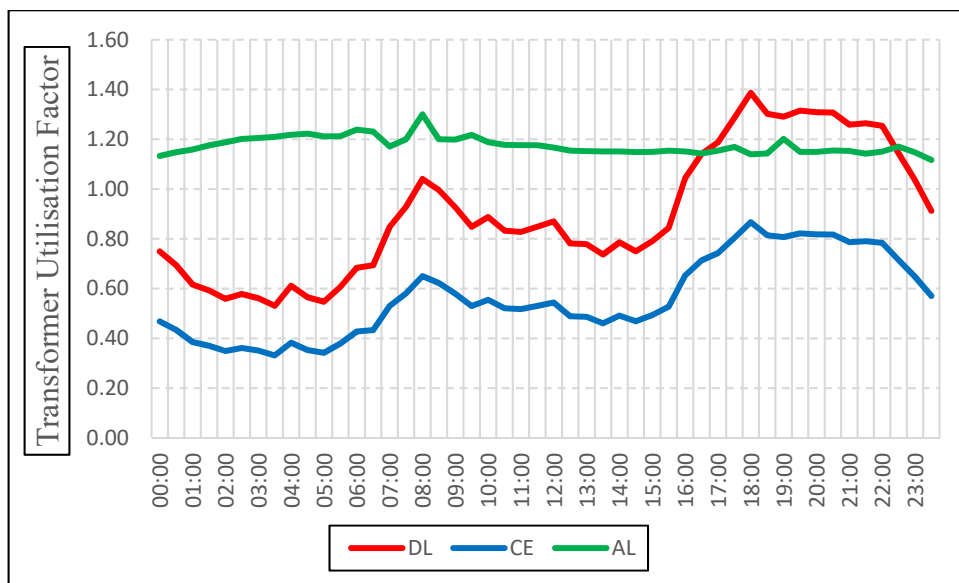


Fig. 5.4(b) Transformer Utilisation Factors on a Winter weekday

As seen in Fig. 5.4(a), the load demand exceeds the transformer limit before enhancement by an average of about **30%** throughout the evening period in the DL profile. However, in the AL profile, the loading capability of the transformer is above the transformer limit before enhancement throughout the whole period, but it is deficient by about **15%** on average in meeting the evening load demand of the LV area. After the transformer capacity is upgraded, the CE profile shows as seen in Fig.

5.4(a) that the load demand of the LV area is satisfied with the transformer having surplus capacity.

Fig. 5.4(b) shows the utilisation factors of the transformers in each of the loading profiles. In the DL profile, the transformer has an average utilisation factor of about **0.61** during the night, **0.85** during the day and **1.23** in the evening. In the AL profile, the transformer has an almost constant utilisation factor averaging **1.18** throughout the day. However, it is observed in the AL profile that the transformer utilisation factor at night time slightly decreases with time into the day. This is because as the temperature rises from the night to the day, the transformer adapts and adjusts its loading capability accordingly. In the CE profile, the transformer utilisation factor is about **0.5** on average in the morning and afternoon and **0.8** in the evening.

Corresponding thermal behaviours (HST curves) and the cumulative loss of life (LoL) of the transformers under the three investigated loading profiles are presented in Fig. 5.5(a) and (b) respectively. As seen in Fig. 5.5(a), the HST of the transformer in the DL profile is well below the 110°C mark that ensures normal life expectancy until 17:00 hours when the HST increases rapidly. Between 17:00 hours and 22:30 hours the HST is above 120°C reaching **138°C** between 18:00 hours and 19:00 hours.

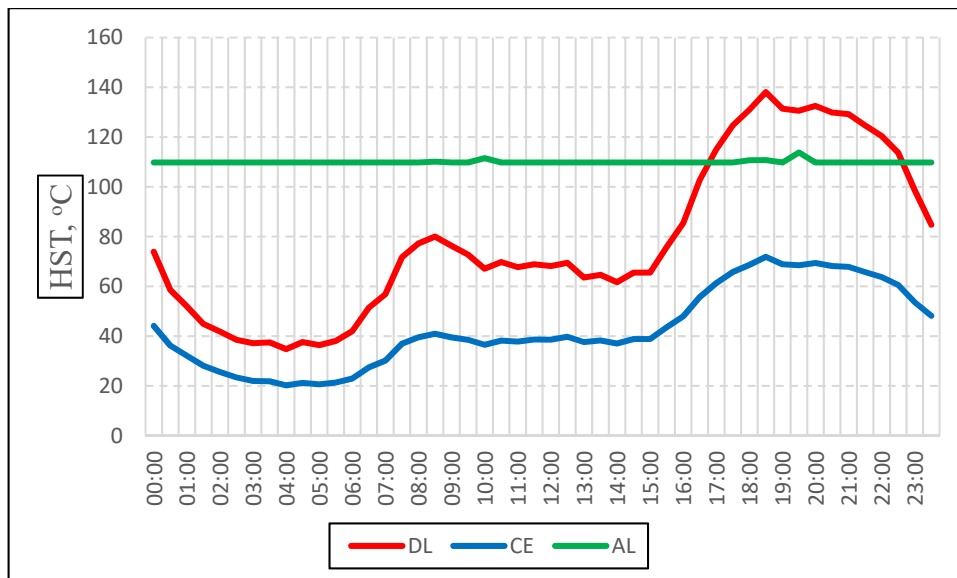


Fig. 5.5(a) HST curves of transformers on a Winter weekday

This implies that the transformer in the DL profile is thermally under-loaded up until 17:00 hours when it is now thermally overloaded for the rest of the evening. The

HST of the transformer in the AL profile of Fig. 5.5(a) is almost constant at **110°C** throughout the day. This implies that the transformer in the AL profile is adequately thermal loaded throughout the day. In the CE profile of Fig. 5.5(a), the HST of the transformer is below 110°C throughout the day reaching a maximum of **72°C** at 18:30 hours. The transformer is therefore thermally under-loaded.

The daily cumulative loss of life of the transformers in each of the loading profiles on a winter weekday are presented in Fig. 5.5(b). For the DL profile, the cumulative loss of life of the transformer is almost nil until 17:00 hours when it increases rapidly to reach a maximum of **0.02%** at the end of the day. The trend is due to the fact that the transformer in DL profile is initially thermally under-loaded until 17:00 hours and thereafter thermally overloaded for the rest of the evening. The daily cumulative loss of life of the transformer in DL profile is about two times above normal. For the AL profile, the cumulative loss of life of the transformer gradually increases from zero at 00:00 hours and reaches a maximum of about **0.01%** at 23:30 hours. This is the normal daily loss of life for a full life expectancy of the transformer.

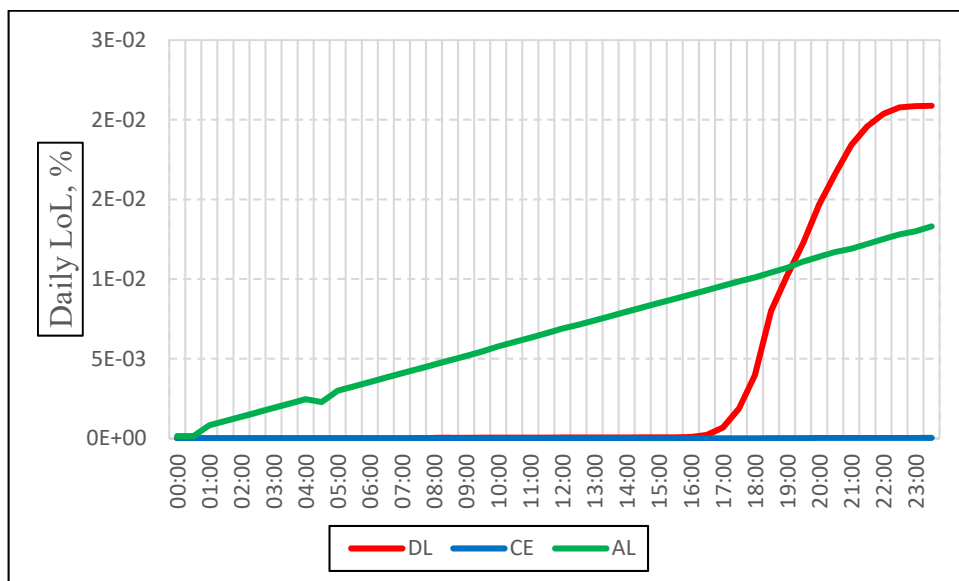


Fig. 5.5(b) Daily cumulative LoL plots of transformers on a Winter weekday

The daily cumulative loss of the transformer in the CE profile is almost zero as seen in Fig. 5.5(b). This is because the transformer is thermally under-loaded throughout the day. This practically implies that under this condition the transformer could out-live its normal life expectancy.

The daily return on utilisation of the transformer in each of the loading profiles on a winter weekday are presented in Fig. 5.6. The daily return on utilisation of transformer in DL and CE profiles are almost equal.

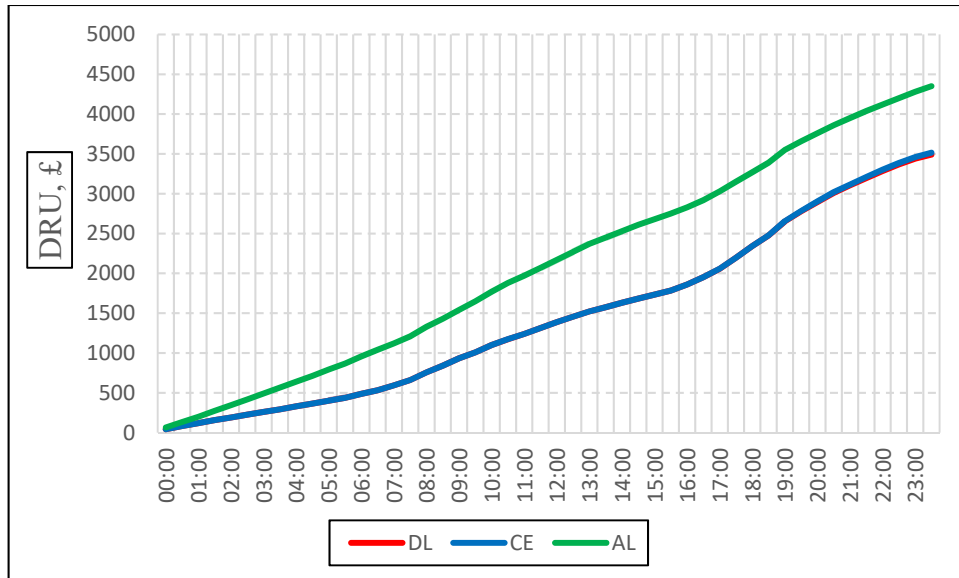


Fig. 5.6 Daily return on utilisation of transformers on a Winter weekday

This is because their *TOCs* are almost equal. The high cost of loss of life of transformer in DL profile almost balances the initial high cost of a higher rating transformer in CE profile. The daily return on utilisation of transformer in DL is the highest at a value of **£4350**, which is £835 more than *DRU* of CE. AL profile has the highest *DRU* because the transformer utilisation factor is relatively high and the loss of life of the transformer is moderately normal.

In order to make informed technical and financial decisions as to which loading method is the best, similar results of the transformer thermal behaviours, utilisation factor and *DRU* are presented for a typical summer weekday.

5.7.2 Typical Summer Weekday Results

Fig. 5.7(a) shows the load demand of the LV area and the transformer loading profiles of the three investigated situations on a typical Summer weekday and Fig. 5.7(b) shows the transformer utilisation factors for the three investigated situations.

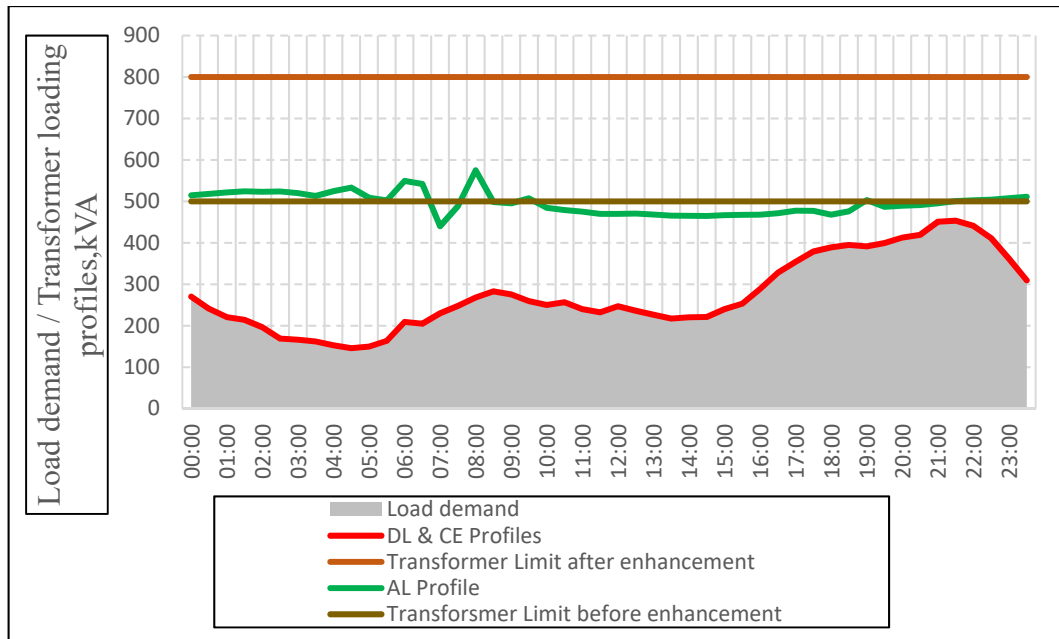


Fig. 5.7(a) Transformer Loading profiles on a Summer weekday

As seen in Fig. 5.7(a), the load demand of the LV area on a typical Summer weekday is such that the transformer capacity (even before enhancement) can withstand either in DL profile or AL profile. It is observed in the AL profile that the loading capability of the transformer is below the transformer limit at some period in the day. There is big capacity surplus between the load demand and the transformer limit after enhancement. This is reflected in the low utilisation factor of the transformer in the CE profile as seen in Fig. 5.7(b). The utilisation factor in the CE profile is below **0.4** for seventeen hours (almost $\frac{3}{4}$ of the day) with only a peak of **0.57** for one hour between 21:00 hours and 22:00 hours.

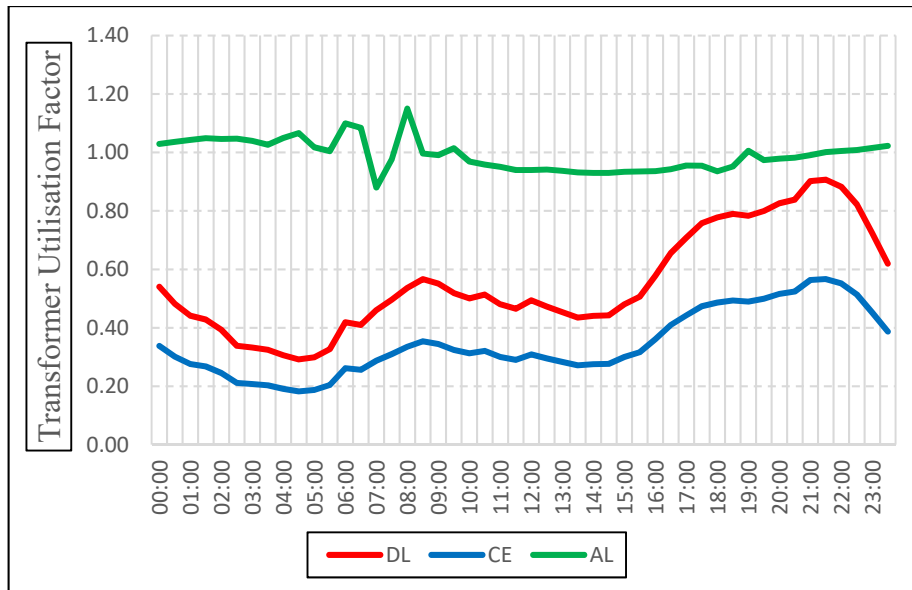


Fig. 5.7(b) Transformer Utilisation Factors on a Summer weekday

In the DL profile, the transformer has an average utilisation factor of about **0.38** during the night, **0.49** during the day and **0.79** in the evening. In the AL profile, the transformer has an average utilisation factor of about **1.04**, **0.97** during the day and **0.98** in the evening.

Corresponding thermal behaviours (HST curves) and the cumulative loss of life (LoL) of the transformers under the three investigated loading profiles on a typical Summer weekday are presented in Fig. 5.8(a) and (b) respectively.

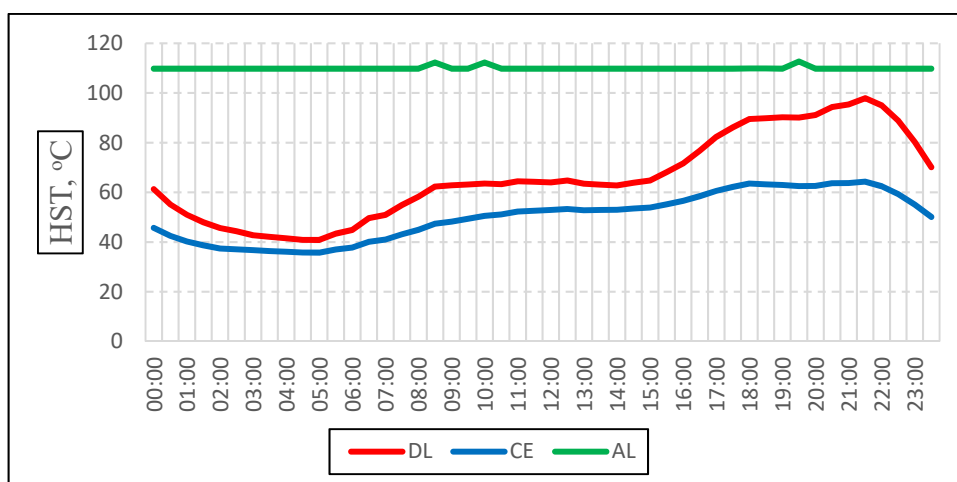


Fig. 5.8(a) HST curves of transformers on a Summer weekday

The HSTs in both DL and CE profiles are below the 110°C mark throughout the day. This indicates that the transformers in both cases are thermally under-loaded. The highest HST in the DL profile is 98°C at 21:30 hours while the highest HST in the CE profile is 64°C occurring at 18:00 hours and 21:30 hours. Accordingly, the daily cumulative loss of life of the transformers in DL and CE is virtually zero as seen in Fig. 5.8(b).

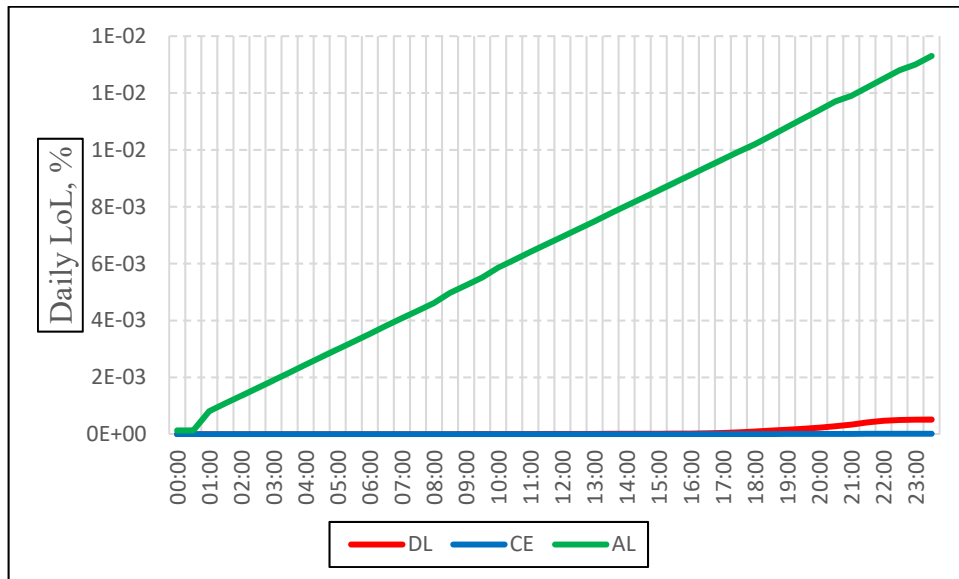


Fig. 5.8(b) Daily cumulative LoL plots of transformers on a Summer weekday

For the AL profile, the HST is almost constant at 110°C throughout the day as seen in Fig. 5.8(a). This implies that the transformer is adequately thermal loaded. For the AL profile, the cumulative loss of life of the transformer gradually increases from zero at 00:00 hours and reaches a maximum of about 0.01% at 23:30 hours as seen in Fig. 5.8(b). This is the normal daily loss of life for a full life expectancy of the transformer.

The daily return on utilisation of the transformer in each of the loading profiles on a Summer weekday are presented in Fig. 5.9. The daily return on utilisation of transformer in DL and CE profiles are almost equal at £2140. The daily return on utilisation of transformer in DL is £3660.

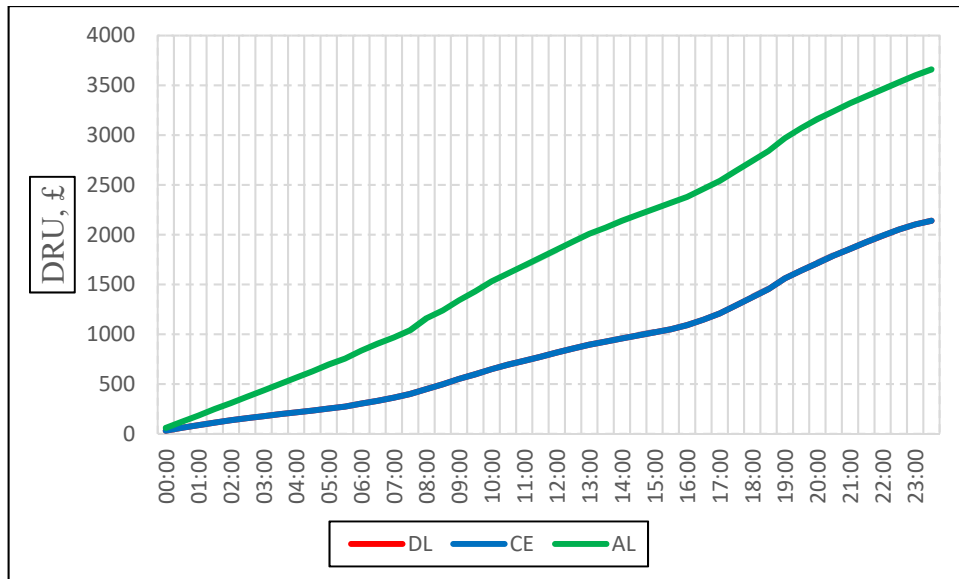


Fig. 5.9 Daily return on utilisation of transformers on a Summer weekday

5.8 COMPARISON OF RESULTS

Table 5.2 below gives a concise comparison of the transformer performances under the three investigated loading situations on both Winter weekday and Summer weekday in 2050. It is observed that upgrading the transformer capacity as done in CE has no comparative advantage over DL and AL in Summer. The transformer in CE is under-utilised in Summer.

Table 5.2 Comparison of transformer performances under different loading situations

Season	Utilisation Factor (Daily Average)			Daily LoL (%)			DRU (£)			Average excess load above Transformer limit (%)		
	DL	CE	AL	DL	CE	AL	DL	CE	AL	DL	CE	AL
Winter	0.90	0.56	1.18	0.02	~0	0.01	3491	3515	4350	30	0	15
Summer	0.55	0.35	0.99	~0	~0	0.01	2139	2140	3660	0	0	0

In DL, the Winter evening load demand exceeds the transformer limit by an average of about **30%** thereby overloading the transformer. The transformer has a high daily

loss of life, which is about two times higher than normal. This means that the useful life of the transformer could be shortened by a factor of **2** under this condition.

In the CE profile, the transformer is able to carry the load requirement of the LV area without any deficit and almost **zero** daily loss of life of the transformer in both Winter and Summer. However, the capacity utilisation factor of the transformer is low especially in Summer.

Transformer in AL has high utilisation factor and a daily loss of life value that ensures full useful life of transformer in both Winter and Summer. The high utilisation factor and normal daily loss of life combine to make the transformer in AL gives the highest daily return on utilisation in both Winter and Summer. The only drawback of the transformer in AL is the deficiency in meeting Winter load demand by an average of **15%**. However, with good load management and demand response the deficiency can be addressed without upgrading the transformer.

5.9 SUMMARY

An adaptive thermal loading method of distribution transformer serving LV area distribution network characterised by significant uptake of EVs and HPs was presented. The aim was to provide a cost-effective solution to the problems of transformer overloading and its attendant consequences of possible premature failure of transformer and restriction of further uptake of EVs and HPs.

A distribution transformer serving a real and typical urban LV distribution network in the UK was the case study. The thermal modelling of the transformer was developed based on IEC 60076-7:2005 standard. Then, the proposed adaptive thermal loading method was applied on the transformer when serving the future load of the LV area on a typical Winter weekday and a typical Summer weekday in 2050 following the integration of significant number of EVs and HPs in the area.

The proposed adaptive thermal loading method was formulated as a non-linear programming function that optimises the capacity utilisation factor of the transformer in accordance with the real and present operating and environmental conditions by maximising daily return on the transformer utilisation. Constraints to the optimisation problem are the thermal and load conditions that ensure the normal life expectancy of

the transformer is not compromised. The optimisation problem of the proposed adaptive thermal loading method was solved using Analytical Solver[®] – a commercial optimization software package from the Frontline Solvers.

To verify the usefulness of the proposed method, three situations were investigated:

- 1) **Dumb loading (DL)**: The transformer is allowed to carry the load demand of the LV area without any intervention. This is a do-nothing situation.
- 2) **Capacity enhancement (CE)**: The capacity of the transformer is upgraded to a higher rating, i.e. replace the transformer with one of higher rating.
- 3) **Adaptive loading (AL)**: The transformer is allowed to carry the load demand of the LV area based on the proposed adaptive thermal loading method.

The following were observed from the results:

- i) In DL, the transformer was overloaded by an average of **30%** in the evening of a Winter weekday and suffered a high daily loss of life (**0.02%**), two times above normal loss of life.
- ii) In AL, the transformer had high capacity utilisation factor, a daily average of **1.18** on a typical Winter weekday but was deficient in meeting the evening load demand by an average of **15%**. The loss of life of the transformer on a typical Winter weekday in AL was normal (**0.01%**) for a full life expectancy.
- iii) In CE, the transformer had a daily average capacity utilisation factor of **0.56**, on a typical Winter weekday. There was no deficiency in meeting the Winter load demand of the LV area and the transformer suffered virtually **zero** loss of life.

- iv) The daily average capacity utilisation factors of the transformers in CE, DL and AL on a Summer weekday were **0.35**, **0.55** and **0.99** respectively. All the load demand of the LV area was adequately met in all the investigated situations. Therefore, the higher rating transformer in CE had no comparative advantage over the transformer in DL and AL on a typical Summer weekday.

- v) On a typical Summer weekday, the daily loss of life of transformer in both DL and CE was virtually **zero** and the loss of life was normal (**0.01%**) for the transformer in AL.

- vi) The transformer in AL had the highest *DRU* of **£4350** and **£3660** on a Winter and a Summer weekday respectively.

CHAPTER 6

MANAGEMENT OF ELECTRIC VEHICLE CHARGING LOAD FOR OPTIMAL CAPACITY UTILISATION OF LOW VOLTAGE DISTRIBUTION TRANSFORMER

6.1 INTRODUCTION

The impacts of significant uptake of EVs and HPs in a LV distribution network area on the loading of the distribution transformer have been investigated in Chapter 4. The need for load management technique in addition to adaptive thermal loading of transformers in LV distribution networks characterised by significant uptake of EVs and HPs has been demonstrated in Chapter 5. For effective management of increased load demand and deferral of asset reinforcement, while allowing further uptake of EVs and HPs, adaptive thermal loading of transformers must be complemented with a load management technique in terms of DSR.

This Chapter presents a de-centralised load management technique, which exploits the advantage of long periods of EVs parking, to coordinate and control their charging without disrupting normal daily trips of the EV owners. In the proposed load management technique, two charging regimes are introduced:

- 1) **Controlled Charging Regime (CCR)** – This is between 16:30 hours and 06:00 hours of the next day. Within this period, charging of EVs are coordinated and controlled. The system aims at meeting the daily charge energy requirement of all the EVs in the LV area within this period without thermally overloading the transformer or violating any operational constraint. The process involves sorting the connected EVs according to their batteries' state of charge (SoC) and determining the number of EVs that could be placed on the network for charging during a time interval based

on their SoC and network constraints including thermal limit of the transformer.

- 2) **Uncontrolled Charging Regime (UCR)** – This is between 06:00 hours and 16:30 hours of the same day. In this period the charging of EVs are not coordinated.

The usefulness of the proposed load management technique is shown in a case study.

6.2 DAILY COMMUTING PATTERNS AND EVS USE

Understanding the timing and duration of EVs availability for charging, which is a function of the EV owners daily trips patterns, would help DNOs to make cost-effective infrastructure and operational decisions. Amongst the key observations from [142] hinted that most EV owners are either full time employed or self-employed and most EV owners charge at home. Therefore, understanding the daily commuting patterns of EV owners is crucial for proper design and implementation of the proposed controlled charging technique. According to [194], average start time of ‘outbound’ commuting journeys is 07:51 hours and the average start time of ‘homebound’ commuting journey is 16:23 hours. Fig. 6.1 is showing the daily trip patterns of commuters between the year 1998 and 2014 from the National Travel Survey as reported in [194]. From the UK Time Use Survey (UKTUS) data set [195], an average of 88 minutes (1.5 hrs) is spent on daily trips out of total 1440 minutes while the average time spent sleeping and resting is 517 minutes (8.6 hrs). Therefore, it can implied from the foregoing that an EV would be parked at home for at least eight hours. Also, the probability of the parking period falling between 16:23 hours to 07:51 hours of the next day is high – more than 70% as seen in Fig. 6.1.

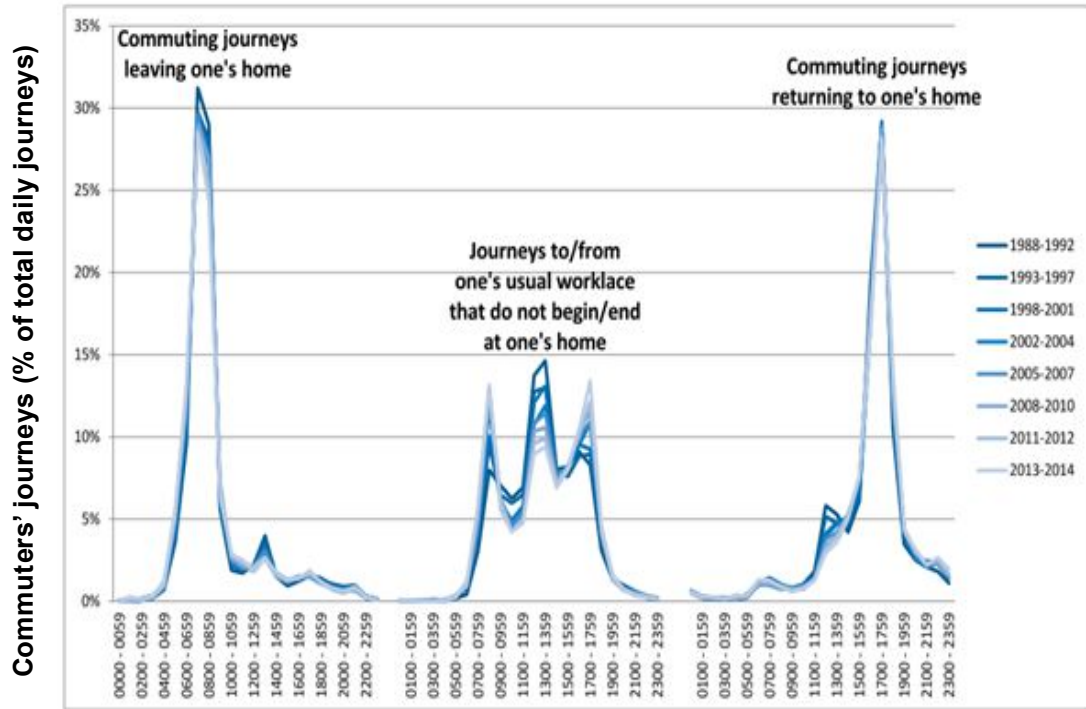


Fig. 6.1 Daily trip patterns of commuters (National Travel Survey) as reported in [194]

6.3 THE ARCHITECTURE OF THE DE-CENTRALISED LOAD MANAGEMENT TECHNIQUE

Fig. 6.2 shows the architecture of the proposed load management. The principal components of the architecture are EV Smart Charge Controller (EVSCC) located at the EV Owners' homes, the EV Load Controller (EVLC) located at the substation and the Distribution Transformer Monitor (DTM) located at the substation. The DTM is a special hardware device that collects, measures, records and processes key parameters of the distribution transformer such as load currents, temperature, oil level and the voltage [196]–[198]. The DTM is the interface device between the EVLC and the distribution transformer.

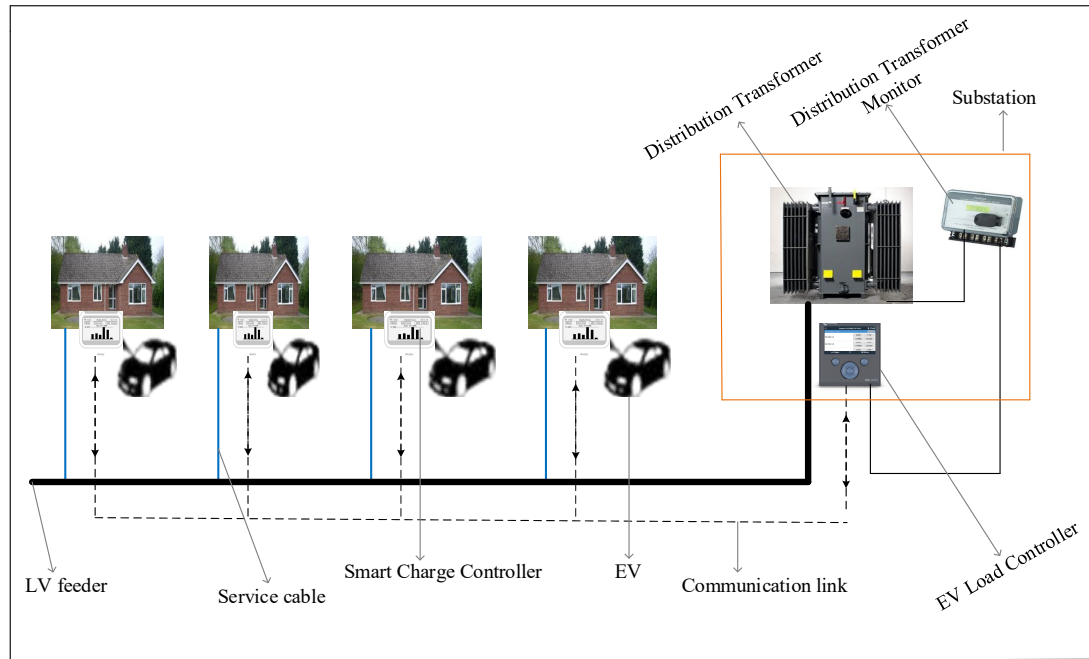


Fig. 6.1 The Architecture of the load management

The EVs are connected to the EVSCC for charging process to begin. The EVSCCs read the SoC of the batteries of the connected EVs, send their readings to the EVLC and await the control signal. The EVLC sorts the SoC in ascending order, calculates the charge energy and checks the DTM if the transformer can accommodate all the EVs at that period without violating any operational constraints, for example, thermal limits of the transformer and feeders, voltage deviation limits, etc. If the transformer can accommodate all the EVs at that period, a ‘YES’ control signal is sent to each of the EVSCCs to commence charging. But in the event that the transformer can only accommodate some but not all the EVs, the EVLC determines the number of EVs to be sent a ‘YES’ control signal (i.e. the number of EVs to be charged) through their EVSCCs giving priority to EVs with low SoC. The process is repeated at the next time interval. The cycle continues until all the connected EVs are fully charged. It is important to mention that the process described above is only operational during the period of Controlled Charging Regime but not during the period of Uncontrolled Charging Regime.

The two-way communication links between the EVSCCs and EVLC could be implemented either through Wireless Mesh Network (WMN) or WiMAX (Worldwide Interoperability for Microwave Access). Both WMN and WiMAX are not expensive, easy to implement and capable of wireless coverage reach of large area [199]–[201].

The uniqueness of this architecture is that it offers a de-centralised and autonomous system of EV charge management at the LV distribution network level devoid of complex interactions and exchange of information between EV owners, EV load aggregators and the DNOs.

6.4 THE DESIGN FORMULATION

The objective of the proposed load management is to ensure that the distribution transformer is able to meet, at all times, the load demand of the LV area it is serving without violating any operational constraint or affecting the normal activities of the residents of the LV area.

Firstly, to achieve the objective, the load on the transformer at a time interval t is broken into two components:

- Non-EV load – all other domestic loads excluding EVs charging load.
- EV load – exclusively EVs charging load.

Then, the transformer load is modulated by varying the EV load in an optimisation objective function which aims at maximising the transformer capacity utilisation subject to operational constraints and non-disruption of normal daily trips of EV owners in the LV area. This can be expressed mathematically as in equation (6.1).

$$L_{(t)} = \max \sum_{t=1}^T \left[L_{nonEV(t)} + P_{chg} \sum_{i=1}^N EV_{i(t)} \right] \quad (6.1)$$

Where:

$L_{(t)}$ is the load (kW) on transformer at time interval t .

$L_{nonEV(t)}$ is the Non-EV load (kW) at time interval t .

P_{chg} is the charger power rating (kW).

EV is the Electric Vehicle as an entity.

t is the index of time interval.

T is the total number of time intervals covering the Controlled Charging

Regime period.

i is the identifier index for EVs.

N is the total number of EVs.

The optimisation objective function of equation (6.1) is subject to the following constraints:

$$L_{nonEV}(t) \geq L_{nonEV_{forecasted}(t)} \quad (6.2)$$

$$P_{chg} \sum_{t=1}^T \sum_{i=1}^N EV_i(t) \geq P_{battery} \sum_{i=1}^N (1 - SoC_{i_{initial}}) \quad (6.3)$$

$$SoC_{i_{initial}} \geq 0.3 \quad (6.4)$$

$$L(t) \leq Trx_{limit}(t) \quad (6.5)$$

Where:

$L_{nonEV_{forecasted}(t)}$ is the forecasted domestic load (kW) at time interval t .

$L_{nonEV}(t)$ is the actual Non-EV (domestic) load (kW) at time interval t .

P_{chg} is the charger power rating (kW).

EV is the Electric Vehicle as an entity.

$P_{battery}$ is the battery power rating (kW) of EV.

$SoC_{i_{initial}}$ is the SoC (%) of the battery of EV_i at the time of plugging in.

$L(t)$ is the load (kW) on transformer at time interval t .

$Trx_{limit}(t)$ is the transformer load limit at time interval t .

t is the index of time interval.

T is the total number of time intervals covering the Controlled Charging

Regime period.

i is the identifier index for EVs.

N is the total number of EVs.

The constraint expressed in equation (6.2) ensures that the domestic (non-EV) load of the LV area is always met even when the load forecast is by mistake less than the

actual. Equation (6.3) aims at ensuring that the daily charge requirement of all connected EVs are met (i.e. the SoC of EVs are restored back to 100% before the start of the next day's trips) within the period of the Controlled Charging Regime. In equation (6.3), it is assumed that the EVs are connected for charging via a Mode 3 (AC) dedicated EV charging system operating at **3.7kW (16A)** as defined by BS EN 61851-1 standards [58]. Mode 3 charging system is capable of smart charging and it incorporates control, communications and protection functions [202].

In Equation (6.4), it is assumed that the initial SoC of EV batteries at the time of connection is limited to a minimum of 30%. The reason for this assumption has been previously explained in **Section 4.6 of Chapter 4**.

The constraint of equation (6.5) is to ensure that the transformer is not at any time loaded beyond its limit. The limit in this context refers to the adaptive thermal limit of the transformer that ensures optimal capacity utilisation under the real and present conditions without compromising the full useful life of the transformer. These limits have been previously determined in **Section 5.7 of Chapter 5** for a transformer serving a typical UK urban LV network area on a typical Winter weekday and a typical Summer weekday in the year 2050.

The algorithm of the load management is presented in Fig. 6.3.

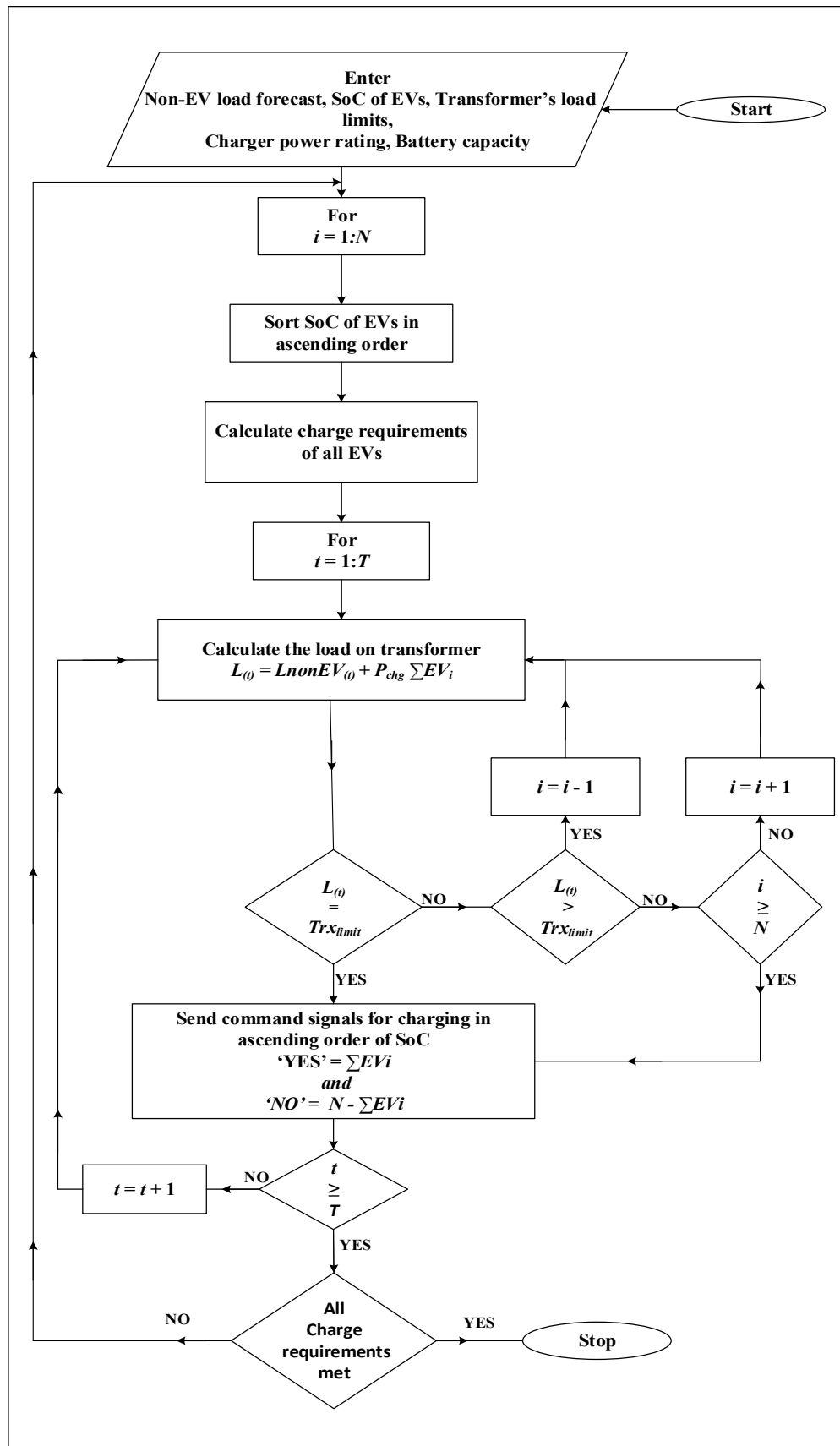


Fig. 6.3 The Algorithm of the load management

6.5 CASE STUDY

The LV area distribution network described in **Section 4.3** is the case study. By the year 2050, the LV area distribution network is projected to be hosting **256 EVs** and **207 HPs** under the most optimistic uptake scenario as seen in **Table 4.6** and **Table 4.8** of **Section 4.5** and **Section 4.7** respectively in **Chapter 4**. Powerflow simulation of the LV area distribution network was performed when the transformer is serving the LV area in the year 2050 on a typical winter weekday and a typical summer weekday. Fig. 6.4 and Fig. 6.5 show the half-hourly Non-EV and EV load demand of the LV area on a typical winter weekday and a typical summer weekday respectively.

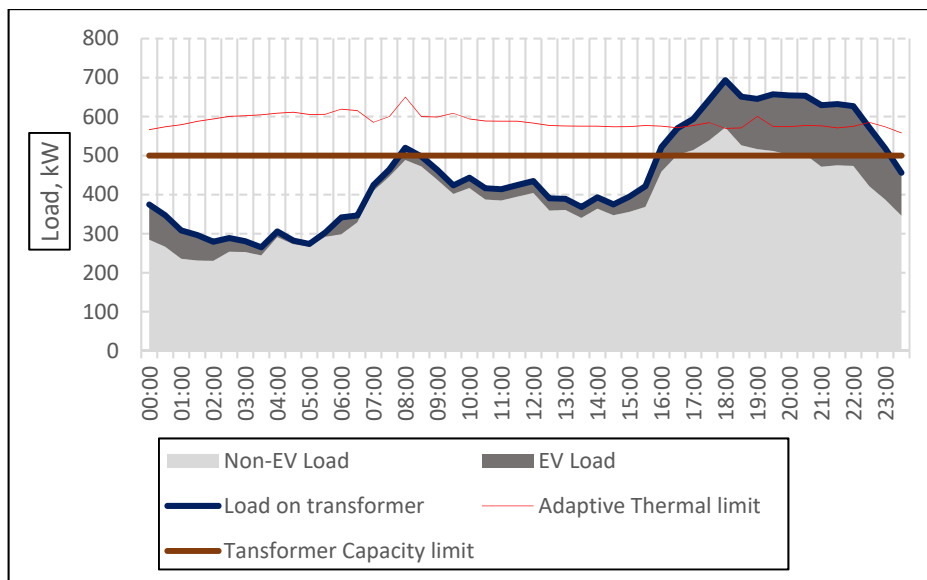


Fig. 6.4 Half-hourly Non-EV and EV load demand on a winter weekday in the year 2050

As seen from Fig. 6.4, on a winter weekday in the year 2050 the combined Non-EV and EV load demand of the LV area outstrips both the transformer capacity limit and adaptive thermal limit. But the severity of the overloading condition is much reduced with the transformer adaptive thermal limit relative to its capacity limit. Reasons for the overloading condition on a winter weekday are increased use of HPs (see **Fig. 4.10** in **Chapter 4**) and increased charging of EVs coinciding with the peak of the non-EV loads (see **Fig. 4.5** in **Chapter 4**). However, on a summer weekday in the year 2050, the load demand of the LV area is well contained within both the transformer capacity limit and adaptive thermal limit as seen in Fig. 6.5.

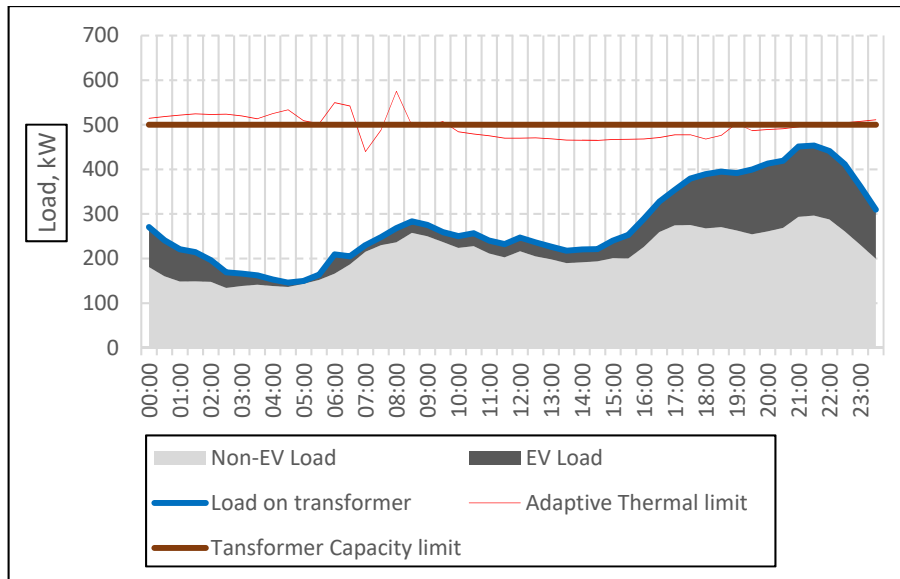


Fig. 6.5 Half-hourly Non-EV and EV load demand on a summer weekday in the year 2050

It has been shown in **Section 4.15 of Chapter 4** that there is no violation of voltage drop limit or ampacity limit of any cable even as the transformer is overloaded in the winter of the year 2050. The challenge is how to manage the transformer overloading cost-effectively without affecting the comfort or normal activities of the residents of the LV area. Good management of the overloading condition would create more headroom for further integration of EVs and HPs.

The proposed load management technique is applied on the LV area when its transformer is serving the future load demand of the area on a typical winter weekday in the year 2050. Table 6.1 gives the analysis of the total charge requirements of EVs in the LV area as estimated from the method and equation (4.9) described in **Section 4.6 of Chapter 4**.

Table 6.1 Analysis of the charge requirements of EVs

Number of EVs (Units)	Initial SoC		Energy required for charging (kWh)	Minimum plugging Time (hrs)
	(%)	(kWh)		
5	70	17	35	1.9
26	67	16	208	2.2
30	63	15	270	2.4
26	58	14	260	2.7
30	54	13	330	3.0
30	50	12	360	3.2
23	46	11	299	3.5
26	42	10	364	3.8
26	38	9	390	4.1
26	33	8	416	4.3
8	30	7	136	4.6
Total 256			3068	

From Table 6.1, it is seen that a total charge of 3,068kWh is required and the minimum initial SoC of EVs is 30%. With the assumed constant charging power of 3.7kW and battery capacity of 24kWh, a minimum plugging time of 5 hours per EV would be necessary to guarantee all EVs are fully restored to 100% SoC considering the minimum initial SoC of 30%.

6.6 RESULTS OF CASE STUDY

The optimisation objective function of equation (6.1) subject to the constraints of equations (6.2) to (6.5) was solved using ‘Analytical Solver[®]’ commercial optimisation software [193]. The model was diagnosed as “QCP NonCvx” and was solved using the standard GRG Nonlinear Solver Engine. Solution was found in 11.45 seconds at the 9th iteration, with all the constraints and optimality conditions satisfied, on a 3-GHz, 8-GB, 64-bit Windows 10 personal computer.

Fig. 6.6 shows the half-hourly contribution of the Non-EV and the EV load components to the transformer load of the LV area and the number of EVs that could receive charging at half-hourly interval on a winter weekday in the year 2050 after applying the proposed load management technique.

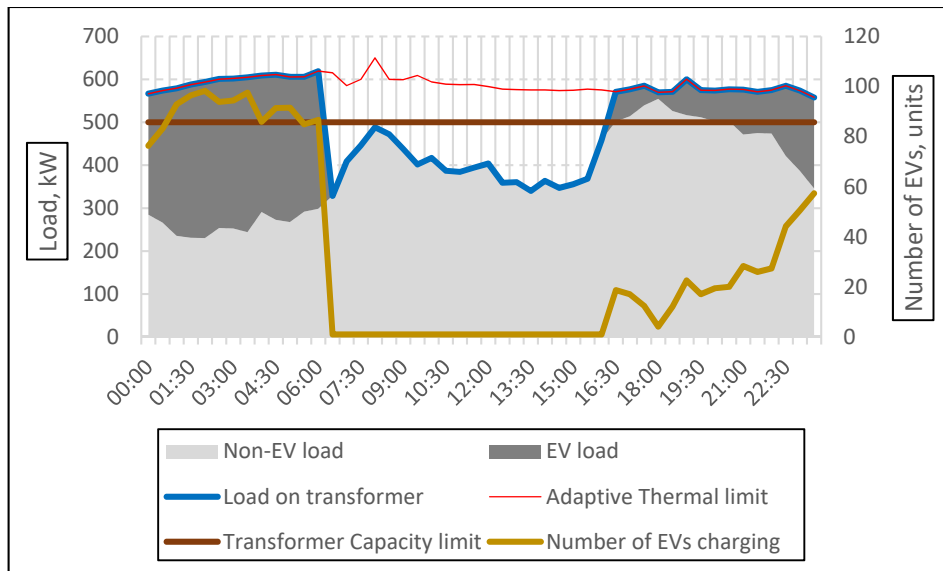


Fig. 6.6 Half-hourly contribution of Non-EV and EV load components to transformer load after applying load management technique

The transformer is no more overloaded. Although, the load outstrips the nominal capacity of the transformer, but it is kept within the confines of the transformer adaptive thermal limits. The useful normal life expectancy and therefore, the normal operation of the transformer is not compromised. Between 16:30 hours and 20:30 hours, the Non-EV component of the total load demand exceeds the transformer nominal capacity. Therefore, hinging the decision for the need of load management on the transformer nominal capacity would require more complex solution than taking the advantage of the flexibility of the charging of EVs as in the present case. This underscores the importance of why the need for load management and/or transformer capacity reinforcement or otherwise should not be based on static nominal capacity of transformers but rather on their adaptive thermal ratings.

The charging of the EVs is scheduled to avoid the peak of the Non-EV load. At the peak of the Non-EV load, only 4 EVs could receive charging. As the Non-EV load decreases, more EVs are allowed to be charged. At 02:00 hours, as many as 98 EVs could be charged at once.

During the Controlled Charging Regime, a total of **5,738kWh** of energy is available for EVs charging. This is almost **double** the daily charge requirements of **3,068kWh** of the 256 EVs in the LV area in the year 2050. The valley region of the total load on transformer between 06:00 hours and 16:30 hours is the Uncontrolled Charging Regime. During this period, EV owners could charge their vehicles at their own liberty as the possibilities of overloading the transformer are remote.

With the potential of more availability of energy (kWh) for charging of EVs during the Controlled Charging Regime and the liberty of charging of EVs during the Uncontrolled Charging Regime, the LV area distribution network could accommodate further uptake of EVs beyond the year 2050 without immediate need for capacity reinforcement.

6.7 SUMMARY

A de-centralised load management technique, which proffers solution to the issue of distribution transformer overloading in LV area distribution networks hosting considerable number of EVs and HPs, was developed.

A typical urban LV area distribution network in the UK was the case study. The load management technique was applied on the case study LV area when the transformer serving the area is carrying the future load demand of the area on a typical winter weekday in the year 2050.

The proposed de-centralised load management technique exploits the flexibility in the charging of EVs, by taking advantage of long periods of EVs parking, to coordinate and control their charging without disrupting normal daily trips of EV owners or violating operational limits of the network.

It was established that at least 70% of EVs are parked for at least 8 hours between 16:23 hours and 07:51 hours of the next day in a typical residential LV area distribution network. On this premise, two charging regimes were proposed in the load management technique:

- 1) **Controlled Charging Regime (CCR)** – This is between 16:30 hours and 06:00 hours of the next day. Within this period, charging of EVs are coordinated and controlled. The process involves sorting the connected EVs

according to the SoC of their batteries and determining the number of EVs that could be placed on the network for charging during a time interval based on their SoC and network constraints including thermal limit of the transformer.

- 2) **Uncontrolled Charging Regime (UCR)** – This is between 06:00 hours and 16:30 hours of the same day. In this period the charging of EVs are not coordinated.

It was assumed that the EVs were connected for charging via a Mode 3 (AC) dedicated EV charging system, which incorporates control, communications and protection functions, operating at **3.7kW (16A)** as defined by BS EN 61851-1 standards. It was also further assumed that the capacity of battery for EVs was 24kWh and were not depleted below 30% SoC.

The coordination and control of the charging of the EVs was assumed by means of a wireless two-way communication link between the EVSCCs at EV owners' premises and the EVLC at the substation. The EVSCCs send the SoC of connected EV batteries to the EVLC at the beginning of the Controlled Charging Regime and at intervals while the regime lasts. The EVLC reads and sorts EV batteries in ascending order of their SoC and sends control signals for charging to as many EVs as the transformer could withstand at that interval based on the present condition of the transformer as analysed by the DTM.

To manage the load on the transformer, the load demand of the LV area was divided into Non-EV load component and EV load component. Then the load on the transformer was modulated by varying the EV load component in an optimisation objective function which aims at maximising the transformer capacity utilisation subject to operational constraints and non-disruption of normal daily trips of EV owners.

The optimisation objective function was solved using Analytical Solver[®] and the following were observed from the results:

- i) The transformer that was previously overloaded by about **30%** for about **5 hours** in the evening was no more overloaded. Although, the load outstripped the nominal capacity of the transformer, but it was kept within the confines of the transformer adaptive thermal limits.

- ii) A total of **5,738kWh** of energy was available for EVs charging during the Controlled Charging Regime. This almost **double** the daily charge requirements of **3,068kWh** of the 256 EVs in the LV area in 2050.

- iii) Considering the amount of available energy (kWh) for charging of EVs during the Controlled Charging Regime and also with the potential and liberty of EV owners to charge their EVs during the Uncontrolled Charging Regime, the LV area distribution network could accommodate further uptake of EVs beyond 2050 without immediate need for capacity reinforcement.

CHAPTER 7

CONCLUSIONS AND SUGGESTIONS FOR FUTURE WORK

7.1 FULFILLING THE AIM OF THE STUDY

This thesis investigated the load management of EVs and HPs in the emerging Electricity System. The key question that the thesis aimed at addressing is – how can the new and additional electric load demand of EVs and HPs on the Electricity System be managed to help achieve the CO₂ emission reduction targets in the most economic manner? The study carried out in Chapter 4 showed that overloading of distribution transformers is the main challenge that may restrict significant uptake of EVs and HPs at the LV distribution network. The proposed solutions in this thesis are:

1. **Adaptive thermal loading of distribution transformers:** An adaptive thermal model for loading of distribution transformers has been developed and tested on a real LV distribution network hosting a significant uptake of EVs and HPs (Chapter 5). Results showed that the loadability/capacity utilisation of distribution transformers improved by as much as 18% above their nameplate rating in winter.
2. **De-centralised load management technique combined with adaptive thermal loading of distribution transformers:** A de-centralised load management technique combined with adaptive thermal loading of distribution transformers was developed and tested on the transformer of a real LV distribution network hosting future uptake level (up to the year 2050) of EVs and HPs (Chapter 6). Results showed that the transformer could withstand the load requirements of the uptake level of EVs and HPs up to the year 2050 without compromising its normal life expectancy.

7.2 THESIS CONTRIBUTIONS

The main contributions of this thesis are summarised:

1. The development of an algorithm for estimating the GHG emissions reduction due to the electrification of the road transportation sector. This is particularly useful for the policy makers in setting targets for the reduction of GHG emissions vis-à-vis the uptake of EVs and deployment of renewable energy sources in the electricity system.
2. The development of a dispatch model for power system which is suitable for analysing the impacts of charging patterns of EVs on power system scheduling, grid emission intensity, GHG emissions and costs of emission abatement. The dispatch model will aid the PSOs to assess their operational philosophy under different EV charging patterns and take actions as appropriate.
3. The development of an algorithm for the operational model of variable speed Air Source Heat Pump (ASHP) for the provision of both domestic hot water and space heating in residential buildings. The model is useful in determining the operational profiles of HPs in residential buildings. The model was used in the impact study of EVs and HPs on the residential LV distribution network.
4. The development of an adaptive thermal model for loading of distribution transformers under varying operating environments and conditions. The model is useful for the DNOs in their planning and operations. Given the weather and load forecasts, the model enables DNOs to optimally schedule load on distribution transformers.
5. The development of a de-centralised load management technique that incorporates a wireless two-way communication between EVs and distribution transformer of residential LV network to manage the charging of EVs and avoid transformer overloading. The concept is useful in that it ensures the maximisation of distribution transformer

capacity and extends the hosting capability of the transformer for further uptake of EVs and HPs. This is particularly useful for the DNOs.

7.3 CONCLUSIONS

This thesis proposed a de-centralised load management technique of EVs combined with adaptive thermal loading of distribution transformers to address the problem of overloading due to the uptake of EVs and HPs in the quest to reducing GHG emissions.

7.3.1 Estimating the True GHG Emissions Reduction due to EVs Integration

An algorithm was developed and used to calculate the annual CO₂ emissions at the UK power grid due to the charging of EVs between the period of 2009 and 2013. The algorithm also calculated CO₂ emissions savings on the road if internal combustion engine (ICE) cars are replaced with EVs. The difference between the CO₂ emissions savings on the road and CO₂ emissions at the grid due to the charging of EVs gives the true estimate of the CO₂ emissions reduction or otherwise in the real context.

Results showed that as the reduction of CO₂ emissions due to uptake of EVs is increasing from 2009 to 2013 so is the average CO₂ emissions intensity of the ICE cars decreasing from 2009 to 2013. The implication of the foregoing statement is that a point could be reached when further uptake of EVs might not contribute to CO₂ emissions reduction if either or both of the following is the case:

- Average CO₂ emissions intensity of ICE cars continues to decrease and there is not appropriate increase of renewable energy sources (RES) and other low carbon sources in the electricity generation mix.
- Average CO₂ emissions intensity of ICE cars continues to decrease and there is not significant increase in the average efficiency of EVs.

7.3.2 Dispatch Model for Analysing Impacts of EVs Charging Patterns on Power System Scheduling, Grid Emissions Intensity and Emissions Abatement Cost

A dispatch model was developed based on the correlation identified from historical data between system load demand and capacity factors of generating units. A 50% uptake of EVs was assumed. Two types of EV charging patterns were used in the work. In one of the patterns, the charging of the EVs is based on the time of use tariff, designated as Time-Of-Use Charging (TOUC), which encourages charging of EVs during the off-peak period at night. In the other pattern, EV owners charge their cars without regard to time of use tariff, designated as Without-Time-Of-Use Charging (WTOUC). The model was then used to dispatch the generating resources to meet system load demand under the two charging patterns of EVs.

From the results the following conclusions can be made:

- Charging pattern that encourages charging of EVs in the off-peak period may affect the optimal use of generating technologies/resources with storage capability e.g. Pumped hydro unit.
- Average grid emission intensity could be higher with the charging pattern of EVs based on time-of-use tariff. This was the case in this work because there was less contribution from the Pumped hydro unit.
- Marginal increase in grid emissions and marginal increase in electricity generation costs are likely to be lower in the TOUC pattern than in the WTOUC pattern. Therefore, emissions abatement costs are likely to be higher in WTOUC than in the TOUC.

7.3.3 EVs and HPs Integration in LV Distribution Networks

The impacts of integration of EVs and HPs, in a real LV network were investigated. Four scenarios were formulated based on the season and projected uptakes of EVs and HPs in the years 2020, 2030, 2040 and 2050. Calculations were made by scaling down the national projected number of EVs and HPs to estimate the uptake of EVs and HPs

in a typical residential LV area distribution network. Average minimum daily energy requirement of an EV was estimated to be **7.2kWh** and the possible maximum daily energy requirement was estimated to be **16.8kWh**. Average electricity demand profiles of HP for a typical winter weekday and a typical summer weekday were created by modelling the operation of HP and implementing the model in MATLAB. The modelled operation of the HP was validated against an actual field trial project.

For all the scenarios in all the years considered, power flow simulations of the LV area distribution network were carried out using GridLAB-D, an agent-based power system simulation software. The results of this study showed that the first possible factor that may restrict further uptake of EVs and HPs at residential LV distribution networks is the issue of transformer overloading.

7.3.4 Adaptive Thermal Loading of Distribution Transformers

An adaptive thermal loading method of distribution transformer in a low carbon LV network was presented. The focus had been to propose and demonstrate a cost-effective solution which encourages intensive capacity utilization of existing distribution transformer in a low carbon LV network hosting considerable number of EVs and HPs. A distribution transformer serving a typical real urban LV network in the UK was used as the case study. The thermal behaviours of the transformer were analysed when carrying the load demand of the LV area on a winter weekday and a summer weekday in year 2050 following considerable uptake of EVs and HPs in the area. In the method, a non-linear programming optimisation function was formulated that optimises the capacity utilisation factor of the transformer in accordance with the real and present operating and environmental conditions by maximising daily return on the transformer utilisation. Constraints to the optimisation problem are the thermal and load conditions that ensure the normal life expectancy of the transformer is not compromised. Three situations were investigated to verify the usefulness of the proposed method:

- 1) **Dumb loading (DL):** The transformer is allowed to carry the load demand of the LV area without any intervention. This is a do-nothing situation.
- 2) **Capacity enhancement (CE):** The capacity of the transformer is upgraded to a higher rating, i.e. replace the transformer with one of higher rating.

- 3) Adaptive loading (AL):** The transformer is allowed to carry the load demand of the LV area based on the proposed adaptive thermal loading method.

Results showed that the loading capability of the transformer increased by about **18%** over its static rating in winter with the proposed method of loading. Whereas in summer, the loading capability of the transformer decreased by about **1%** below its static rating.

7.3.5 Management of EVs Charging

A de-centralised load management technique exploiting the flexibility in the charging of EVs was presented. Two charging regimes were assumed. The Controlled Charging Regime between 16:30 hours and 06:00 hours of the next day and the Uncontrolled Charging Regime between 06:00 hours and 16:30 hours of the same day. During the Controlled Charging Regime, it was assumed the charging of EVs is coordinated and controlled by means of a wireless two-way communication link between EV Charge Controllers at EV owners' premises and the EV Load Controller at the local LV substation. The EV Load Controller sorts the EVs batteries in ascending order of their SoC and sends command signals for charging to as many EVs as the transformer could allow at that interval based on the condition of the transformer analysed by the Distribution Transformer Monitor.

A typical urban LV area distribution network in the UK was used as the case study. The technique was applied on the LV area when its transformer was carrying the future load demand of the area on a typical Winter weekday in year 2050. To achieve the load management, load demand was decomposed into Non-EV load and EV load. Then the load on transformer was managed by varying the EV load in an optimisation objective function which maximises the capacity utilisation of the transformer subject to operational constraints and non-disruption of daily trips of EV owners.

Results showed improved hosting capability of the LV distribution network for EVs and HPs in terms of energy available for the charging of EVs. In the case study, a total of **5,738kWh** energy was available for charging of EVs during the Controlled Charging Regime. This is almost double of the daily charge requirement of **3,068kWh** of **256** EVs (representing **63%** uptake) in the LV area.

7.4 SUGGESTIONS FOR FURTHER WORK

Possible paths for future work are:

- In the work about the impacts of EV charging patterns on Power System scheduling, grid emissions intensity and net emissions abatement cost presented in Chapter 3, the EV charging profiles used in the work are mostly suitable for residential LV distribution network. Therefore, consideration could be given to EV charging profiles from commercial LV area distribution network to be included in the study to further the work.
- In Chapter 4, variable speed ASHP was assumed, reasons being that ASHP requires no elaborate installation process of digging of ground to lay ducts and its power consumption varies with the heating need of ambience at a particular time. However, in practice, there would be different types of HPs installed at different residential buildings. Future work could look at an aggregation of combination of different types of HPs – Ground Source, Air Source, Constant speed, Variable speed, etc. Also, based on the present situation, the battery of Nissan Leaf 24kWh, being the most driven EV in the UK, was used in the work. In the future, different battery models based on the currently available EVs could be used in the work to reflect the reality of that time.
- For the thermal modelling of transformer in Chapter 5, the exponential equations solution model of the IEC 60076-7:2005 was used. This is suitable for the half-hourly resolution of the load and ambient temperature available for use in the work. However, for smaller resolution of temperature and load, the difference equations solution is more appropriate and will give more details especially when solved by numerical analysis solution. The only caveat though, is that the time resolution must not be greater than one-half of the winding time constant.
- All EV owners are assumed to participate in the load management scheme presented in Chapter 6, allowing the DNOs to coordinate and control the charging of their EVs during the Controlled Charging Regime. The agreement between the EV owners and DNOs should be regulated on contractual basis,

for the mutual benefits of the parties involved. Such agreement was not covered in this work. Considering such regulated agreement between the EV owners and DNOs could extend this work further. As well the work could be extended by practically implementing the model, especially the two-way communication between the EVSCCs and EVLC at the LV substation. Also, in the future, different battery models based on the currently available EVs could be used to reflect the reality of that time. Finally, as the V2G technology matures and costs of EV batteries drop such that V2G deployment becomes economical from the perspective of EV owners, the concept could be inserted in the present work to extend it further.

REFERENCES

- [1] Intergovernmental Panel on Climate Change (IPCC), “AR5 Climate Change 2014: Mitigation of Climate Change,” New York, 2014.
- [2] D. Attenborough, “COP 24: Opening words of the UN Charter.” United Nations, Katowice, pp. 1–2, 2018.
- [3] Intergovernmental Panel on Climate Change (IPCC), “Global Warming of 1.5 °C,” Geneva, 2018.
- [4] Climate Action Tracker (CAT), “2100 Warming Projections,” *Temperatures*, 2017. [Online]. Available: <https://climateactiontracker.org/global/temperatures/>. [Accessed: 08-Dec-2018].
- [5] Department for Business, Energy and Industrial Strategy (DBEIS), “2016 UK Greenhouse Gas Emissions, Final Figures,” *Statistical Release: National Statistics*, no. February. London, pp. 1–51, 2018.
- [6] Parliament of UK, “Climate change: Action!,” *Spore*, vol. 1, no. 136. Statute Law Database, p. 15, 2008.
- [7] Parliament of UK, “Finance Act 2000: Part II Climate Change Levy.” Statute Law Database, p. 622, 2000.
- [8] Office of Gas and Electricity Markets (Ofgem), “Guidance for generators: Co - location of electricity storage facilities with renewable generation supported under the Renewables Obligation or Feed-in Tariff schemes (Version 2).” London, pp. 1–36, 2018.
- [9] Office of Gas and Electricity Markets (Ofgem), “Feed-in Tariffs: Guidance for Licensed Electricity Suppliers (Version 10).” Ofgem, London, pp. 1–132, 2018.
- [10] Department for Business, Energy and Industrial Strategy (DBEIS), “THE RENEWABLE HEAT INCENTIVE: A REFORMED SCHEME.” London, pp. 1–116, 2016.
- [11] Office for Low Emission Vehicles (OLEV), “Reformed Plug-In Car Grant extended into next decade - GOV.UK,” *News story*, 2018. [Online]. Available:

- <https://www.gov.uk/government/news/reformed-plug-in-car-grant-extended-into-next-decade>. [Accessed: 10-Dec-2018].
- [12] M. Eshani, Y. Gao, S. Longo, and K. Ebrahimi, *Modern Electric, Hybrid Electric, and Fuel Cell Vehicles*, 3rd ed. Boca Raton: CRC Press, 2018.
- [13] Department of Energy (DOE), Office of Energy Efficiency & Renewable Energy, “Fuel Economy Guide.” [Online]. Available: <https://www.fueleconomy.gov/feg/PowerSearch.do?action=noform&path=1&year1=1984&year2=2019&vtype=Electric>. [Accessed: 08-May-2016].
- [14] H. S. Das, C. W. Tan, and A. H. M. Yatim, “Fuel cell hybrid electric vehicles: A review on power conditioning units and topologies,” *Renew. Sustain. Energy Rev.*, vol. 76, pp. 268–291, Sep. 2017.
- [15] A. Hepbasli and Y. Kalinci, “A review of heat pump water heating systems,” *Renew. Sustain. Energy Rev.*, pp. 1–19, 2008.
- [16] International Energy Agency (IEA), “Heat pumps for cooling and heating Subtask 5, Report n:o 3,” Finland, 2011.
- [17] T. Nowak, “Heat Pumps: Integrating technologies to decarbonise heating and cooling,” 2018.
- [18] A. Michael and E. Baster, “Modelling the performance of Air Source Heat Pump Systems,” University of Strathclyde, 2011.
- [19] M. Forsén, “Heat pumps: technology and environmental impact,” 2005.
- [20] Natural Resource Canada’s Office of Energy Efficiency (NRC), *Heating and cooling with a heat pump*. 2004.
- [21] Wärmepumpen-Testzentrum WPZ, “Information sheet of the Heat Pump Test Center WPZ,” *WPZ – Bulletin*, vol. 41, no. 2. University of applied science NTB, Buchs, pp. 1–24, 2013.
- [22] G. Martinopoulos, K. T. Papakostas, and A. M. Papadopoulos, “A comparative review of heating systems in EU countries, based on efficiency and fuel cost,” *Renew. Sustain. Energy Rev.*, vol. 90, pp. 687–699, Jul. 2018.
- [23] B. Wyse, “Investigation into the Time-Shifting Of Domestic Heat Loads,” University of Strathclyde, 2011.

-
- [24] R. Domitrovic, “Variable-Speed Heat Pumps for Energy Efficiency and Demand Response,” California, 2014.
- [25] K. Herold, R. Radermacher, and S. Klein, *Absorption Chillers and Heat Pumps, Second Edition*. CRC Press, 2016.
- [26] D. Del Col, M. Azzolin, G. Benassi, and M. Mantovan, “Energy efficiency in a ground source heat pump with variable speed drives,” *Energy Build.*, vol. 91, pp. 105–114, Mar. 2015.
- [27] Department for Transport (DfT), “Vehicle Licensing Statistics: Annual 2017,” *Statistical Release*, no. April. 2018.
- [28] Office of Gas and Electricity Markets (Ofgem), “Public reports and data: Domestic RHI.” [Online]. Available: <https://www.ofgem.gov.uk/environmental-programmes/domestic-rhi/contacts-guidance-and-resources/public-reports-and-data-domestic-rhi>. [Accessed: 30-Dec-2018].
- [29] T. R. Hawkins, B. Singh, G. Majeau-Bettez, and A. H. Stromman, “Comparative Environmental Life Cycle Assessment of Conventional and Electric Vehicles,” *J. Ind. Ecol.*, vol. 17, no. 1, pp. 53–64, 2013.
- [30] E. Crossin and P. J. . Doherty, “The effect of charging time on the comparative environmental performance of different vehicle types,” *Appl. Energy*, vol. 179, pp. 716–726, 2016.
- [31] L. A.-W. Ellingsen, B. Singh, and A. H. Stromman, “The size and range effect: lifecycle greenhouse gas emissions of electric vehicles,” *Environ. Res. Lett.*, vol. 11, no. 054010, pp. 1–8, 2016.
- [32] J. P. Helveston, Y. Liu, E. M. Feit, E. Fuchs, E. Klampfl, and J. J. Michalek, “Will subsidies drive electric vehicle adoption? Measuring preferences in the U.S. and China,” *Transp. Res. Part A*, vol. 73, pp. 96–112, 2015.
- [33] G. Zhou, X. Ou, and Z. Xiliang, “Development of electric vehicles use in China: A perspective of life-cycle energy consumption and greenhouse gas emissions,” *Energy Policy*, vol. 59, pp. 875–884, 2013.
- [34] O. Zehner, “Unclean at any speed,” *IEEE Spectr.*, vol. 50, no. 7, pp. 40–45, 2013.

-
- [35] J. Petersen, “Plug-in Vehicles and Their Dirty Little Secret - Renewable Energy World,” *Renewable Energy World*, 2011. [Online]. Available: <https://www.renewableenergyworld.com/articles/2011/01/plug-in-vehicles-and-their-dirty-little-secret.html>. [Accessed: 16-Dec-2018].
- [36] R. Edwards, J.-F. Larivé, D. Rickeard, and W. Weindorf, “Well-to-Wheels analysis of future automotive fuels and powertrains in the European context WELL-TO-TANK (WTT) Report,” Luxembourg, 2014.
- [37] H. Ma, F. Balthasar, N. Tait, X. Riera-Palou, and A. Harrison, “A new comparison between the life cycle greenhouse gas emissions of battery electric vehicles and internal combustion vehicles,” *Energy Policy*, vol. 44, pp. 160–173, 2012.
- [38] L. Canals Casals, E. Martinez-Laserna, B. Amante García, and N. Nieto, “Sustainability analysis of the electric vehicle use in Europe for CO2 emissions reduction,” *J. Clean. Prod.*, vol. 127, pp. 425–437, Jul. 2016.
- [39] C. Grant, R. Hsu, P. Keegan, and W. Kallock, “Plug-in Electric Vehicles and Electric Cooperatives, Vol.2: Managing the Financial and Grid Impacts of Plug-in Electric Vehicles,” Virginia, 2015.
- [40] D. B. Richardson, “Electric Vehicles and the electric grid: A review of modelling approaches, impacts, and renewable energy integration,” *Renew. Sustain. Energy Rev.*, vol. 19, pp. 247–254, 2013.
- [41] J. Todd, J. Chen, and F. Clogston, “Creating the Clean Energy Economy: Analysis of the Electric Vehicle Industry,” Washington, DC, 2013.
- [42] I. G. Unda, “Management of Electric Vehicle Battery Charging in Distribution Networks,” Cardiff, 2012.
- [43] E. Sortomme, “Combined bidding of regulation and spinning reserves for unidirectional Vehicle-to-Grid,” in *2012 IEEE PES Innovative Smart Grid Technologies (ISGT)*, 2012, pp. 1–7.
- [44] T. K. Miao, V. K. Ramachandaramurthy, and J. Y. Yong, “Integration of electric vehicles in smart grid: A review on vehicle to grid technologies and optimisation techniques,” *Renew. Sustain. Energy Rev.*, vol. 53, pp. 720–732, 2016.

-
- [45] H. Bevrani and T. Hiyama, *Intelligent Automatic Generation Control*. New York: DRC Press, Taylor and Francis Group, 2011.
- [46] J. Zhao, C. Wan, Z. Xu, and K. P. Wang, “Spinning Reserve Requirement Optimization Considering Integration of Plug-In Electric Vehicles,” *IEEE Trans. Smart Grid*, vol. 8, no. 4, pp. 2009–2021, 2017.
- [47] M. Ansari, A. T. Al-Awami, E. Sortomme, and M. A. Abido, “Coordinated Bidding of Ancillary Services for Vehicle-to-Grid Using Fuzzy Optimization,” *IEEE Trans. Smart Grid*, vol. 6, no. 1, pp. 261–270, 2015.
- [48] E. Sortomme and M. A. El-Sharkawi, “Optimal Combined Bidding of Vehicle-to-Grid Ancillary Services,” *IEEE Trans. Smart Grid*, vol. 3, no. 1, pp. 70–79, Mar. 2012.
- [49] E. Sortomme and M. A. El-Sharkawi, “Optimal Charging Strategies for Unidirectional Vehicle-to-Grid,” *IEEE Trans. Smart Grid*, vol. 2, no. 1, pp. 131–138, Mar. 2011.
- [50] M. Dubarry, A. Devie, and K. McKenzie, “Durability and reliability of electric vehicle batteries under electric utility grid operations: Bidirectional charging impact analysis,” *J. Power Sources*, vol. 358, pp. 39–49, Aug. 2017.
- [51] K. M. Tan, V. K. Ramachandaramurthy, J. Y. Yong, S. Padmanaban, L. Mihet-Popa, and F. Blaabjerg, “Minimization of Load Variance in Power Grids—Investigation on Optimal Vehicle-to-Grid Scheduling,” *Energies*, vol. 10, no. 11, p. 1880, Nov. 2017.
- [52] M. Uddin, M. F. Romlie, M. F. Abdullah, S. Abd Halim, A. H. Abu Bakar, and T. Chia Kwang, “A review on peak load shaving strategies,” *Renew. Sustain. Energy Rev.*, vol. 82, pp. 3323–3332, Feb. 2018.
- [53] M. A. López, S. de la Torre, S. Martín, and J. A. Aguado, “Demand-side management in smart grid operation considering electric vehicles load shifting and vehicle-to-grid support,” *Int. J. Electr. Power Energy Syst.*, vol. 64, pp. 689–698, Jan. 2015.
- [54] E. Heydarian-Forushani, M. E. H. Golshan, and M. Shafie-khah, “Flexible interaction of plug-in electric vehicle parking lots for efficient wind integration,” *Appl. Energy*, vol. 179, pp. 338–349, Oct. 2016.

-
- [55] M. Wang, Y. Mu, H. Jia, J. Wu, X. Yu, and Y. Qi, "Active power regulation for large-scale wind farms through an efficient power plant model of electric vehicles," *Appl. Energy*, vol. 185, pp. 1673–1683, Jan. 2017.
- [56] B. Drysdale, J. Wu, and N. Jenkins, "Flexible demand in the GB domestic electricity sector in 2030," *Appl. Energy*, vol. 139, pp. 281–290, Feb. 2015.
- [57] Frontier Economics, "Future potential for DSR in GB," London, 2015.
- [58] British Standards Institution (BSI), *BS EN 61851-1:2011 Electric vehicle conductive charging system. General requirements*. London: BSI, 2011.
- [59] P. Papadopoulos, S. Skarvelis-Kazakos, I. Grau, L. M. Cipcigan, and N. Jenkins, "Electric vehicles' impact on British distribution networks," *IET Electr. Syst. Transp.*, vol. 2, no. 3, p. 91, 2012.
- [60] C. H. Dharmakeerthi, N. Mithulannanthan, and T. . Saha, "Impact of electric vehicle fast charging on power system voltage stability," vol. 57, pp. 241–249, 2014.
- [61] G. Mills and I. MacGill, "Potential power system and fuel consumption impacts of plug in hybrid vehicle charging using Australian National Electricity Market load profiles and transportation survey data," *Electr. Power Syst. Res.*, vol. 116, pp. 1–11, Nov. 2014.
- [62] W.-P. Schill and C. Gerbaulet, "Power system impacts of electric vehicles in Germany: Charging with coal or renewables?," *Appl. Energy*, vol. 156, pp. 185–196, 2015.
- [63] A. Foley, B. Tyther, P. Calnan, and B. Ó Gallachóir, "Impacts of Electric Vehicle charging under electricity market operations," *Appl. Energy*, vol. 101, pp. 93–102, Jan. 2013.
- [64] P. Zhang, K. Qian, C. Zhou, B. G. Stewart, and D. M. Hepburn, "A Methodology for Optimization of Power Systems Demand Due to Electric Vehicle Charging Load," *IEEE Trans. Power Syst.*, vol. 27, no. 3, pp. 1628–1636, Aug. 2012.
- [65] J. Villar, C. A. Diaz, J. Arnau, and F. A. Campos, "Impact of plug-in-electric vehicles penetration on electricity demand, prices and thermal generation dispatch," in *2012 9th International Conference on the European Energy*

- Market*, 2012, pp. 1–8.
- [66] M. Majidpour and W.-P. Chen, “Grid and Schedule Constrained Electric Vehicle Charging Algorithm Using Node Sensitivity Approach,” in *2012 International Conference on Connected Vehicles and Expo (ICCVE)*, 2012, pp. 304–310.
- [67] K. H. Jansen, T. M. Brown, and G. S. Samuelson, “Emissions impacts of plug-in hybrid electric vehicle deployment on the U.S. western grid,” *J. Power Sources*, vol. 195, no. 16, pp. 5409–5416, 2010.
- [68] United Nations Framework Convention on Climate Change (UNFCCC), *Paris Agreement*, no. December. 2015, p. 32.
- [69] Committee on Climate Change (CCC), “The Fifth Carbon Budget: The next step towards a low-carbon economy,” 2015.
- [70] P. M. Connor, L. Xie, R. Lowes, J. Britton, and T. Richardson, “The development of renewable heating policy in the United Kingdom,” *Renew. Energy*, vol. 75, pp. 733–744, Mar. 2015.
- [71] M. Chaudry, M. Abeysekera, S. H. R. Hosseini, N. Jenkins, and J. Wu, “Uncertainties in decarbonising heat in the UK,” *Energy Policy*, vol. 87, pp. 623–640, Dec. 2015.
- [72] V. Bianco, F. Scarpa, and L. A. Tagliafico, “Estimation of primary energy savings by using heat pumps for heating purposes in the residential sector,” *Appl. Therm. Eng.*, vol. 114, pp. 938–947, Mar. 2017.
- [73] M. Jarre, M. Noussan, and M. Simonetti, “Primary energy consumption of heat pumps in high renewable share electricity mixes,” *Energy Convers. Manag.*, vol. 171, pp. 1339–1351, Sep. 2018.
- [74] R. Gupta and R. Irving, “Possible effects of future domestic heat pump installations on the UK energy supply,” *Energy Build.*, vol. 84, pp. 94–110, Dec. 2014.
- [75] Parliament of UK, *Automated and Electric Vehicles Act 2018*. London: House of Commons, 2018.
- [76] A. D. Hilshey, P. D. H. Hines, P. Rezaei, and J. R. Dowds, “Estimating the

- impact of electric vehicle smart charging on distribution transformer aging,” *IEEE Trans. Smart Grid*, vol. 4, no. 2, pp. 905–913, 2013.
- [77] S. U. Karki, S. B. Halbhavi, and S. G. Kulkarni, “Study on Challenges in Integrating Renewable Technologies,” *Int. J. Adv. Res. Electr. Electron. Instrum. Eng.*, vol. 3, no. 8, pp. 10972–10977, 2014.
- [78] H. Farzin, M. Moeini-Aghtaie, and M. Fotuhi-Firuzabad, “Reliability Studies of Distribution Systems Integrated with Electric Vehicles under Battery-Exchange Mode,” *IEEE Trans. Power Deliv.*, vol. 31, no. 6, pp. 2473–2482, 2016.
- [79] D. Pudjianto *et al.*, “Smart control for minimizing distribution network reinforcement cost due to electrification,” *Energy Policy*, vol. 52, pp. 76–84, Jan. 2013.
- [80] A. Navarro-Espinosa and L. F. Ochoa, “Probabilistic Impact Assessment of Low Carbon Technologies in LV Distribution Systems,” *IEEE Trans. Power Syst.*, vol. 31, no. 3, pp. 2192–2203, 2016.
- [81] R.-C. Leou, C.-L. Su, and C.-N. Lu, “Stochastic Analyses of Electric Vehicle Charging Impacts on Distribution Network,” *IEEE Trans. Power Syst.*, vol. 29, no. 3, pp. 1055–1063, May 2014.
- [82] A. Navarro-Espinosa and P. Mancarella, “Probabilistic modeling and assessment of the impact of electric heat pumps on low voltage distribution networks,” *Appl. Energy*, vol. 127, pp. 249–266, Aug. 2014.
- [83] M. A. Awadallah, B. N. Singh, and B. Venkatesh, “Impact of EV Charger Load on Distribution Network Capacity: A Case Study in Toronto,” *Can. J. Electr. Comput. Eng.*, vol. 39, no. 4, pp. 268–273, 2016.
- [84] M. Neaimeh *et al.*, “A probabilistic approach to combining smart meter and electric vehicle charging data to investigate distribution network impacts,” *Appl. Energy*, vol. 157, pp. 688–698, Nov. 2015.
- [85] M. Akmal, B. Fox, J. D. Morrow, and T. Littler, “Impact of heat pump load on distribution networks,” *IET Gener. Transm. Distrib.*, vol. 8, no. 12, pp. 2065–2073, 2014.
- [86] C. Protopapadaki and D. Saelens, “Heat pump and PV impact on residential

- low-voltage distribution grids as a function of building and district properties,” *Appl. Energy*, vol. 192, pp. 268–281, Apr. 2017.
- [87] S. Deb, K. Tammi, K. Kalita, and P. Mahanta, “Impact of Electric Vehicle Charging Station Load on Distribution Network,” *energies*, vol. 11, no. 178, pp. 1–25, 2018.
- [88] A. N. M. M. Haque, P. H. Nguyen, F. W. Bliiek, and J. G. Slootweg, “Demand response for real-time congestion management incorporating dynamic thermal overloading cost,” *Sustain. Energy, Grids Networks*, vol. 10, pp. 65–74, Jun. 2017.
- [89] J. Hu, A. Saleem, S. You, L. Nordström, M. Lind, and J. Østergaard, “A multi-agent system for distribution grid congestion management with electric vehicles,” *Eng. Appl. Artif. Intell.*, vol. 38, pp. 45–58, Feb. 2015.
- [90] R. Liao, J. Hao, L. Ynag, and S. Grzybowski, “Study on aging characteristics of mineral oil/natural ester mixtures paper insulation,” in *International Conference on Dielectric Liquids*, 2011, pp. 1–4.
- [91] A. N. M. M. Haque, D. S. Shafiullah, P. H. Nguyen, and F. W. Bliiek, “Real-Time Congestion Management in Active Distribution Network based on Dynamic Thermal Overloading Cost,” *Power Syst. Comput. Conf.*, pp. 1–7, 2016.
- [92] B. Shahbazi, M. Savaghebi, and M. Shariati, “A Probabilistic Approach for Power Transformer Dynamic Loading Capability Assessment,” *Int. Rev. Electr. Eng.*, vol. 5, no. 3, pp. 952–960, 2010.
- [93] R. Jongen, P. Morshuis, J. Smit, A. Jansesn, Gulski, and Edward, “A statistical approach to processing power transformer failure data,” in *CIGRE 19th International Conference on Electricity Distribution*, 2007.
- [94] IEEE Standards Association, *IEEE Guide for Loading Mineral- Oil-Immersed Transformers and Step-Voltage Regulators*, vol. 2011, no. March. 2012.
- [95] International Electrotechnical Commission (IEC), “IEC 60076-7:2005-Power transformers-Part 7: Loading Guide for Oil-Immersed Power Transformers,” 2005.
- [96] W. Andrew and A. Amditi, “D6.3 NeMo Hyper-Network validation,” *hyper-*

- Network for electroMobility (NeMo) D6.3: Integration and Validation*, 2017. [Online]. Available: <https://nemo-emobility.eu/deliverables/>. [Accessed: 05-Dec-2018].
- [97] S. Carter, G. Williamson, J. King, V. Levi, and J. McWilliam, “Key findings of DS2030 – a study into future GB distribution network operations,” *CIREN - Open Access Proc. J.*, vol. 2017, no. 1, pp. 2390–2393, Oct. 2017.
- [98] Competition and Markets Authority, “Energy market investigation,” London, 2016.
- [99] M. H. Roos, D. A. M. Geldtmeijer, H. P. Nguyen, J. Morren, and J. G. Slootweg, “Optimizing the technical and economic value of energy storage systems in LV networks for DNO applications,” *Sustain. Energy, Grids Networks*, vol. 16, pp. 207–216, Dec. 2018.
- [100] I. I. Avramidis, V. A. Evangelopoulos, P. S. Georgilakis, and N. D. Hatziaargyriou, “Demand side flexibility schemes for facilitating the high penetration of residential distributed energy resources,” *IET Gener. Transm. Distrib.*, vol. 12, no. 18, pp. 4079–4088, Oct. 2018.
- [101] N. Kelly, A. Samuel, and J. Hand, “Testing integrated electric vehicle charging and domestic heating strategies for future UK housing,” *Energy Build.*, vol. 105, pp. 377–392, Oct. 2015.
- [102] Y. Gao, B. Patel, Q. Liu, Z. Wang, and G. Bryson, “Methodology to assess distribution transformer thermal capacity for uptake of low carbon technologies,” *IET Gener. Transm. Distrib.*, vol. 11, no. 7, pp. 1645–1651, May 2017.
- [103] J. Hu, H. Morais, M. Lind, and H. W. Bindner, “Multi-agent based modeling for electric vehicle integration in a distribution network operation,” *Electr. Power Syst. Res.*, vol. 136, pp. 341–351, Jul. 2016.
- [104] R. Rana and S. Mishra, “Day-Ahead Scheduling of Electric Vehicles for Overloading Management in Active Distribution System via Web-Based Application,” *IEEE Syst. J.*, pp. 1–11, 2018.
- [105] Department of Energy and Climate Change (DECC), “2014 UK Greenhouse Gas Emissions, Provisional Figures.” National Statistics, pp. 1–33, 2015.

-
- [106] Committee on Climate Change (CCC), “Reducing the UK’s carbon footprint.” Committee on Climate Change, London, pp. 1–110, 2013.
- [107] L. Wilson, “Shades of Green: Electric Cars’ Carbon Emissions Around the Globe,” 2013.
- [108] P. Katsis, T. Papageorgiou, and L. Ntziachristos, “Modelling the Trip Length Distribution Impact on the CO₂ Emissions of Electrified Vehicles,” *Energy and Power*, vol. 4, no. 1A, pp. 57–64, 2014.
- [109] C. Pineiro and D. Xenias, “e-Mobility Fleet Schemes and Market Potentials in Austria,” eBRIDGE Project (EU), 2014.
- [110] Department for Regional Development, “Travel Survey for Northern Ireland In-depth Report 2008-2010.” National Statistics, Belfast, pp. 1–54, 2011.
- [111] Department for Regional Development, “Travel Survey for Northern Ireland In-depth Report 2011-2013.” National Statistics, Belfast, pp. 1–56, 2014.
- [112] Department for Transport (DfT), “Road traffic estimates in Great Britain: 2015 Tables.” National Statistics, London, 2015.
- [113] Department for Transport (DfT), “Table VEH0102: Licensed vehicles at the end of the year by body type, Great Britain from 1994; also United Kingdom from 2014.” DVLA/DfT, 2015.
- [114] Driver and Vehicle Agency (DVA), “Northern Ireland Transport Statistics: 2013-2014 Vehicle registrations.” DVA, Belfast, 2015.
- [115] Department of Energy and Climate Change (DECC), “Energy Consumption in the UK (2015): Transport energy consumption in the UK between 1970 and 2014.” National Statistics, London, 2015.
- [116] Department for Transport (DfT), “Table VEH0203: Licensed cars at the end of the year by propulsion / fuel type, Great Britain from 1994; also United Kingdom from 2014.” DVLA/DfT, London, 2015.
- [117] International Energy Agency, “Statistics of UK on Electricity and Heat.” 2012.
- [118] Nissan Motor (GB) Ltd., “Nissan™ Official UK Website.” [Online]. Available: <https://www.nissan.co.uk/>. [Accessed: 05-Mar-2015].
- [119] Department of Energy and Climate Change (DECC), “2015 Government GHG

- Conversion Factors for Company Reporting: Methodology Paper for Emission Factors Final Report,” London, 2015.
- [120] Environmental Protection Agency (EPA), “Inventory of U.S. Greenhouse Gas Emissions and Sinks: 1990–2011,” Washington, DC, 2013.
- [121] Intergovernmental Panel on Climate Change (IPCC), “2006 IPCC Guidelines for National Greenhouse Gas Inventories.” Geneva, 2006.
- [122] Department of Energy and Climate Change (DECC), *Digest of United Kingdom Energy Statistics 2015*. 2015.
- [123] Department of Energy and Climate Change (DECC), “2014 UK Greenhouse Gas Emissions , Provisional Statistical release,” no. March, p. 44, 2015.
- [124] Department of Energy and Climate Change (DECC), “Energy Trends.” National Statistics, London, pp. 1–92, 2015.
- [125] Index Mundi, “Countries ranked by CO2 emissions from electricity and heat production, total (% of total fuel combustion).” [Online]. Available: <https://www.indexmundi.com/facts/indicators/EN.CO2.ETOT.ZS/rankings>. [Accessed: 06-Mar-2015].
- [126] Department for Business, Energy and Industrial Strategy (DBEIS), “Plant installed capacity, by connection, United Kingdom.” National Statistics, London, 2016.
- [127] Great Britain National Grid status, 2016. [Online]. Available: <https://www.gridwatch.templar.co.uk/>. [Accessed: 10-Mar-2016].
- [128] EirGrid Group, “Smart Grid Dashboard.” [Online]. Available: <http://smartgriddashboard.eirgrid.com/#ni>. [Accessed: 15-Mar-2016].
- [129] System Operator for Northern Ireland (SONI), “System Information.” [Online]. Available: <http://www.soni.ltd.uk/how-the-grid-works/system-information/>. [Accessed: 11-Mar-2016].
- [130] H. E. Thornton, A. S. Adam, B. J. Hoskins, and J. D. Brayshaw, “The relationship between wind power, electricity demand and winter weather patterns in Great Britain,” *Environ. Res. Lett.*, vol. 12, no. 6, pp. 1–11, 2017.
- [131] Department for Transport (DfT), “Table VEH0203: Licensed cars at the end of

- the year by propulsion / fuel type, Great Britain from 1994; also United Kingdom from 2014.” 2016.
- [132] Department for Transport (DfT), “National Travel Survey: 2015 Report,” London, 2016.
- [133] Department for Transport (DfT), “Vehicle Licensing Statistics: Annual 2015.” pp. 1–14, 2016.
- [134] DVLA/DVA/DfT, “Ultra low emission vehicles (ULEVs) registered for the first time, including top 10 models for the latest year, United Kingdom from 2010 Q1.” 2016.
- [135] National Grid, “Future Energy Scenarios,” no. July. pp. 1–228, 2015.
- [136] J. Bates and S. Henry, “Carbon factor for wood fuels for the Supplier Obligation Final report,” Oxford, 2009.
- [137] Biomass Availability and Sustainability Information System (BASIS), “Report on conversion efficiency of biomass,” 2015.
- [138] Mott MacDonald, “UK Electricity Generation Costs Update,” Brighton, 2010.
- [139] Society of Motor Manufacturers and Traders (SMMT), “New Car CO 2 Report 2016,” 2016.
- [140] Department of Energy & Climate Change (DECC), “2014 UK Greenhouse Gas Emissions, Final Figures,” 2016.
- [141] A. Neagoe-Stefana, M. Eremia, L. Toma, and A. Neagoe, “Impact of charging Electric Vehicles in residential network on the voltage profile using Matlab,” in *2015 9th International Symposium on Advanced Topics in Electrical Engineering (ATEE)*, 2015, pp. 787–791.
- [142] UK Power Networks, “Impact of Electric Vehicle and Heat Pump Loads on Network Demand Profiles,” 2014.
- [143] National Grid, “Future Energy Scenarios,” no. July. pp. 1–119, 2017.
- [144] D. P. Chassin, J. C. Fuller, and N. Djilali, “GridLAB-D: An agent-based simulation framework for smart grids,” *J. Appl. Math.*, vol. 2014, pp. 1–12, 2014.

-
- [145] D. P. Chassin, K. Schneider, and C. Gerkenmeyer, "GridLAB-D: An open-source power systems modeling and simulation environment," in *2008 IEEE/PES Transmission and Distribution Conference and Exposition*, 2008, pp. 1–5.
- [146] Office of Electricity Delivery and Energy Reliability, "GridLabD: A Unique Tool to Design the Smart Grid," 2012.
- [147] M. Sisinni, "Deliverable D6.1 MAS2TERING Multi-Agent Systems and Secured coupling of Telecom and Energy gRIDs for Next Generation smartgrid services D6.1-Detailed Use Cases Scenarios," 2016.
- [148] UK Energy Research Centre (UKERC), "ELECTRICITY USER DEMAND PROFILE DATA." [Online]. Available: <http://data.ukedc.rl.ac.uk/simplebrowse/edc/efficiency/residential/LoadProfile/data>. [Accessed: 22-May-2018].
- [149] Department for Communities and Local Government (DCLG), "Table 401: Household projections, United Kingdom, 1961-2039." 2016.
- [150] Department of Energy and Climate Change (DECC), "Domestic energy consumption in the UK between 1970 and 2014," 2015.
- [151] Department for Business, Energy and Industrial Strategy (DBEIS), "Energy consumption in UK," 2017.
- [152] Department for Business, Energy and Industrial Strategy (DBEIS), "QUARTERLY ENERGY PRICES TABLES ANNEX, DECEMBER 2017," 2017.
- [153] T. Knight, E. Kivinen, and D. Fell, "Uptake of Ultra Low Emission Vehicles in the UK A Rapid Evidence Assessment for the Department for Transport," 2015.
- [154] DVLA/DfT, "Licensed cars at the end of the year by propulsion / fuel type, Great Britain from 1994; also United Kingdom from 2014." 2018.
- [155] Office for National Statistics (ONS), "Overview of the UK Population: July 2017," *Article: People, Population and Community*, no. July. pp. 1–17, 2017.
- [156] Office for National Statistics (ONS), "Families and Households: 2017," *Statistical bulletin: People, Population and Community*. pp. 1–16, 2017.

-
- [157] European Commission, “Population on 1st January by age, sex and type of projection 2015-2080,” *eurostat*, 2018. [Online]. Available: http://appsso.eurostat.ec.europa.eu/nui/show.do?dataset=proj_15npms&lang=en. [Accessed: 24-May-2018].
- [158] Office of Gas and Electricity Markets (Ofgem), “Ofgem ’ s proposal to revise the Typical Domestic Consumption Values for gas and electricity , including additional information on the peak and off-peak split for Economy 7 meters , and on the mean consumption for restricted meter customers .” pp. 1–11, 2017.
- [159] Office of Gas and Electricity Markets (Ofgem), “Decision letter: Revision of typical domestic consumption values,” pp. 2–4, 2010.
- [160] Office of Gas and Electricity Markets (Ofgem), “Review of typical domestic consumption values,” p. 31, 2013.
- [161] Office of Gas and Electricity Markets (Ofgem), “Typical Domestic Consumption Values for gas and electricity 2015,” no. May, pp. 2–5, 2015.
- [162] UK Nissan Motor Corporation, “Range and Charging: 2017 Nissan Leaf Electric Car.” [Online]. Available: <https://www.nissan.co.uk/vehicles/new-vehicles/leaf/range-charging.html>. [Accessed: 25-May-2018].
- [163] Department for Transport (DfT), “Analyses from the National Travel Survey,” *Statistical Release*, no. January. 2018.
- [164] C. Wemhoener, “Final report Annex 32 part 3 Economical heating and cooling systems for low energy houses,” 2011.
- [165] C. Wemhöner *et al.*, “Calculation method for the seasonal performance of heat pump compact units and validation,” 2007.
- [166] C. Wemhöner and T. Afjei, “Seasonal performance calculation for residential heat pumps with combined space heating and hot water production (FHBB method),” 2003.
- [167] S. Shao, M. Pipattanasomporn, and S. Rahman, “Development of physical-based demand response-enabled residential load models,” *IEEE Trans. Power Syst.*, vol. 28, no. 2, pp. 607–614, 2013.
- [168] F. Hall and R. Greeno, *Building service handbook*, 6th ed. Oxford: Elsevier

- Limited, 2011.
- [169] P. J. C. Nel, M. J. Booysen, and A. B. van der Merwe, “A computationally inexpensive energy model for horizontal electrical water heaters with scheduling,” *IEEE Trans. Smart Grid*, vol. 9, no. 1, pp. 48–56, 2018.
- [170] Health and Safety Executive (HSE), *Legionnaires’ disease Part 2: The control of legionella bacteria in hot and cold water systems*, 1st ed. Norwich: HSE Books, 2014.
- [171] P. Boait and A. Stafford, “Electrical Load Characteristics of Domestic Heat Pumps and Scope for Demand Side Management,” *Int. Conf. Electr. Distrib.*, vol. 21, no. 0125, pp. 6–9, 2011.
- [172] J. Henderson and J. Hart, *BREDEM 2012 – A technical description of the BRE Domestic Energy Model*, Version 1. Wtaford: BRE, 2015.
- [173] R. Hendron and J. Burch, “Development of Standardized Domestic Hot Water Event Schedules for Residential Buildings,” *ASME 2007 Energy Sustain. Conf.*, vol. 29, no. August, pp. 253–72, 2008.
- [174] Kingspan (UK), “Vented Hot Water Cylinders,” *Albion cylinder: Technical and Installation Documents*, 2016. [Online]. Available: <https://www.kingspan.com/gb/en-gb/products/hot-water-cylinders/vented-hot-water-cylinders>. [Accessed: 26-Jun-2016].
- [175] Department for Communities and Local Government (DCLG), “Housing Stock profile, 2014-15.” 2015.
- [176] HM Government, “The Building Regulations 2010: Conservation of fuel and power in existing dwellings - Approved Document Part L1B,” no. October. 2010.
- [177] UK Met Office, “Archive services - Met Office.” [Online]. Available: <https://www.metoffice.gov.uk/learning/library/archive/services>. [Accessed: 12-May-2016].
- [178] W. H. Kersting, *Distribution System Modeling and Analysis*, 3rd ed. Florida: CRC Press, 2012.
- [179] C. AJ, M. A. Salam, Q. M. Rahman, F. Wen, S. P. Ang, and W. Voon, “Causes

- of transformer failures and diagnostic methods – A review,” *Renew. Sustain. Energy Rev.*, vol. 82, pp. 1442–1456, Feb. 2018.
- [180] Office of Gas and Electricity Markets (Ofgem), “Know your rights,” *Factsheets: Domestic consumers Electricity - distribution*. pp. 1–12, 2015.
- [181] Department for Environment, Food and Rural Affairs (Defra), “Estimating energy saving potential from transformers and evaluating their impact on the feasibility of renewable energy systems,” 2013.
- [182] A. Abu-Siada and S. Islam, “A novel online technique to detect power transformer winding faults,” *IEEE Trans. Power Deliv.*, vol. 27, no. 2, pp. 849–857, Apr. 2012.
- [183] D. Martin, Y. Cui, C. Ekanayake, M. Hui, and T. Saha, “An updated model to determine the life remaining of transformer insulation,” *IEEE Trans. Power Deliv.*, vol. 30, no. 1, pp. 395–402, Feb. 2015.
- [184] V. A. Primo, B. Garcia, and J. C. Burgos, “Applicability of nanodielectric fluids to the improvement of transformer insulation properties,” in *Proceedings of the 2016 IEEE International Conference on Dielectrics, ICD 2016*, 2016, vol. 1, pp. 76–79.
- [185] L. Yang, S. Gao, B. Deng, J. Zang, W. Sun, and E. Hu, “Inhibition method for the degradation of oil–paper insulation and corrosive sulphur in a transformer using adsorption treatment,” *IET Gener. Transm. Distrib.*, vol. 10, no. 8, pp. 1893–1900, 2016.
- [186] P. W. R. Smith, Z. D. Wang, M. Daghrhah, D. Walker, Q. Liu, and P. Mavrommatis, “Design of experimental setup to study factors affecting hot spot temperature in disc type winding transformers,” in *IET International Conference on Resilience of Transmission and Distribution Networks (RTDN) 2015*, 2015, p. 29 (6 .)-29 (6 .).
- [187] M. Daghrhah, Z. D. Wang, Q. Liu, D. Walker, C. Krause, and G. Wilson, “Experimental investigation of hot spot factor for assessing hot spot temperature in transformers,” in *CMD 2016 - International Conference on Condition Monitoring and Diagnosis*, 2016, pp. 948–951.
- [188] Y. Cui, H. Ma, T. Saha, C. Ekanayake, and D. Martin, “Moisture-Dependent

- thermal modelling of power transformer,” *IEEE Trans. Power Deliv.*, vol. 31, no. 5, pp. 2140–2150, Oct. 2016.
- [189] S. Acharya and P. C. Tapre, “Life assessment of transformer using thermal models,” in *2017 International Conference on Energy, Communication, Data Analytics and Soft Computing (ICECDS)*, 2017, pp. 3515–3520.
- [190] L. Petkovska, M. Dugalovski, G. Cvetkovski, and P. Lefley, “A novel approach to multi-objective efficiency optimisation for a distribution transformer based on the Taguchi method,” in *2014 International Conference on Electrical Machines (ICEM)*, 2014, pp. 2228–2234.
- [191] Nord Pool, “N2EX Day Ahead Auction Prices - UK table.” [Online]. Available: <https://www.nordpoolgroup.com/Market-data1/GB/Auction-prices/UK/Hourly/?view=table>. [Accessed: 16-Aug-2018].
- [192] Office of Gas and Electricity Markets (Ofgem), “Understand your gas and electricity bills.” [Online]. Available: <https://www.ofgem.gov.uk/consumers/household-gas-and-electricity-guide/understand-your-gas-and-electricity-bills>. [Accessed: 16-Aug-2018].
- [193] Frontline Systems Inc., “Analytic Solver® Platform.” [Online]. Available: <https://www.solver.com/analytic-solver®-platform>. [Accessed: 16-Aug-2018].
- [194] S. Le Vine, J. Polak, and A. Humphrey, “Commuting trends in England 1988 - 2015,” London, 2017.
- [195] J. Gershuny and O. Sullivan, “United Kingdom Time Use Survey, 2014-2015,” UK Data Service, 2017.
- [196] S. Rahman, S. K. Dey, B. K. Bhawmick, and N. K. Das, “Design and implementation of real time transformer health monitoring system using GSM technology,” in *2017 International Conference on Electrical, Computer and Communication Engineering (ECCE)*, 2017, pp. 258–261.
- [197] R. R. Pawar and S. B. Deosarkar, “Health condition monitoring system for distribution transformer using Internet of Things (IoT),” in *2017 International Conference on Computing Methodologies and Communication (ICCMC)*, 2017, pp. 117–122.
- [198] M. Jalilian *et al.*, “Design and implementation of the monitoring and control

-
- systems for distribution transformer by using GSM network,” *Int. J. Electr. Power Energy Syst.*, vol. 74, pp. 36–41, Jan. 2016.
- [199] A. Mulla, J. Baviskar, S. Khare, and F. Kazi, “The Wireless Technologies for Smart Grid Communication: A Review,” in *2015 Fifth International Conference on Communication Systems and Network Technologies*, 2015, pp. 442–447.
- [200] A. Mahmood, N. Javaid, and S. Razzaq, “A review of wireless communications for smart grid,” *Renew. Sustain. Energy Rev.*, vol. 41, pp. 248–260, Jan. 2015.
- [201] A. Yarali and S. Rahman, “Wireless Communication for Smart Grids,” in *Second International Conference on Advanced Collaborative Networks, Systems and Applications 2012 (COLLA 2012)*, 2012, pp. 1–9.
- [202] British Electrotechnical and Allied Manufacturers Association (BEAMA), “A GUIDE TO ELECTRIC VEHICLE INFRASTRUCTURE.” London, pp. 1–40, 2015.
- [203] Department for Communities and Local Government (DCLG), “Technical housing standards – nationally described space standard.” DCLG, London, pp. 1–5, 2015.
- [204] M. Stein, *When Technology Fails A Manual for Self-Reliance, Sustainability, and Surviving the Long Emergency*. Chelsea Green Publishing, 2008.
- [205] “Roofing Calculator.” [Online]. Available: <https://www.calculator.net/roofing-calculator.html>. [Accessed: 06-Jan-2019].
- [206] The Chartered Institution of Building Services Engineers London, *CIBSE Concise Handbook*, 3rd ed. Chartered Inst. of Building Services Engineers, 2008.
- [207] B. E. AINSWORTH, W. L. HASKELL, M. C. WHITT, M. L. IRWIN, A. M. SWARTZ, and S. J. STRATH, “Compendium of Physical Activities: an update of activity codes and MET intensities,” *MEDICINE & SCIENCE IN SPORTS & EXERCISE*. pp. 498–516, 2000.
- [208] “Met - Metabolic Rate.” [Online]. Available: https://www.engineeringtoolbox.com/met-metabolic-rate-d_733.html. [Accessed: 06-Jan-2019].
-

APPENDIX A

PARAMETERS AND DATA USED FOR MODELLING THE OPERATION OF HP IN CHAPTER 4

This appendix presents the parameters and data which were used in the modelling of the operation of HP in Chapter 4.

A.1 Parameters of building

Table A.1 Parameters of building

Parameters	Values
Number of bedrooms	Randomised between 2 and 3 bedrooms, since the mean number of bedrooms for all household in GB is 2.8 [175].
Floor area (A_{floor})	Randomised between $90m^2$ and $110m^2$. Range of standard floor area for 2/3 bedroom house [203].
Height of building	$4.6m$ (assuming two storey building). Minimum floor to ceiling height is $2.3m$ [203].
Area of door (A_{door})	$3.02m^2$ (assuming 2 external doors each of size 1981mm by 762mm)
Volume of building (V_{house})	Calculated from 'Floor area' and 'height of building'
Number of occupants (N_{person})	Randomised between 2 and 3, since the mean number of persons per household is 3 [175].
External wall area (A_{wall})	Calculated from the 'Floor area' assuming a wall thickness of 362mm
Overall area of windows (A_{window})	Calculated from 'Area of wall', assuming 15% wall-to-window ratio [204].

Parameters	Values
Overall area of south-facing window (A_{sth_window})	Calculated from 'Area of wall', assuming 12% wall-to-window ratio [204].
Net external wall area (Net_A_wall)	Calculated from 'Area of wall', 'Area of door' and 'Area of window'.
Area of roof (A_wall)	Calculated from 'Area of floor', assuming 45 degrees pitch angle [205].
Number of air change (N_air)	Randomised between 0.5 and 1.0 air changes/hr, standard for bedroom and living room respectively [206]
U-value of floor (U_floor)	Randomised between 0.22 and 0.45 W/m^2K [176], [206].
U-value of wall (U_wall)	Randomised between 0.28 and 0.45 W/m^2K [176], [206].
U-value of roof (U_roof)	Randomised between 0.18 and 0.25 W/m^2K [176], [206].
U-value of door (U_door)	Randomised between 1.8 and 2.0 W/m^2K [176], [206].
U-value of window (U_window)	Randomised between 1.6 and 2.0 W/m^2K [176], [206].
SHGC	Randomised between 0.45 and 0.67 [206].
Heat gain per person (H_person)	93.5W. Calculated from the average of heat emission from reclining/sleeping (83W) and seated/relaxed (104W) [207], [208].
Initial internal space temperature ($T_room_initial$)	Randomised between 14 $^{\circ}C$ and 22 $^{\circ}C$.

A.2 Parameters of DHW tank

Table A.2 Parameters of building

Parameters	Values
Volume of tank (V_{tank})	150 litres [174].
Surface area of tank (A_{tank})	$2.36m^2$ [174].
Thermal transmittance coefficient of tank (U_{tank})	$1.13 W/m^2K$ [174].
Initial DHW temperature ($T_{DHW_initial}$)	Randomised between $47 ^\circ C$ and $60 ^\circ C$.

A.3 Parameters of radiator

The type of radiator used in the model is single-panel, single-convector radiator.

Table A.3 Parameters of radiator

Parameters	Values
Dimension of radiator	Height 700mm, Width 2000mm, and Depth 50mm
Power output	2966W
Area (A_{rad})	$5.6m^2$ (4 units by $1.4m^2$)
Thermal transmittance coefficient (h_{rad})	$38.5 W/m^2K$
Water mass flow rate (m)	$0.078 kg/s$ (this is variable setting)

A.4 Data of weather and water draw events

Table A.4 Temperature, Solar radiation and water draw events

Time	Temperature ($^{\circ}C$)		Solar radiation (W/m^2)		Water draw (litres)
	summer	winter	summer	winter	
00:00	18.4	5.4	0	0	1.20
00:30	17.5	3.4	0	0	0.80
01:00	16.7	1.4	0	0	0.50
01:30	16.2	-0.2	0	0	0.30
02:00	15.7	-2.3	0	0	0.10
02:30	16.2	-3.6	0	0	0.08
03:00	16.7	-5.0	0	0	0.05
03:30	16.6	-5.7	0	0	0.05
04:00	16.6	-6.4	0	0	0.05
04:30	16.5	-6.7	0	0	0.08
05:00	16.4	-7.0	0	0	0.10
05:30	16.6	-7.2	0	0	0.60
06:00	16.9	-7.3	40	0	1.10
06:30	17.4	-7.0	130	0	2.63
07:00	17.8	-6.6	210	0	4.15
07:30	18.5	-6.3	310	0	4.30
08:00	19.2	-6.0	410	0	4.45
08:30	20.4	-5.6	510	0	4.40
09:00	21.6	-5.1	610	30	4.35
09:30	23.4	-4.1	660	70	4.08
10:00	25.1	-3.0	700	100	3.80
10:30	26.4	-2.1	720	80	3.58
11:00	27.6	-1.3	740	50	3.35
11:30	28.3	-0.7	760	60	3.08
12:00	29.0	-0.1	780	70	2.80
12:30	29.1	0.9	790	90	2.50
13:00	30.1	2.0	790	100	2.20
13:30	30.1	2.2	770	120	2.15

Time	Temperature ($^{\circ}\text{C}$)		Solar radiation (W/m^2)		Water draw (litres)
	summer	winter	summer	winter	
14:00	30.0	2.4	750	130	2.10
14:30	29.3	2.4	720	80	2.00
15:00	29.7	2.4	690	30	1.90
15:30	29.7	2.4	610	30	1.95
16:00	29.4	2.2	520	0	2.10
16:30	28.8	2.2	420	0	2.22
17:00	28.1	2.1	310	0	2.35
17:30	27.9	2.2	220	0	2.85
18:00	27.7	2.2	120	0	3.35
18:30	26.9	2.2	120	0	3.58
19:00	26.1	2.3	0	0	3.80
19:30	25.4	2.3	0	0	3.73
20:00	24.6	2.3	0	0	3.65
20:30	23.9	2.3	0	0	3.50
21:00	23.2	2.3	0	0	3.35
21:30	22.2	2.3	0	0	3.08
22:00	21.3	2.2	0	0	2.80
22:30	20.7	2.2	0	0	2.58
23:00	20.1	2.1	0	0	2.35
23:30	19.3	3.8	0	0	1.78

A.5 MATLAB codes used for modelling HP operation in Chapter 4

1. Randomisation of input parameters

```

8 function [p] = generatorpar(n,Low_lim,Up_lim)
n = 100;
Low_lim = 90;
Up_lim = 110;
C_air = 1000;
ro_air = 1.2;
A_floor = (Up_lim-Low_lim).*rand(n,1) + Low_lim;
A_wall = (0.362+sqrt(A_floor)).^2;
A_window = 0.15.*A_wall;
A_door = 3.02;
V_house = (4.8.*A_floor);
Net_A_wall = (A_wall-A_window-A_door);
A_sth_window = (0.12.*A_floor);
A_roof = sqrt(2).*A_wall;
N_person = round((3-2).*rand(n,1) + 2);
SHGC = (0.67-0.45).*rand(n,1) + 0.45;
N_air = (0.5-0.25).*rand(n,1) + 0.25;
U_floor = (0.45-0.22).*rand(n,1) + 0.22;
U_wall = (0.45-0.28).*rand(n,1) + 0.28;
U_roof = (0.25-0.18).*rand(n,1) + 0.18;
U_window = (2-1.6).*rand(n,1) + 1.6;
U_door = (2-1.8).*rand(n,1) + 1.8;
const_EAU_C_v =
(A_floor.*U_floor)+(Net_A_wall.*U_wall)+(A_roof.*U_roof)+(A_window.*U_windo
w)+(A_door.*U_door)+(N_air.*V_house.*0.333);
T_room_initial = (22-14).*rand(n,1) + 14;
T_DHW_initial = (60-47).*rand(n,1) + 47;
delta_C=C_air * ro_air * V_house;
start = round((1-0).*rand(n,1) + 0);

```

Published with MATLAB® R2018a

2. Data processing

```

9. function BuildingData = ProcessData(BuildingData)
    N_time_steps=BuildingData.N_time_steps;
    T_ext=BuildingData.T_ext;
    H_solar_rad=BuildingData.H_solar_rad;
    V_use=BuildingData.V_use;
    H_person=BuildingData.H_person;
    N_person=BuildingData.N_person;
    A_sth_window=BuildingData.A_sth_window;
    SHGC=BuildingData.SHGC;
    T_room_initial=BuildingData.T_room_initial;
    delta_t=BuildingData.delta_t;
    C_air=BuildingData.C_air;
    ro_air=BuildingData.ro_air;
    V_house=BuildingData.V_house;
    const_EAU_C_v=BuildingData.const_EAU_C_v;
    T_flow_SH=BuildingData.T_flow_SH;
    m_SH=BuildingData.m_SH;
    C_SH=BuildingData.C_SH;
    h_rad=BuildingData.h_rad;
    A_rad=BuildingData.A_rad;
    V_DHW=BuildingData.V_DHW;
    T_flow_DHW=BuildingData.T_flow_DHW;
    t_star=BuildingData.t_star;
    C_w=BuildingData.C_w;
    T_DHW_initial=BuildingData.T_DHW_initial;
    T_in_DHW=BuildingData.T_in_DHW;
    U_DHW=BuildingData.U_DHW;
    A_DHW=BuildingData.A_DHW;

    SH_ranges_mat=BuildingData.SH_ranges_mat;
    DHW_ranges_mat=BuildingData.DHW_ranges_mat;

    P_elec_HP=zeros(N_time_steps, 1);
    T_room=zeros(N_time_steps, 1);
    Q_loss=zeros(N_time_steps, 1);
    Q_gain=zeros(N_time_steps, 1);
    HP_SH_value=zeros(N_time_steps, 1);
    HP_SH_flag=2*ones(N_time_steps, 1);
    T_return_SH=zeros(N_time_steps, 1);
    T_rad_SH=zeros(N_time_steps, 1);
    COP_HP_SH=zeros(N_time_steps, 1);

    T_DHW=zeros(N_time_steps, 1);
    HP_DHW_value=zeros(N_time_steps, 1);
    HP_DHW_flag=2*ones(N_time_steps, 1);

```



```

COP_HP_DHW=zeros(N_time_steps, 1);

T_room(1)=T_room_initial;
Q_loss(1)=const_EAU_C_v* (T_room(1) - T_ext(1));
Q_gain(1)=(H_person * N_person) + (A_sth_window * SHGC * H_solar_rad (1));
T_return_SH(1)=(T_flow_SH*(2*m_SH*C_SH - h_rad*A_rad) +
2*(h_rad*A_rad*T_room(1)))/(h_rad*A_rad + 2*m_SH*C_SH);
T_rad_SH(1)=(T_flow_SH+T_return_SH(1))/2.0;
HP_SH_value(1)=h_rad*A_rad *(T_rad_SH(1) - T_room(1));

COP_HP_SH(1)=7.7261 * exp(-0.027*(T_return_SH(1) - T_ext(1)));

T_DHW(1)=T_DHW_initial;

COP_HP_DHW(1)=7.7261 * exp(-0.027*(T_DHW(1) - T_ext(1)));

%% Assuming input data is ok and the first time step is defined
%% in the first line of the Temperature ranges.
min_temp_DHW=DHW_ranges_mat(1,3);
%max_temp_DHW=DHW_ranges_mat(1,4);
min_temp_SH=SH_ranges_mat(1,3);
%max_temp_SH=SH_ranges_mat(1,4);

if T_DHW(1)<min_temp_DHW
    HP_DHW_flag(1)=1.0;
    HP_SH_flag(1)=0.0;
elseif T_DHW(1)>=min_temp_DHW
    HP_DHW_flag(1)=0.0;
    if T_room(1)<min_temp_SH
        HP_SH_flag(1)=1.0;
    else
        HP_SH_flag(1)=0.0;
    end
end

delta_C=C_air * ro_air * v_house;

for i=2:N_time_steps
    T_room(i)=T_room(i-1) - (1800.0 * delta_t * (Q_loss(i-1) - Q_gain(i-1)
- HP_SH_value(i-1)*1000*HP_SH_flag(i-1)) / delta_C);
    Q_loss(i)=const_EAU_C_v* (T_room(i) - T_ext(i));
    Q_gain(i)=(H_person * N_person) + (A_sth_window * SHGC * H_solar_rad
(i));
    T_return_SH(i)=(T_flow_SH*(2*m_SH*C_SH - h_rad*A_rad) +
2*(h_rad*A_rad*T_room(i)))/(h_rad*A_rad + 2*m_SH*C_SH);
    T_rad_SH(i)=(T_flow_SH+T_return_SH(i))/2.0;
    HP_SH_value(i)=h_rad*A_rad *(T_rad_SH(i) - T_room(i));
    COP_HP_SH(i)=7.7261 * exp(-0.027*(T_return_SH(i) - T_ext(i)));

    if HP_DHW_flag(i-1)==0

```

```

    Fac1=V_DHW * T_in_DHW + V_use(i-1) * T_in_DHW + (V_DHW-V_use(i-1))
* (T_DHW(i-1)-T_in_DHW);
    Fac2=0.86 * U_DHW * A_DHW *(T_DHW(i-1) - T_room(i-1)) * delta_t;
    Fac3=V_DHW+V_use(i-1); %% Formula OK????? V_use(i) OR V_use(i-1)
????????????
    T_DHW(i)=(Fac1-Fac2)/Fac3;
elseif HP_DHW_flag(i-1)==1
    T_DHW(i)=T_flow_DHW;
end

HP_DHW_value(i)=(V_DHW * C_w * (T_flow_DHW - T_DHW(i)))/(60.0 *
t_star);

COP_HP_DHW(i)=7.7261 * exp(-0.027*(T_DHW(i) - T_ext(i)));

%%% LOGIC and TEMPERATURE RANGES
flag=0;
j=1;
while flag==0
    if i>=DHW_ranges_mat(j,1) && i<=DHW_ranges_mat(j,2)
        min_temp_DHW=DHW_ranges_mat(j,3);
%         max_temp_DHW=DHW_ranges_mat(j,4);
        flag=1;
    end
    j=j+1;
    if j>size(DHW_ranges_mat, 1) && flag==0
        disp('Error with Domestic Hot Water temperature ranges');
        flag=1;
    end
end

flag=0;
j=1;
while flag==0
    if i>=SH_ranges_mat(j,1) && i<=SH_ranges_mat(j,2)
        min_temp_SH=SH_ranges_mat(j,3);
        max_temp_SH=SH_ranges_mat(j,4);
        flag=1;
    end
    j=j+1;
    if j>size(SH_ranges_mat, 1)&& flag==0
        disp('Error with Space Heating temperature ranges');
        flag=1;
    end
end

if T_DHW(i)<min_temp_DHW
    HP_DHW_flag(i)=1.0;
else
    HP_DHW_flag(i)=0.0;
end

```

```

end

if HP_DHW_flag(i)==0.0
    if T_room(i)>max_temp_SH
        HP_SH_flag(i)=0.0;
    elseif T_room(i)<min_temp_SH
        HP_SH_flag(i)=1.0;
    else
        HP_SH_flag(i)=HP_SH_flag(i-1);
    end
elseif HP_DHW_flag(i)==1.0
    HP_SH_flag(i)=0.0;
end

HP_SH_value(i)=HP_SH_value(i)/1000;
P_elec_HP(i)=HP_SH_value(i)/COP_HP_SH(i)*HP_SH_flag(i) +
HP_DHW_value(i)/COP_HP_DHW(i)*HP_DHW_flag(i);

end
HP_SH_value(1)=HP_SH_value(1)/1000;

if HP_DHW_flag(N_time_steps)==1
    HP_DHW_value(1)=(V_DHW * C_w * (T_DHW_initial - T_flow_DHW))/(60.0 *
t_star);
elseif HP_DHW_flag(N_time_steps)==0
    HP_DHW_value(1)=(V_DHW * C_w * (T_DHW_initial -
T_DHW(N_time_steps)))/(60.0 * t_star);
end

if T_DHW_initial > T_DHW(N_time_steps)
    HP_DHW_flag(1)=1;
else
    HP_DHW_flag(1)=0;
end

P_elec_HP(1)=HP_SH_value(1)/COP_HP_SH(1)*HP_SH_flag(1) +
HP_DHW_value(1)/COP_HP_DHW(1)*HP_DHW_flag(1);

Q_loss=Q_loss/1000;
Q_gain=Q_gain/1000;
% HP_SH_value=HP_SH_value/1000;
% P_elec_HP= P_elec_HP_SH + P_elec_HP_DHW;

BuildingData.T_room=T_room;
BuildingData.Q_loss=Q_loss;
BuildingData.Q_gain=Q_gain;
BuildingData.T_return_SH=T_return_SH;
BuildingData.T_rad_SH=T_rad_SH;
BuildingData.HP_SH_value=HP_SH_value;
BuildingData.COP_HP_SH=COP_HP_SH;
BuildingData.T_DHW=T_DHW;

```

```
BuildingData.HP_DHW_value=HP_DHW_value;  
BuildingData.COP_HP_DHW=COP_HP_DHW;  
BuildingData.HP_SH_flag=HP_SH_flag;  
BuildingData.HP_DHW_flag=HP_DHW_flag;  
BuildingData.P_elec_HP=P_elec_HP;  
end
```

Published with MATLAB® R2018a

3. Implementation and output

```
0. clear  
clc  
  
filename='Building_Data.xlsx';  
  
%%% Read from the excel file  
BuildingData = ReadData(filename);  
  
%%% Process the data and calculations  
BuildingData = ProcessData(BuildingData);  
  
%%% write in the output file  
writeResults(BuildingData, filename);  
  
myFile='worksapce.mat';  
save(myFile, '-v7.3'); % % save the workspace
```

Published with MATLAB® R2018a

APPENDIX B

DETAILS OF THE CASE STUDY LV NETWORK

B.1 One-line diagram of the LV network

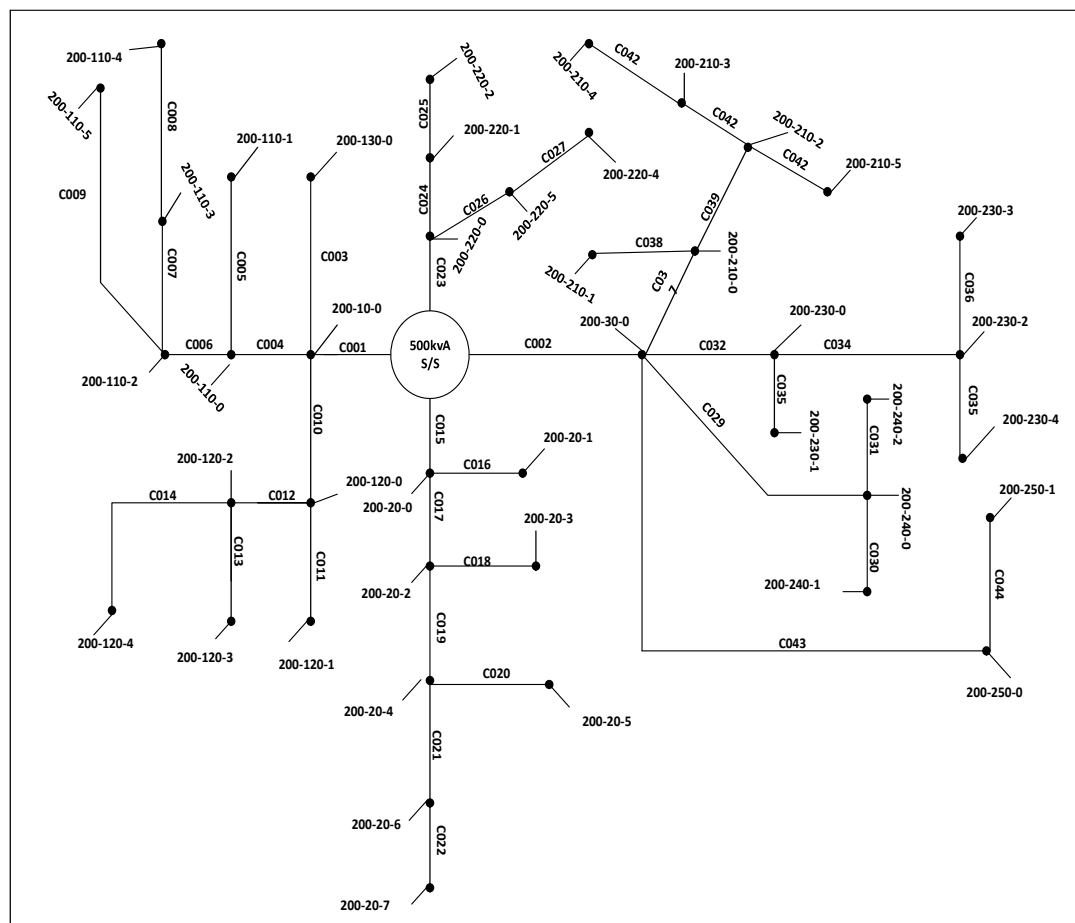


Fig. B.1 One-line diagram of the case study LV network

B.2 Technical parameters of the LV network

Table B.2 Technical parameters of the LV network

S S	Feeder NO.	Feeder identifier	From node	To node	Leng th (m)	Cable size/Ty pe	Cable identif ier	Resistance (Ω /km)		Reactance (Ω /km)		Rati ng (A)
								Pha se	Neut ral	Pha se	Neut ral	
C	10	C10	200	200-10-0	215	300TR	C001	0.100	0.164	0.073	0.011	470.0
C	20	C20	200	200-20-0	120	185TR	C015	0.164	0.164	0.074	0.014	355.0
C	20	C20	200-20-0	200-20-2	30	185TR	C017	0.164	0.164	0.074	0.014	355.0
C	20	C20	200-20-2	200-20-4	15	185TR	C019	0.164	0.164	0.074	0.014	355.0
C	20	C20	200-20-4	200-20-5	120	5c.04Cu	C020	0.703	0.703	0.079	0.079	140.0
C	20	C20	200-20-6	200-20-7	90	5c.04Cu	C022	0.703	0.703	0.079	0.079	140.0
C	20	C20	200-20-2	200-20-3	30	5c.06Cu	C018	0.463	0.463	0.076	0.076	175.0
C	20	C20	200-20-0	200-20-1	100	5c.10Cu	C016	0.276	0.276	0.073	0.073	240.0
C	20	C20	200-20-4	200-20-6	50	5c.10Cu	C021	0.276	0.276	0.073	0.073	240.0
C	30	C30	200	200-30-0	105	300TR	C002	0.100	0.164	0.073	0.011	470.0
C	110	C110	200-110-0	200-110-1	75	5c.04Cu	C005	0.703	0.703	0.079	0.079	140.0
C	110	C110	200-110-2	200-110-3	105	5c.04Cu	C007	0.703	0.703	0.079	0.079	140.0
C	110	C110	200-110-2	200-110-5	85	5c.04Cu	C009	0.703	0.703	0.079	0.079	140.0
C	110	C110	200-10-0	200-110-0	25	5c.10Cu	C004	0.276	0.276	0.073	0.073	240.0
C	110	C110	200-110-0	200-110-2	35	5c.10Cu	C006	0.276	0.276	0.073	0.073	240.0
C	110	C110	200-110-3	200-110-4	90	70TR	C008	0.443	0.443	0.076	0.015	196.0
C	120	C120	200-120-0	200-120-1	55	5c.04Cu	C011	0.703	0.703	0.079	0.079	140.0
C	120	C120	200-120-2	200-120-3	140	5c.04Cu	C013	0.703	0.703	0.079	0.079	140.0
C	120	C120	200-120-2	200-120-4	115	5c.04Cu	C014	0.703	0.703	0.079	0.079	140.0
C	120	C120	200-10-0	200-120-0	35	5c.10Cu	C010	0.276	0.276	0.073	0.073	240.0
C	120	C120	200-120-0	200-120-2	40	5c.10Cu	C012	0.276	0.276	0.073	0.073	240.0
C	130	C130	200-10-0	200-130-0	175	5c.06Cu	C003	0.463	0.463	0.076	0.076	175.0
C	210	C210	200-210-0	200-210-1	30	5c.06Cu	C038	0.463	0.463	0.076	0.076	175.0
C	210	C210	200-210-0	200-210-2	25	5c.06Cu	C039	0.463	0.463	0.076	0.076	175.0
C	210	C210	200-210-2	200-210-3	60	5c.06Cu	C041	0.463	0.463	0.076	0.076	175.0
C	210	C210	200-210-2	200-210-5	60	5c.06Cu	C042	0.463	0.463	0.076	0.076	175.0
C	210	C210	200-210-3	200-210-4	35	5c.06Cu	C040	0.463	0.463	0.076	0.076	175.0
C	210	C210	200-30-0	200-210-0	100	5c.10Cu	C037	0.276	0.276	0.073	0.073	240.0
C	220	C220	200	200-220-0	30	185TR	C023	0.164	0.164	0.074	0.014	355.0
C	220	C220	200-220-1	200-220-2	30	5c.06Cu	C025	0.463	0.463	0.076	0.076	175.0
C	220	C220	200-220-3	200-220-5	50	5c.06Cu	C028	0.463	0.463	0.076	0.076	175.0
C	220	C220	200-220-0	200-220-1	50	5c.10Cu	C024	0.276	0.276	0.073	0.073	240.0

C	220	C220	200-220-0	200-220-3	25	5c.10Cu	C026	0.276	0.276	0.073	0.073	240.0
C	220	C220	200-220-3	200-220-4	65	5c.10Cu	C027	0.276	0.276	0.073	0.073	240.0
C	230	C230	200-230-2	200-230-4	70	4c.10AL	C035	0.456	0.456	0.073	0.073	185.0
C	230	C230	200-230-2	200-230-3	20	4c.10AL	C036	0.456	0.456	0.073	0.073	185.0
C	230	C230	200-30-0	200-230-0	55	4c.20AL	C032	0.234	0.234	0.069	0.069	270.0
C	230	C230	200-230-0	200-230-1	45	4c.20AL	C033	0.234	0.234	0.069	0.069	270.0
C	230	C230	200-230-0	200-230-2	40	4c.20AL	C034	0.234	0.234	0.069	0.069	270.0
C	240	C240	200-30-0	200-240-0	50	5c.06Cu	C029	0.463	0.463	0.076	0.076	175.0
C	240	C240	200-240-0	200-240-1	50	5c.06Cu	C030	0.463	0.463	0.076	0.076	175.0
C	240	C240	200-240-0	200-240-2	30	5c.06Cu	C031	0.463	0.463	0.076	0.076	175.0
C	250	C250	200-250-0	200-250-1	130	120TR	C044	0.253	0.253	0.073	0.015	265.0
C	250	C250	200-30-0	200-250-0	250	300TR	C043	0.100	0.164	0.073	0.011	470.0